TECHNISCHE UNIVERSITÄT MÜNCHEN

Institut für Diabetes und Krebs, Helmholtz Zentrum München

&

Chair for Metabolic Programming, TUM School of Life Sciences

Mechanisms of inflammatory gene repression by the Glucocorticoid Receptor

Laura Escoter Torres

Vollständiger Abdruck der von der Fakultät TUM School of Life Sciences der Technischen Universität München zur Erlangung des akademischen Grades eines

Doktors der Naturwissenschaften (Dr. rer. nat.)

genehmigten Dissertation.

Vositzende: Prof. Dr. Ilona Grunwald Kadow

Prüfende/-r der Dissertation:

1. Prof. Dr. Nina Henriette Uhlenhaut

2. Prof. Dr. Dirk Haller

3. Prof. Dr. Roland Schüle

Die Dissertation wurde am 24.06.2020 bei der Technischen Universität München eingereicht und durch die Fakultät TUM School of Life Sciences am 16.11.2020 angenommen.

Acknowledgements

First, I would like to thank my supervisor, Prof. Dr. N. Henriette Uhlenhaut, for her support and guidance through each stage of this project. I specially appreciate the time, effort, ideas and feedback, which has greatly contributed to my professional and scientific development. Also, I value the generous funding from the ERC grant allocated to Prof. Uhlenhaut.

I am grateful to Prof. Dirk Haller for his support and scientific advice during our annual meetings discussing the progress of my PhD project. My special thanks go to Prof. Dr. Matthias Tschöp, director of the Institute for Diabetes and Obesity, and Prof. Dr. Stephan Herzig, director of the Institute for Diabetes and Cancer, for their input on this project as well as for leading two great international dynamic institutes with very talented scientists.

I would like to acknowledge Dr. Franziska Greulich for her assistance with NGS analysis and our various scientific discussions that significantly contributed to this work. Also, a strong thank you to Dr. Michael Wierer for the successful collaboration with the proteomics analysis.

I am deeply thankful to all the members of the MolEndo group, IDO and IDC for their help and support. I would like to acknowledge Dr. Omar García González, Michaël Hubert and Dr. Céline Jouffe specially for their crucial support and for making my time in the lab an unforgettable experience. Also, I appreciate the valuable scientific remarks from Dr. Manuel Gil Lozano. Similarly, my thanks to all team members: Kostas, Katerina, Teresa, Büsra, Afzal, Ken, Charlotte, Cinzia, Kinga, Kristina, Fabiana, Ashfaq, Suhail, Sybille and Ivonne for creating a vibrant, challenging and interactive professional environment. Also, thank you to Kei, Laurent, Caterina, Isabelle, Serge, Roger and Maria from the Nestlé Institute of Health Sciences in Lausanne to motivate me to pursue a PhD.

Lastly, but most important, a big thank you to my husband Christian Kerecsényi, my family and friends for their unconditional love, support and motivation. Thank you for always being there for me.

Table of contents

Abstract

The Glucocorticoid Receptor (GR) is an important immunosuppressive and anti-inflammatory drug target. It belongs to the nuclear receptor family of ligand-controlled transcription factors. Upon binding of its ligands such as cortisone or dexamethasone, GR translocates to the nucleus to regulate the expression of target genes either positively or negatively. The anti-inflammatory effects of glucocorticoids (GC) are mostly attributed to the repression of inflammatory genes by GR. Transcriptional repression by GR is mainly thought to occur via “tethering” or transrepression. In this mechanism, GR interacts with DNA-bound pro-inflammatory transcription factors (i.e. NF-κB and AP-1) to repress transcription and interfere with their activity without direct DNA binding. On the contrary, direct DNA binding by GR is generally believed to mediate gene activation, and the up-regulation of metabolic genes, for example, is thought to cause many of the adverse effects of treatment with GCs. However, the exact mechanisms mediating activation or repression still remain unknown.

However, here the generation of a new mouse line, named $GR^{\Delta Zn}$, with a point mutation in the DNA-binding domain of GR, reveals that DNA binding is essential for both transcriptional activation and repression. This mutant tethers via protein-protein interactions to NF-κB but no longer recognises specific DNA sequences. The application of genomic NGS and proteomic techniques, under inflammatory conditions, showed that DNA recognition is actually required for the assembly of a functional co-regulator complex to mediate glucocorticoid responses. Both mouse embryonic fibroblasts and macrophages from $GR^{\Delta Zn}$ mice fail to respond to treatment with GC under any of the conditions tested, even though tethered sites can be detected near inflammatory genes.

These findings challenge the model of transcriptional repression by tethering and in turn highlight the importance of DNA binding by GR in the control of inflammatory responses. These results may contribute to the development of safer immunomodulators with fewer side effects.

Zusammenfassung

Der Glukokortikoid Rezeptor (GR) ist ein wichtiges immunsuppressives und entzündungshemmendes Wirkstoffziel in der medizinischen Forschung. Er gehört zur Familie der Kern-Hormon Rezeptoren - ligandengesteuerter Transkriptionsfaktoren. Bei der Bindung seines Liganden, z.B. Cortison oder Dexamethason, transloziert der GR in den Zellkern und reguliert dort die Expression seiner Zielgene entweder positiv oder negativ. Die entzündungshemmende Wirkung von Glukokortikoiden (GC) wird hauptsächlich auf die Unterdrückung entzündlicher Geneexpression durch den GR zurückgeführt. Es wird angenommen, dass die Repression der Transkription durch GR via "Tethering" oder Transrepression erfolgt. Dabei interagiert der GR mit DNA-gebundenen entzündungsfördernden Transkriptionsfaktoren (z.B. NF-κB und AP-1), um die Genexpression zu unterdrücken und deren Aktivität ohne direkte DNA-Bindung zu stören. Im Gegensatz dazu wird im Allgemeinen angenommen, dass der GR durch die direkte DNA-Bindung vor allem die Aktivierung von Zielgenen vermittelt. Vor allem die Hochregulierung von metabolischen Genen verursacht dabei Nebenwirkungen in der Glukokortikoidtherapie. Die genauen Mechanismen, welche die Aktivierung oder Unterdrückung der Genexpression durch den GR vermitteln, sind weitgehend noch unbekannt.

In meiner Doktorarbeit konnte ich durch die Erzeugung einer neuen Mauslinie namens $GR^{\Delta Zn}$ mit einer Punktmutation in der DNA-Bindedomäne des GRs zeigen, dass die DNA-Bindung sowohl für die Transkriptionsaktivierung als auch für die Repression entscheidend ist. Diese Mutante bindet an NF-κB über Protein-Protein-Wechselwirkungen, erkennt jedoch keine spezifischen DNA-Sequenzen mehr. Unter Verwendung von „Next-Generation“ Sequenzierungs- (NGS) und proteomischen Techniken konnte ich zeigen, dass die DNA-Erkennung tatsächlich für den Aufbau eines funktionellen GR-Co-Regulator-Komplexes zur Vermittlung des Glukokortikoideffektes erforderlich ist. Embryonale Mausfibroblasten als auch murine Makrophagen von $GR^{\Delta Zn}$ Mäusen sprechen unter keiner der getesteten Bedingungen auf die Behandlung mit GC an, obwohl ich die Bindung des GRs an einige Stellen im Genom nachweisen konnte.

Diese Ergebnisse stellen das Modell der Transkriptionsrepression durch „Tethering“ in Frage und unterstreichen wiederum die Bedeutung der DNA-Bindung für die GR-vermittelte Kontrolle der Entzündungsreaktion. Des Weiteren tragen diese Ergebnisse zur Entwicklung sicherer Immunmodulatoren mit weniger Nebenwirkungen bei.

Abbreviations

ACTH	adrenocorticotropic hormone
AKC	ammonium chloride potassium
BCA	bicinchoninic acid
BMDM	bone marrow-derived macrophages
bp	base pair
BSA	bovine serum albumin
cDNA	complementary DNA
ChIP	chromatin immunoprecipitation
CRH	corticotrophin-releasing hormone
CRISPR	clustered regularly interspaced short palindromic repeats
DAPI	4′,6-diamidino-2-phenylindole
DBD	DNA binding domain
DEG	differentially expressed gene
Dex	dexamethasone
DMEM	Dulbecco's modified eagle's medium
DNA	deoxyribonucleic acid
DSG	disuccinimidyl glutarate
DTT	dithiothreitol
EDTA	ethylenediaminetetraacetic acid
EMSA	electrophoretic mobility shift assay
ENCODE	encyclopedia of DNA elements
ES	embryonic stem
FBS(d)	foetal bovine serum (dialyzed)
FDR	false discovery rate
GBS	GR binding site
GC	glucocorticoid
GEO	gene expression omnibus
GO	gene ontology
GR	glucocorticoid receptor
GRE	glucocorticoid response element
H&E	hematoxylin and eosin
HEPEs	2-(4-(2-hydroxyethyl)piperazin-1-yl)ethanesulfonic acid
HPA	hypothalamic-pituitary-adrenal
i.e.	id est, "that is"
IGB	integrated genome browser
IgG	immunoglobulin G
IP	immunoprecipitaiton
KO	knock out
LBD	ligand binding domain
LPS	lipopolysaccharide
M-CSF	macrophage colony stimulating factor
MEF	mouse embryonic fibroblast

mRNA	messenger RNA
MS	mass spectrometry
NGS	Next Generation Sequencing
NR	nuclear receptor
NTD	N-terminal transactivation domain
NTP	nucleoside triphosphate
PBS	phosphate buffered saline
PCR	polymerase chain reaction
PFA	paraformaldehyde
qPCR	quantitative PCR
RNA	ribonucleic acid
rpm	revolutions per minute
RT-PCR	reverse transcriptase polymerase chain reaction
SDS	sodium dodecyl sulfate
SEM	standard error of the mean
TBS-T	tris buffered saline with tween 20
TF	transcription factor
TPA/PMA	tetradecanoylphorbol acetate
TSS	transcription start site
UCSC	University of California, Santa Cruz
ZT	‚Zeitgeber‘

All gene names are indicated in *italics.* All protein names are written in regular font. Compounds and chemicals are abbreviated according to common nomenclature.

Index of Tables

Index of Figures

1. Introduction

1.1 Glucocorticoid signalling in health and disease

Glucocorticoids (GC) are steroid hormones present in all vertebrates that regulate various physiological processes such as, lung development, glucose metabolism, and inflammatory and stress responses. GC were discovered in 1946 when Edward Kendall isolated four steroidal compounds from adrenal extracts. One of the compounds is what we now know as cortisol, which was synthesized later by Sarett (Kendall 1949, Sarett 1946). Later on, Philip Hench discovered the therapeutic potential of cortisol by treating a patient suffering from rheumatoid arthritis (Hench, Kendall and et al. 1949). Kendall and Hench were awarded the Nobel Prize in Physiology or Medicine, together with Reichstein, in 1950 “for their discoveries relating to the hormones of the adrenal cortex, their structure and biological effects”. Nowadays, synthetic glucocorticoids, such as dexamethasone (Dex) or prednisolone are widely prescribed drugs for many inflammatory and autoimmune diseases.

1.1.1 HPA axis and physiological roles of glucocorticoids

Synthesis and secretion of cortisol in humans and corticosterone in rodents, is regulated in a diurnal- and stress-responsive manner. In normal healthy conditions, circulating levels of GC are subjected to tight regulation with levels peaking at the beginning of the active phase of the day. Synthesis and release of GC is regulated at different levels of the hypothalamic-pituitary-adrenal (HPA) axis (Biddie, Conway-Campbell and Lightman 2012). Briefly, stress and/or circadian clock signals the hypothalamus to release corticotrophin-releasing hormone (CRH), which induces the release of adrenocorticotropic hormone (ACTH) synthesis and secretion from the pituitary gland. ACTH then induces adrenal synthesis and secretion of GC, which interacts with specific receptors in target tissues. Homeostasis in GC levels is achieved by the negative feedback loop on the pituitary and hypothalamus (Gjerstad, Lightman and Spiga 2018) (**Figure 1**).

GC regulate numerous essential physiological and developmental processes, ranging from lung maturation to glucose metabolism and immune responses. Endogenous GC play important homeostatic roles in adult mammals. For instance, GC stimulate

gluconeogenesis in the liver to provide energy as part of daily rhythmic energy metabolism and for the “fight or flight” response (Kadmiel and Cidlowski 2013, Herman et al. 2016). In a “fight or flight” context, GC increase vascular tone and alertness, mobilise glucose and importantly prime the immune system to prepare the body for a potential injury.

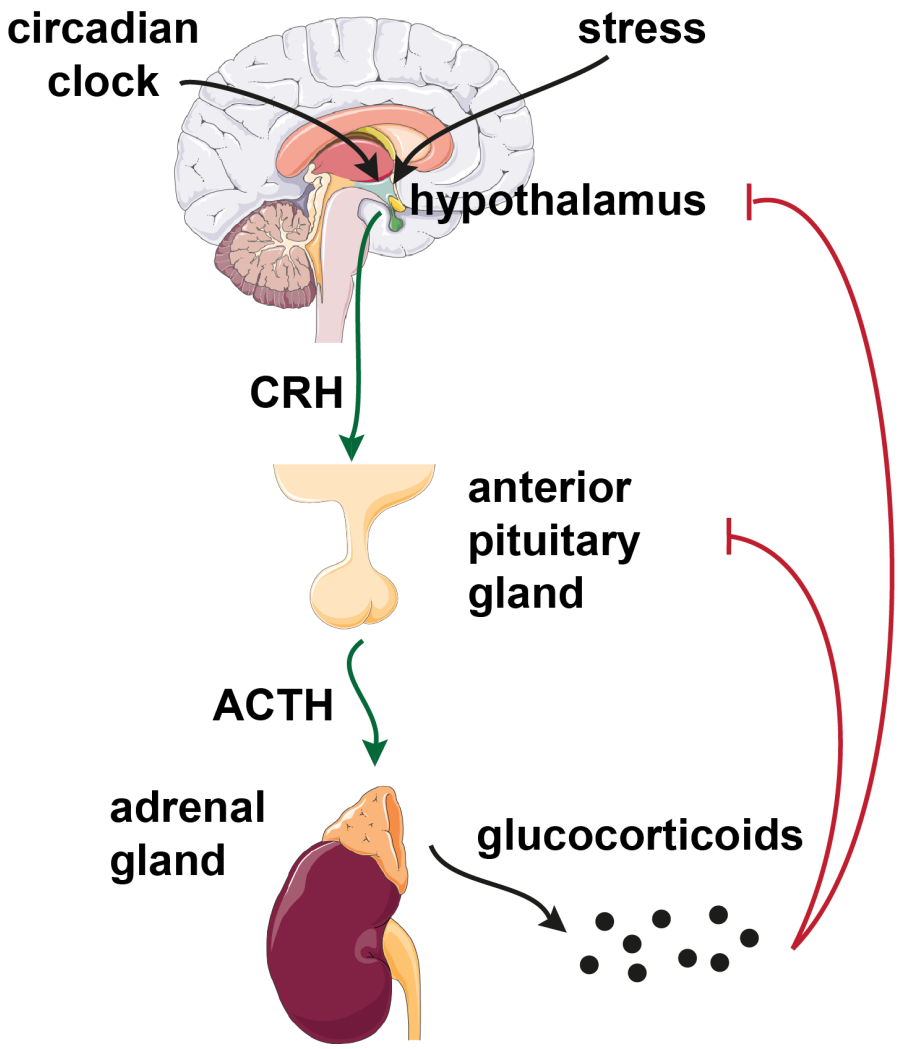

Figure 1. Regulation of glucocorticoid hormone secretion by the hypothalamic-pituitary-adrenal axis.
External and internal signals trigger the hypothalamus to release corticotropin releasing hormone (CRH), which in turn will signal the pituitary gland to secrete adrenocorticotropic hormone (ACTH). Then, ACTH signals the adrenal glands to secrete glucocorticoids (GC). GC regulate in a negative feedback loop the release of CRH and ACTH. Image adapted from (Oakley and Cidlowski 2013).

1.1.2 Clinical use and side effects of glucocorticoids

Due to their potent anti-inflammatory actions, GC are widely used as a treatment for acute and chronic inflammatory diseases, such as asthma, allergies, rheumatoid arthritis, skin conditions, multiple sclerosis etc. (**Figure 2**). Currently, it is estimated that 1-3% of the adult Western population are receiving GC, demonstrating their broad applications (McDonough, Curtis and Saag 2008). Administration of GC strongly suppresses the immune system. Nearly all immune cell types are sensitive to GC (Strehl et al. 2019). For example, macrophages, which sense infectious agents and secrete pro-inflammatory cytokines, are strongly silenced in presence of GC (Ehrchen, Roth and Barczyk-Kahlert 2019). Other immune cells also react to GC resulting in strong immunosuppression effects. Cell migration, maturation and apoptosis are regulated by the synthetic glucocorticoid dexamethasone in dendritic cells and neutrophils (Cao et al. 2013). Phagocytosis is enhanced in neutrophils and macrophages (Matyszak et al. 2000, Tuckermann et al. 2005). Also, GC suppress antibody production in B cells and induce apoptosis in B and T cells (Alnemri et al. 1992, Goossens and Van Vlierberghe 2016, Wang et al. 2003). The powerful immunosuppressive effects of glucocorticoids are advantageous to avoid organ rejection after transplantation and against some types of cancer, such as lymphoma (Ramamoorthy and Cidlowski 2016, De Lucena and Rangel 2018). Also, respiratory conditions such as asthma and chronic obstructive pulmonary disease (COPD) can be treated with corticosteroids. GC suppress cytokines, chemokines and cell adhesion molecules improving the airway epithelium (Schleimer 2004). Another beneficial effect of treatment with GC is the lung maturation of premature babies (Olaloko, Mohammed and Ojha 2018). Topical application of corticosteroids rapidly improves skin conditions, such as psoriasis and eczema, due to their anti-proliferative effects on keratinocytes and regulation of epithelial integrity and immune function (Sevilla and Perez 2018). Pain from inflammation of the joints and surrounding tissues in rheumatoid arthritis can be improved by treatment with GC. Also, ocular inflammation such as conjunctivitis, keratitis and uveitis can be treated with GC (Holland, Fingeret and Mah 2019).

GC have been used for over 70 years as anti-inflammatory drugs; however, treatment often comes with undesired adverse effects (**Figure 2**). Shortly after their first clinical use, side effects such as weight fluctuation, rounding of the face, glucose metabolism alterations, osteoporosis and other were observed (Hench 1952). Generally, a dose

superior to >30 mg/day of prednisolone is considered high (Buttgereit et al. 2002). Glucocorticoids signal the liver to replenish and release glucose to maintain energy homeostasis under physiological conditions as well as in response to stress (i.e. physical or mental). Prolonged exposure to high levels of cortisol induces adipocyte hypertrophy, glucose intolerance and insulin resistance (Kuo et al. 2015). Other side effects include hypertension, muscle and skin atrophy, osteoporosis, glaucoma, impaired wound healing and psychological effects such as insomnia, depression and anxiety (Hartmann et al. 2016, Muller and Holsboer 2006, Pimenta, Wolley and Stowasser 2012).

Long-term exposure to high levels of glucocorticoids due to chronic external administration or secretion from endocrine tumours, often causes a pathological condition known as Cushing's syndrome (Raff and Carroll 2015). Its symptoms include weight gain, round face and neck, weak muscles, stretch marks and susceptibility to infection. On the other side, chronic deficiency in GC levels results in Addison's disease with extreme fatigue, weight loss and low blood pressure and glucose levels. Separating beneficial therapeutic properties from adverse side effects based on a molecular understanding of GC action together with the glucocorticoid receptor (GR) is a long-term goal in biomedical research.

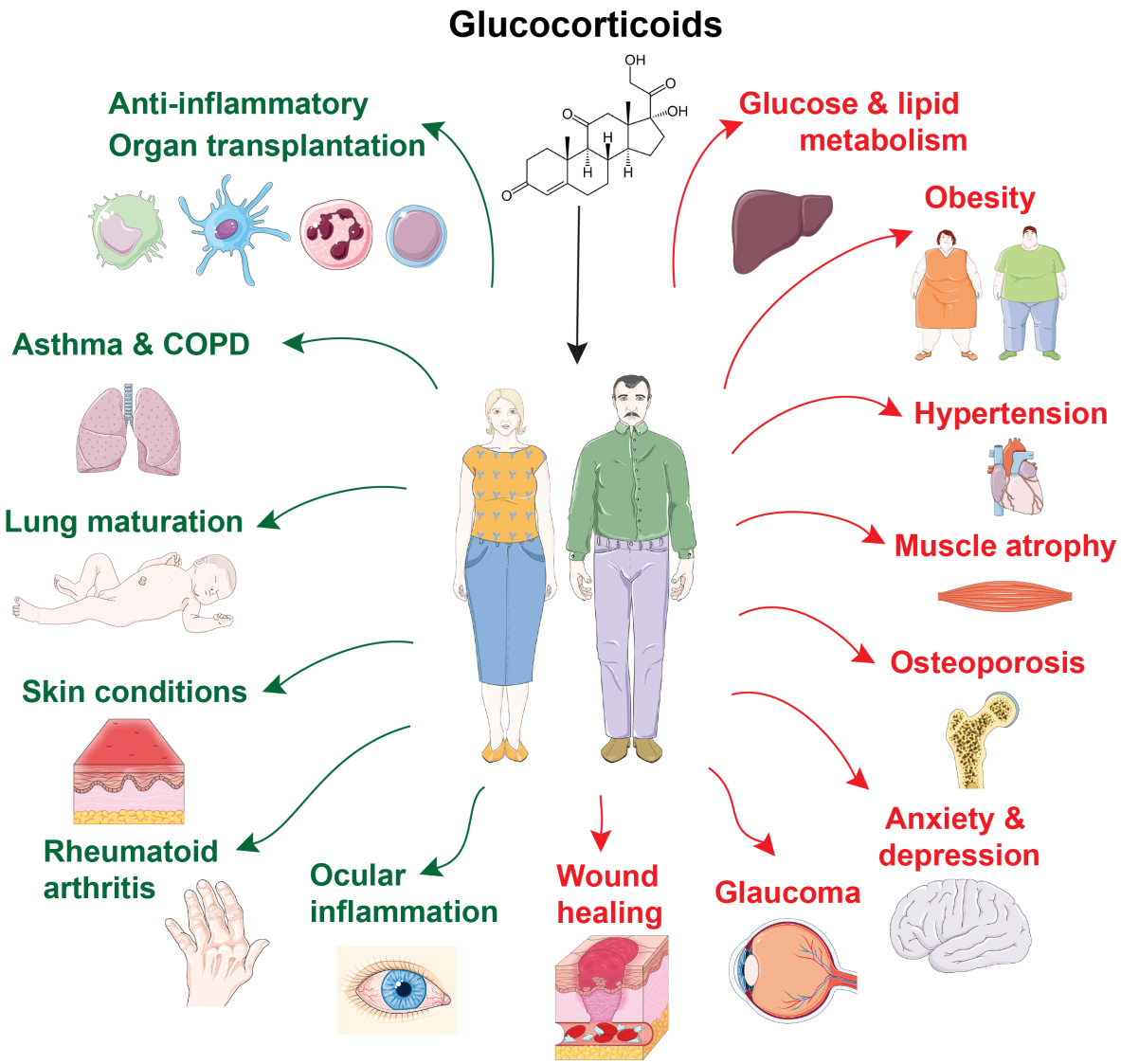

Figure 2. Beneficial and adverse effects of therapy with glucocorticoids.
Green; beneficial effects. Red; undesired side effects. Image adapted from (Oakley and Cidlowski 2013). Glucocorticoid molecule; cortisone (Hardy, Raza and Cooper 2020).

1.2 Immunomodulation by the glucocorticoid receptor

1.2.1 The glucocorticoid receptor

The GR belongs to the nuclear receptor (NR) superfamily of ligand activated transcription factors (TF). This family is formed by 48 and 49 NRs in humans and mice, respectively (Zhang et al. 2004). Most NRs have the special property of being activated by small lipophilic ligands to then modulate gene transcription and therefore regulate

development, reproduction and general physiological homeostasis (**Figure 3**). GR is part of the NR subfamily 3, group C that is formed by: the glucocorticoid, mineralocorticoid, progesterone and androgen receptors.

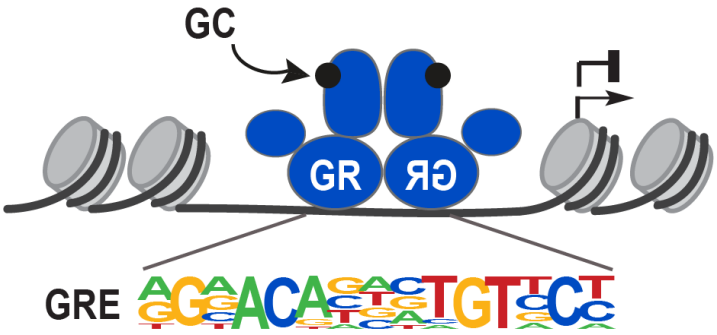

Figure 3. Glucocorticoid receptor gene regulation. The dimeric glucocorticoid receptor (GR) binds specific genomic DNA sequences named Glucocorticoid Response Elements (GREs) to activate and repress target genes. GC; glucocorticoid, hormone ligand.

The GR gene, *NR3C1* in humans and *Nr3c1* in mice, is encoded in chromosome 5 and 18, respectively. The gene contains nine exons and can generate several isoforms including GRα and GRβ, by alternative splicing of exon 9 (Lu and Cidlowski 2005, Hartmann et al. 2016). GRα is the predominant isoform and GC are able to bind GRα but not GRβ. Also, GRβ appears to antagonize the activity of GRα (Kino, Su and Chrousos 2009). All NRs share a highly conserved structural organization. The GR protein consists of three major domains, the N-terminal transactivation domain (NTD), the central DNA binding domain (DBD) and the C-terminal ligand binding domain (LBD) (Giguere et al. 1986). The region between the DBD and the LBD contains a nuclear localisation signal that when exposed allows the translocation to the nucleus (**Figure 4**). The DBD domain is composed of several conserved amino acids that fold into two zinc finger structures and is essential to recognise specific DNA sequences. Each zinc finger is formed by four cysteine amino acids with one central zinc ion.

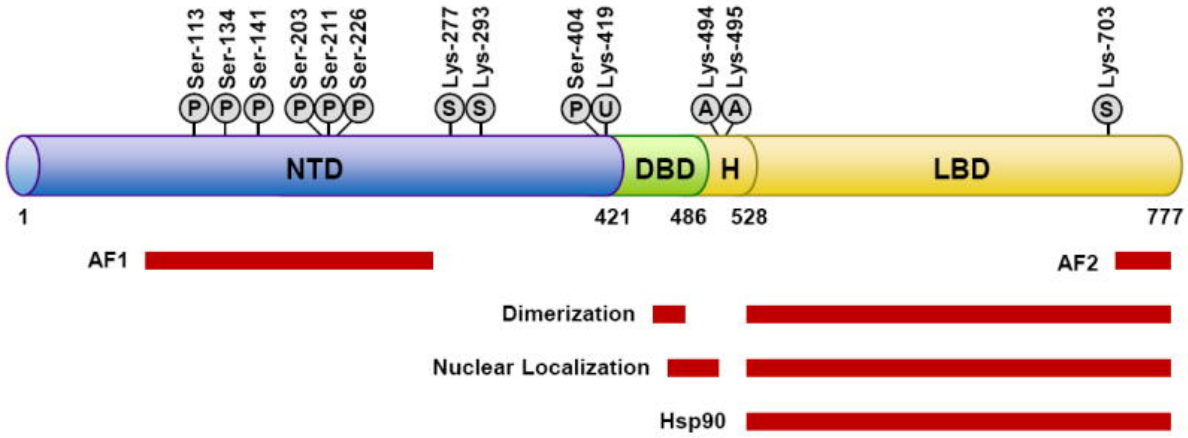

Figure 4. The glucocorticoid receptor functional protein domains.
N-terminal domain (NTD), DNA-binding domain (DBD), ligand binding domain (LBD), flexible hinge region (H) and activation function 1 and 2 (AF1, AF2). Post-translational modifications: phosphorylation (P), sumoylation (S), ubiquitination (U) and acetylation (A). Red: regions relevant for: transactivation, dimerization, nuclear transport and interaction with the heat shock protein 90 (Hsp90). Amino acid numbers refer to human GR. Image from (Oakley and Cidlowski 2013).

In the presence of ligand, GR undergoes a conformational change that triggers the release from cytoplasmic heat shock proteins (Hsp) such as Hsp90, and exposes GR's nuclear localisation signals (Pratt and Toft 2003). Then, GR is imported to the nucleus via importinα to bind to specific genomic sequences. GR binds to enhancer regions and promoters to activate or repress target genes (Lim et al. 2015, Glass and Saijo 2010). The classical DNA binding site for GR are the glucocorticoid response elements (GREs), which are typically composed by two imperfect 6 bp palindromic sites separated by a 3 base pair (bp) spacer. The consensus GRE has the following sequence: GnACAnnnTGTnC, where n stands for any nucleotide. Also, the crosstalk with the nearby TF, chromatin remodelling and histone acetyltransferase (HATs) and co-regulators influences the transcriptional immunomodulation by the GR.

The diversity in transcriptional activity of GR is partly due to post-translational modifications. GR can be phosphorylated at serine/threonine residues and acetylated, ubiquitinated and/or sumoylated at lysine residues. The most characterised GR phosphorylation sites are human S203, 211 and 226 (mouse S212, 220 and 234). Cell-specific kinases such as cyclin-dependent kinases (CDKs) complexes, extracellular signal-regulated kinases (ERKs), mitogen-activated protein kinases (MAPKs) kinases and glycogen synthase kinase 3 (GSK-3) have been shown to phosphorylate GR to modulate its activity (Galliher-Beckley and Cidlowski 2009). In addition, ubiquitination

of GR at K419 was shown to influence the turnover and degradation by the proteasome (Deroo et al. 2002). Finally, GR can be sumoylated, which can affect the interaction with coregulators (Druker et al. 2013).

1.2.2 Mechanisms of GR-mediated gene regulation

Hormone binding by GR results in nuclear translocation that allows the receptor to recognise and bind to specific DNA regions and regulate its target genes. Even though the immunosuppressive effects of GC are known for many years, the exact mechanisms are in fact of great complexity. Lipopolysaccharide (LPS), a small component of the wall of Gram-negative bacteria, is commonly used to study inflammation. Under inflammatory conditions, the Toll-like receptor 4 (TLR4) activates a signalling cascade in macrophages that end with the nuclear translocation of nuclear factor-κB (NF-κB) and activator protein 1 (AP-1). These two TF, in combination with others, then activate the expression of pro-inflammatory genes (Oeckinghaus and Ghosh 2009, Zenz et al. 2008). TLR4 signalling pathway ultimately activates NF-κB via degradation of cytosolic IκB kinase (IKK) complex that allows NF-κB to translocate to the nucleus. Also, TLR4 activates AP-1 via the MAPK signalling pathway.

1.2.2.1 Genomic actions of the GR

The “classical” effects of the GR are the genomic effects, where ligand-bound GR mediates transcriptional activation and repression. In the nucleus, GR homodimerizes and binds GREs found in *cis*-regulatory elements. These genomic regions can be in sense or antisense orientation and close to the transcription starting site (TSS) of a target gene (promoter region) or up to several hundred base pairs away, upstream or downstream, of a target gene (enhancer). In addition, multiple TF can bind close by in the genome and regulate transcription in a co-operative manner. To mediate transcriptional activation, GR binds classical GREs. However, several mechanisms are proposed for transcriptional repression of GR target genes. For example: trans-repression or tethering to other DNA-bound TF, negative GREs (nGREs), non-classical GREs, GREs overlapping with other motifs (composite GREs), unknown motifs, DNA as an allosteric modulator of GR as well as consensus classical GREs are all mechanisms proposed to play a role in gene repression (**Figure 5**). Also, GR interacts

with a variety of co-activators and chromatin-remodelling complexes to modulate transcriptional activity.

Chromatin immunoprecipitation (ChIP) followed by massively parallel sequencing (ChIP-Seq) is a powerful tool to map the genome-wide binding profile (cistrome) of a particular protein. In ChIP-Seq, proteins are first crosslinked to DNA, then the genomic DNA is fragmented, the protein of interest is immunoprecipitated and the DNA fragments are sequenced to identify the set of binding sites. The development of Next Generation Sequencing (NGS) and ChIP-Seq technologies greatly expanded the ability to study the genome and transcriptional regulation.

The lack of canonical GREs in some ChIP-Seq peaks has been traditionally explained by GR tethering to other DNA-bound TF via protein-protein interactions (Scheschowitsch, Leite and Assreuy 2017, Desmet and De Bosscher 2017). Most frequently, GR tethering to NF-κB (Ray and Prefontaine 1994), AP-1 (Yang-Yen et al. 1990), STAT3 (Langlais et al. 2012) and others has been suggested as the main mechanism of down-regulation of inflammatory genes. Tethering can also be named transrepression. GR has been shown to repress a luciferase reporter that contains a NF-κB response element or AP-1, but not a classical GRE, driving the expression of a luciferase reporter gene (Bladh et al. 2005, Rogatsky, Waase and Garabedian 1998), concluding that GR did not directly bind DNA but instead repressive actions were mediated by tethering. Both, the NF-κB subunit, p65 (also known as RelA) and AP-1 can interact directly with GR (Ray and Prefontaine 1994, Jonat et al. 1990). Finally, GR tethering to STAT3 was studied by Langlais and co-authors in mouse pituitary tumour cell line, AtT-20. Signal transducer and activator of transcription 3 (STAT3) is a TF that is activated by cytokines and the MAPK pathway to regulate innate immune responses (Hillmer et al. 2016). Intriguingly, STAT3 tethering to GR synergistically increased gene expression. On the contrary, GR tethering to STAT3 resulted in gene repression (Langlais et al. 2012).

The definition of negative GRE (nGRE) is complex and heterogeneous. The first nGRE motif was identified in the promoter region of the GR-repressed *Pro-opiomelanocortin* (*POMC*) gene (Drouin et al. 1989). nGREs have been detected in various genes from different cell types, for example: in milk (*bovine prolactin PRL3*), bone (*Osteocalcin*), skin structure (*Keratins*) and inflammation (*Il1β*) (Subramaniam, Cairns and Okret

1997, Aslam et al. 1995, Radoja et al. 2000, Zhang, Zhang and Duff 1997). Negative GREs were initially described as GR-bound sequences that resemble the classical GRE. However, they can also be a DNA sequence with mismatch/es at conserved position/s of the motif near a repressed target. A variation of nGRE, named “inverted repeat (IR) nGRE” was shown to associate with repression by direct GR binding (Surjit et al. 2011). These IR nGREs vary from the canonical GRE or nGRE motifs. Instead, they are inverted repeats of CTCC with a spacing of 0 to 2 base pairs. However, the presence of IR nGREs in ChIP-Seq sequences and their significance for repression of inflammatory genes requires more studies.

Another mechanism of gene regulation is a composite or combinatorial binding of GR to imperfect GREs that overlap with motifs from other TF (Siersbaek et al. 2011). For example, the *proliferin* promoter region, has a composite element that is regulated by GR and AP-1 (Mordacq and Linzer 1989, Miner and Yamamoto 1992). Also, the GR DBD domain was shown to bind a novel motif, inside the NF-κB consensus sequence. The AATTT nucleotides at the promoter regions of *CCL2*, *IL-8*, *PLAU*, *RELB* and *ICAM1* genes was bound by crystallised GR’s DBD. This novel site is highly conserved between species (Hudson et al. 2018). Finally, at overlapping sites, TF might compete for a specific binding site, adding another layer of complexity to the transcriptional modulation by GR.

Several studies have shown that GR mostly binds open chromatin regions, meaning DNase-I accessible regions, contributing to the high cell-type specific binding of GR (Biddie et al. 2011, John et al. 2011). In a subset of sites though, GR does seem to act as a pioneer factor (Swinstead et al. 2016). Another factor that can fine tune the activity of GR is the DNA itself acting as an allosteric modulator. A single base pair can differentially affect GR’s DBD conformation and transcriptional activity (Meijsing et al. 2009, Schone et al. 2018). Also, addition of a single GR binding site upstream of *IL1β* and *IL1R2* genes using CRISPR/Cas9 in U2OS cells was sufficient for GR to regulate them (Thormann et al. 2019).

Finally, GR directly binding to canonical high affinity GREs is the classical and widely accepted mechanism for gene activation, but not repression. Examples of activated targets with GREs are *GC-induced leucine zipper* (*Gilz* or *Tsc22d3*), *Serum/glucocorticoid-regulated kinase 1* (*Sgk1*) or *Period 1* (*Per1*) (Itani et al. 2002).

However, the discovery of GREs in enhancers near both activated and repressed genes in bone marrow-derived macrophages (BMDM) treated with LPS and Dex defies these models. This observation points out direct GRE binding's role in GR-mediated inflammatory gene repression. Also, the models described above are insufficient to predict up- or down-regulation by GR (Uhlenhaut et al. 2013, Hoffman et al. 2018, Hemmer et al. 2019, Hudson et al. 2018).

In conclusion, despite great progress made with Next Generation Sequencing (NGS) techniques and genome wide analysis, the exact mechanisms of inflammatory gene repression by GR remains unknown.

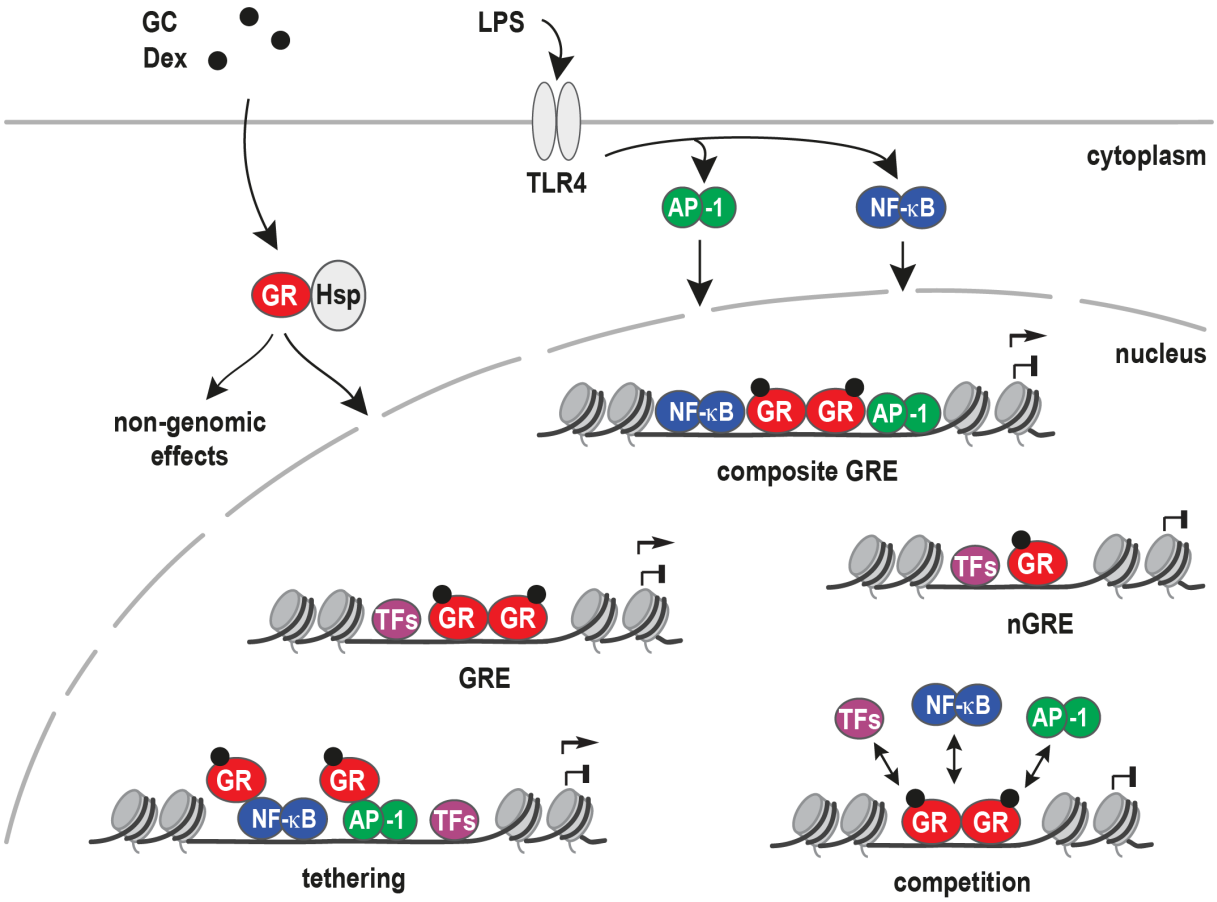

Figure 5. Mechanisms of gene regulation by the glucocorticoid receptor.
Glucocorticoids (GC) diffuse to the cytoplasm where they bind the glucocorticoid receptor (GR). Ligand binding changes GR's conformation and releases it from the heat shock proteins (HSP) before translocating to the nucleus. Lipopolysaccharide (LPS) binds to Toll-like receptor 4 (TLR4) in macrophages and starts a signalling cascade that results in the nuclear translocation of NF-κB and AP-1 transcription factors that bind and regulate pro-inflammatory genes. Mechanisms that have been proposed to mediate GR's anti-inflammatory actions are: binding to Glucocorticoid Response Elements (GREs), composite or combinatory GREs, negative (nGRE), tethering to DNA-bound TF or competition between TF for binding sites. Also, non-genomic rapid effects of GC can take place. Image from (Escoter-Torres et al. 2019).

1.2.2.2 Non-genomic actions of GR

Some effects of GC, such as bronchodilatation, are so rapid (within minutes) that they seem unlikely to be a result of gene transcription effects but rather non-genomic actions of the GR (Buttgereit and Scheffold 2002). These actions are thought to i) not require GR's direct action, or ii) take place via membrane or cytosolic GR (Proven et al. 2003, Bartholome et al. 2004, Spies et al. 2006). Non-genomic functions have been described in several cell types (i.e. macrophages, lung epithelial cells and T cells) (Long et al. 2005, Matthews et al. 2008, Lowenberg et al. 2006). Mechanistically, GR has been shown to be involved in the loss of Mitogen- and Stress-activated protein Kinsase-1 (MSK1) recruitment at promoters of inflammatory genes as well as nuclear export of MSK1 via cytosolic GR (Beck et al. 2008).

1.2.2.3 Tissue specificity and multimerization of GR

The right levels of expression of a particular factor in a tissue are important for proper physiological function and homeostasis. As previously discussed, the GR/GC effects are very diverse and tissue specific. That can be partially due to differential isoform expression of *NR3C1,* but also the chromatin landscape and DNA accessibility is cell type and tissue specific. A study from Farley and co-authors showed that the binding affinity of a TF to an enhancer correlates with expression of the target gene in a tissue-specific manner. In other words, to achieve the precise expression of a given protein in a tissue/organ, both high and low affinity enhancers with the right spacing are essential. This work was done in invertebrate squid-like animals named ciona (Farley et al. 2016).

In addition to specific enhancer and DNA accessibility, the residence time of a factor bound to DNA and the number of oligomerization state have been proposed to play a role in regulation of gene transcription. Originally, GR (and any other TF) was thought to bind DNA in a static manner to regulate transcriptional outcome. However, with advanced fluorescence microscopy techniques, GR's oligomeric state can be now visualized in live cells. The time that GR stays bound to DNA is much shorter than previously thought, it is in fact in the range of seconds or less (Gebhardt et al. 2013). Also, only a portion of available molecules are bound to DNA at a particular time. This suggests that TF and co-regulators have rather a fast "binding - no binding" interaction

at genomic response elements (Paakinaho et al. 2017). GR has been described to act as a monomer, dimer and also tetramer (Wrange, Carlstedt-Duke and Gustafsson 1986, Tsai et al. 1988, Wrange, Eriksson and Perlmann 1989, Payvar et al. 1983). Also, upon DNA binding, GR undergoes a conformational change that promotes the formation of tetramers via the LBD domain (Meijsing et al. 2009, Presman et al. 2016).

1.2.3 Glucocorticoid action on macrophages and target genes

Potent anti-inflammatory and immune-supressing effects of GC affect both the innate and the adaptive immune system. Macrophages are innate immune cells that mediate defence responses by removal of pathogens and regulate tissue homeostasis (Hirayama, Iida and Nakase 2017). Macrophages are the first line of defence against pathogens and reside in many different tissues. They are among the most effective producers of pro-inflammatory mediators that mediate the recruitment of immune cells. Depending on the activating stimulus, they can be classified into M1-like and M2-like macrophages. The classically activated macrophages, M1-like macrophages, mediate pro-inflammatory actions. They are activated when exposed to lipopolysaccharide (LPS), interferon gamma (INFγ) or tumour necrosis factor alpha (TNF-α). They can also be activated by pathogen- and danger-associated molecular patterns (PAMPs and DAMPs respectively) (Roh and Sohn 2018). In macrophages, the pathogenic agent signals to TLRs, which activate the NF-κB and AP-1 signalling pathways to induce transcription of pro-inflammatory cytokines and chemokines. Some of those cytokines can be silenced by GC. (Medzhitov and Horng 2009, Hayden and Ghosh 2004). On the other hand, M2-like macrophages, are characterised by their anti-inflammatory potential and are activated by cytokines involved in inflammatory resolution, like IL-4, IL-10 and IL-13. GC can also polarize macrophages to an M2-like phenotype by regulating the expression of anti-inflammatory proteins (Gordon 2003, Martinez and Gordon 2014).

GC can strongly modulate macrophage activity by repressing transcription of pro-inflammatory genes as well as inducing genes that antagonize pro-inflammatory signalling. Examples of down-regulated pro-inflammatory genes are: chemokines, interleukins and matrix metalloproteinases (Ehrchen et al. 2019). Transcription of the chemokines, which attract immune cells to the site of inflammation, are repressed by

GC (i.e. *Ccl2* and *Cxcl2*) (Uhlenhaut et al. 2013). GC also inhibit the transcription of several pro-inflammatory interleukins produced by human macrophages (i.e. *Il6, Il8, Il1β, Il12* and *TNFα*) (Ma et al. 2004). Proteins form the matrix metallopeptidases (Mmp) family are also repressed by GC. (i.e. *Mmp9, Mmp12* and *Mmp13*). Mmps are proteases that degrade the extracellular matrix and participate in the chemotaxis (Rollins et al. 2017). An example of GC-induced genes that antagonize the pro-inflammatory signalling is the *GC-induced leucine zipper* (*Gilz or Tsc22d3*) gene, which binds to the NF-κB subunit p65 to supress gene transcription (Berrebi et al. 2003). Also, *MAPK phosphatase 1* (*Mkp1* or *Dusp1*) is activated by the GR and limits the MAPK pathway via negative feedback loop (Abraham et al. 2006). Similarly, the *I kappa B* (*IκBα* and *β*) inhibitory protein, traps NF-κB in inactive cytoplasmic complexes in mice and human (Auphan et al. 1995). Also, the *Kruppel-like transcription factors* (*Klf*) are important for GC-induced inflammatory response (Sasse et al. 2013). Finally, a classic GR-induced target gene is the circadian rhythm gene *Per1* (Balsalobre et al. 2000). The up-regulation of anti-inflammatory genes emphasizes the fact that both gene repression and activation are required for the immunomodulatory effects of GC.

1.3 Mechanistic insights into immunomodulation from GR mutants

A strategy to study diverse aspects of GR gene regulation is the generation of transgenic mice that express mutated versions (deletion, chimeric or point mutants) of the receptor, reviewed by (Beck, De Bosscher and Haegeman 2011, Escoter-Torres et al. 2019).

Importantly, GR-deficient mice die shortly after birth due to respiratory failure. They present sever impairment of lung inflation and development from day E15.5 *post coitum* (p.c.). The HPA axis was impaired resulting in enlarged adrenal glands with increased expression of cortical steroid biosynthetic enzymes. Also, GR^{KO} mice showed decreased transcript levels of the following hepatic gluconeogenic enzymes: *glucose 6-phosphatase* (*G6Pase*), *tyrosine aminotransferase* (*TAT*), *serine dehydratase* (*SDH*) and *phosphoenolpyruvate carboxykinase* (PEPCK) in livers of new born mice (Cole et al. 1995).

One mutant mouse model expressing a dimerization-defective GR (GR^{dim}) has been intensively studied over the past 20 years. The GR^{dim} mutant was originally designed following the principle that GR required dimerization to activate, but not to repress target genes. Initially, GR was thought to tether to inflammatory TF (i.e. NF-κB and AP-1) as a monomer, and therefore the "dim" mutation that abolishes dimerization would separate the activation from repression mechanisms of the receptor. Monomer GR was considered to mediate the beneficial anti-inflammatory effects via tethering. And dimeric GR was thought to drive the activation of metabolic genes (Hubner et al. 2015). Homozygous mice with the GR A465T (dim) mutation in the second zinc finger of the DBD can live, under certain genetic backgrounds, unlike the global GR^{KO}, that die shorty after birth (Reichardt et al. 1998, Reichardt et al. 2001, Cole et al. 1995). GR^{dim} responded to treatment with CGs in phorbol ester-induced skin irritation inflammation model. The authors concluded that GR monomer and thus tethering was sufficient for inflammatory gene repression. However, the authors sparked the belief that DNA binding was not essential for repression. After, in other models of inflammation, such as LPS/TNFα-induced shock, arthritis or allergy models, GR^{dim} did not repress inflammation and cytokine production as efficient as wild type mice (Vandevyver et al. 2012, Silverman et al. 2013, Kleiman et al. 2012, Tuckermann et al. 2007, Baschant et al. 2011, Vettorazzi et al. 2015, Klassen et al. 2017). Also, later on, the GR^{dim} cistrome in macrophages and liver was studied. Importantly, half site GREs were enriched in the GR^{dim} binding sites, supporting a model of "half-site-facilitated-tethering" where DNA sequence mediates repression (Lim et al. 2015).

Other GR mutant mice have been studied, for example the sumoylation-deficient GR K310R and the GR-C3. The K310R mutation showed sumoylation at this site to be required for GC-mediated anti-inflammatory effects in skin inflammation. Also, reduced nuclear receptor co-repressor 2 (NCoR) also known as silencing mediator of retinoid and thyroid hormone receptor (SMRT) recruitment to GR, NF-κB and AP-1 genomic binding was observed in this mutant (Hua, Ganti and Chambon 2016a, Hua, Paulen and Chambon 2016b). Additionally, a knock-in mouse that expresses the GR isoform C3 was generated by Cidlowski and co-authors. These mice died after birth but could be rescued with prenatal GC administration. Also, this knocked-in mice were more sensitive to LPS administration and generally showed impaired repression of

inflammatory response. These results suggest that GR-C3 might mediate anti-inflammatory actions (Oakley et al. 2018).

Many other GR mutations have been studied *in vitro*, mainly in immortalized cell lines. One particularly interesting mutation is the rat GR R488Q (human R469Q) in the DBD. This mutation was shown to selectively repress AP-1 gene transcription and not NF-κB (Bladh et al. 2005). Another relevant mutant is the double DBD point mutant rat GR P493R/A494S, also known as GR LS7. This mutant was reported to repress NF-κB and AP-1 mediated gene transcription, but not transcriptional activation, separating therefore activation vs repression GR-mediated transcriptional regulation (Liden et al. 1997).

In conclusion, the generation of GR mutant models provides a valuable tool to study the molecular function of GR. The GR^{dim} mutant was shown to dissociate monomeric and dimeric actions of the GR. However, it does not dissociate direct DNA binding from tethering actions, since it was shown to bind half site GREs in macrophages and liver (Lim et al. 2015). A different approach to address the requirement of direct DNA binding for target gene repression by GR, is the characterization of the DNA-binding impaired GR C437G mouse mutant, named $GR^{\Delta Zn}$. Several human GR DBD mutants including the GR C421G, mouse C437G, were characterised *in vitro* in CAT reporter assays as well as gel shift assays by Hollenberg and Evans (Hollenberg and Evans 1988). The cysteine 421 in the first zinc finger of the hGR DBD was shown to be critical for DNA binding and transcriptional activation, indicating the importance of DNA binding for transcriptional regulation (**Figure 6**).

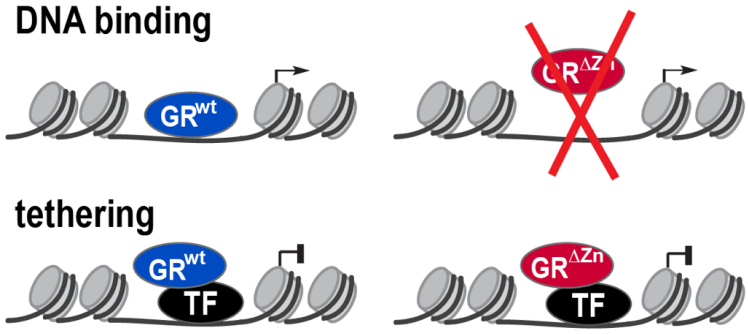

Figure 6. Schematic illustrating the DNA binding-impaired $GR^{\Delta Zn}$ mutant.
The GR zinc finger mutant separates direct DNA binding, which is abolished, from tethering to other transcription factors (TF), which is maintained.

2. Scope of the thesis

The hypothesis of this thesis was that this new $GR^{\Delta Zn}$ mouse will allow dissection of both direct and indirect (tethering) DNA binding mechanisms of gene regulation by GR. The two main aims of this work are:

1. Characterisation of the DNA-binding impaired mouse mutant line $GR^{\Delta Zn}$

The $GR^{\Delta Zn}$ mouse line was generated to study the requirement of direct DNA binding for transcriptional activation and repression by GR. After thoroughly validating the integrity of the $GR^{\Delta Zn}$ protein with maintained GR properties such as protein stability, post-translational modifications, nuclear translocation and protein-protein interactions, the phenotype of homozygous mutants was characterised. Key GR target tissues such as innate immune cells, lungs, adrenal glands, livers and fibroblasts were studied.

2. Characterisation of the genomic and transcriptional effects of the $GR^{\Delta Zn}$ mutant

The genomic occupancy of the DNA binding-impaired $GR^{\Delta Zn}$ protein under inflammatory conditions in mouse embryonic fibroblasts (MEFs) was investigated. The tethered and the direct binding sites in the genome were determined by ChIP-Seq and the genomic binding was correlated with RNA-Seq data to measure the transcription of target genes. The effect of the DNA binding impairment in the interaction with co-regulators was measured by proteomics (ChIP-MS).

Mainly, the role of DNA binding by GR in the repression of inflammatory genes was investigated. Ultimately, understanding these molecular mechanisms may contribute to the development of novel anti-inflammatory drugs with reduced side effects.

3. Material and methods

3.1 Chemicals, commercial kits, antibodies and primers

Table 1. List of chemicals and reagents.

Chemical/reagent	Provider
Agarose	VWR Chemicals
Bovine serum albumin (BSA)	Sigma Aldrich
Chelex	Sigma Aldrich
Complete Mini protease inhibitor	Roche Applied Science
DAPI	Sigma Aldrich
Dexamethasone (Dex)	Sigma Aldrich
Dialyzed Foetal Bovine Serum (dFBS)	Sigma Aldrich
DMEM (high glucose)	Sigma Aldrich
DMEM (phenol red-free)	Thermo Fisher Scientific GmbH
dNTP	Thermo Fisher Scientific GmbH
Dynabeads M-280 sheep anti-rabbit IgG-10	Thermo Fisher Scientific GmbH
Dithiothreitol (DTT)	Serva Electrophoresis GmbH
EDTA	G-Biosciences
Eosin Y	Sigma Aldrich
Eukitt mounting medium	Sigma Aldrich
Ethanol	AppliChem GmbH
Foetal Bovine Serum (FBS)	Sigma Aldrich
Ficoll paque	Thermo Fisher Scientific GmbH
Formaldehyde (16%), methanol-free	Thermo Fisher Scientific GmbH
Formalin 10%, neutral buffered	Sigma Aldrich
Fugene HD transfection reagent	Promega
Glycerol	Carl Roth GmbH
Glycine	Sigma Aldrich
GoTaq Green DNA Polymerase	Promega
Hematoxylin Gill no.3	Sigma Aldrich
HEPES buffer	Carl Roth GmbH
Igepal (NP-40)	Sigma Aldrich
Isopropyl alcohol	Merck Millipore

Lipopolysaccharide (LPS)	OMNILAB
Macrophage-SFM medium	Thermo Fisher Scientific GmbH
Magnesium chloride	Carl Roth GmbH
M-CSF	PeproTech
Methanol	Sigma Aldrich
Milk powder	Carl Roth GmbH
Mounting medium	Dako
Opti-MEM reduced serum medium	Thermo Fisher Scientific GmbH
Paraformaldehyde (PFA)	Sigma Aldrich
Penicillin/Streptomycin	Sigma Aldrich
Phorbol 12-myristate 13-acetate (TPA/PMA)	Sigma Aldrich
Phosphate-buffered saline (PBS)	Thermo Fisher Scientific GmbH
Phosphatase inhibitor	Thermo Fisher Scientific GmbH
Power SYBR Green Master mix	Thermo Fisher Scientific GmbH
Protein G-coupled Dynabeads	Thermo Fisher Scientific GmbH
Proteinase K	Sigma Aldrich
Rnase A (Dnase-free)	AppliChem GmbH
Sepharose A/G beads for ChIP-qPCR	Biomol GmbH
Sepharose beads CL4B for ChIP-MS	GE healthcare
Sodium dodecyl sulfate (20%)	Sigma Aldrich
Sodium pyruvate	Sigma Aldrich
Triton-X	AppliChem GmbH
Trypsin (0,25%) EDTA	Sigma Aldrich
Tween-20	AppliChem GmbH
Xylene	AppliChem GmbH

Table 2. List of commercial kits and reagents.

Product	**Provider**	**Product**
BCA reagent	Thermo Fisher Scientific	23228
Bradford reagent	Biorad	500-0205
DNA plasmid plus maxi	Qiagen	12963
Dual-Glo, Luciferase assay	Promega	E2940

HaeIII restriction enzyme	NEB	R0108
High sensitivity DNA kit	Agilent Technologies	5067-4626
KAPA HyperPrep kit (96rnxs)	Roche	7962363001
Library Quantification (Illumina/ROX)	Roche	7960336001
MinElute PCR purification kit	Qiagen	28006
QIAquick gel extraction kit	Qiagen	28706
QuantiTect reverse transcription kit	Qiagen	205314
Qubit dsDNA HS kit	Thermo Fisher Scientific	Q32854
RNA 6000 Nano reagents	Agilent Technologies	5067-1511
RNAiMAX Lipofectamine	Thermo Fisher Scientific	13778075
RNeasy micro kit (low input)	Qiagen	74004
RNeasy mini kit	Qiagen	74106

Table 3. List of primary and secondary antibodies.

Antibody*	**Technique****	**Provider**	**Product number**
actin (M)	WB	Santa Cruz	sc-56459
GR (R)	ChIP, MS, IP	Proteintech	24050-1-AP
GR (M)	WB	Santa Cruz	sc-393232
GR (R)	IF	Cell Signaling	12041
GR-P, human Ser203 (R)	WB	Abbexa	abx011845
GR-P, human Ser211 (R)	WB	Cell Signaling	4161S
GR-P, human Ser226 (R)	WB	Cell Signaling	97285
GRIP-1 (R)	ChIP	Abcam	Ab10491
GRIP-1 (R)	WB	Cell Signaling	96687
IgG (M), HRP-conjugated	WB	Jackson	115-035-206
p65 (R)	ChIP	Abcam	ab7970
p65 (R)	WB	Cell Signaling	6956
IgG (R)	ChIP, MS, IP	Cell Signaling	2729
IgG (R), Cy5-conjugated	IF	Dianova	711-175-152
IgG (R), HRP-conjugated	WB	Santa Cruz	sc-2317
AKT (R)	WB	Cell Signaling	4691
AKT-P, Ser473 (R)	WB	Cell Signaling	4060
ERK1 and ERK2 (R)	WB	Cell Signaling	9102

ERK1/2-P, Thr202/Tyr204 (R)	WB	Cell Signaling	4376
Gsk3b (R)	WB	Cell Signaling	9316
Gsk3b-P, Ser9 (R)	WB	Cell Signaling	9336

* Host species antibody: R = rabbit and M = mouse. ** Chromatin immunoprecipitation (ChIP), immunocytofluorescence (IF), immunoprecipitation (IP), mass spectrometry (MS), western blot (WB).

Table 4. List of ChIP-qPCR primers.

Locus	Forward (5'-3')	Reverse (3'-5')
FoxL2	GCTGGCAGAATAGCATCCG	TGATGAAGCACTCGTTGAGGC
MEFs		
Ccl2	GGAGAAAACGGGAAACCCCA	ATTGTGCAATCTGCTGTCGC
Fkbp5	CTCAGCAGCTGGGTAAGTGG	TGCAGGAGCGGTTGATCTG
Gilz	CCCGGGACTAGGGTACAGAA	GCCACAAGGGTGTGGTTTGA
Il6	GGAGCCCACCAAGAACGATAG	CAGAGAGGAACTTCATAGCGGT
Klf9	CACAGCCCTTCTGACTCACC	CCGAGTATGGTTCTGCCTCG
Per1	GTAGGTCCCGCAAAGAGAACC	GACAGCGGTCCTGTACAAAAG
Macrophages		
Ccl2	GATCTGGCTGGAGAAAACGG	TCTGCTGTCGCAACACTCGT
Dusp1	ACAGACAGAATGGTGGTTTTTACTCC	CCCCTTGCTTTCAAATGTTACAC
Il1β	GGGAAGAGGCTATTGCTACCC	ATGCCCATTTCCACCACGAT
Mmp13	TGCACCAAACACATCAAACTTTCTG	CTTAGTAACTAGGGCAAACCCCC
Nos2	TGCCAAGAGATGCAGTTGAGG	GCTTGGGTTCGAGGCCTAC
Per1	TGGAACATCCTGTTCTCAGCG	AAGGAAGGCTGTGGCCAAC
Liver		
Acox2	GACGGCACATTGAGTTCC	ATGACTACGCAAGGCACAC
Adh5	ACTAGGTTTGGTTCCGTGGT	TCGCGCATCTAAAGCAATGA
Fah	CCAGTTCTCTCAACGTGCCT	AGCCTTAACCTGAGCCAACC
Gbe1	TACTTCCGAGCAGCGTTTGT	AGGTCGCTCTTCGATGTTGG
Hilpda	GACTCCCCGAGAACTCTGC	AGCCCCAAAGACAAACGGAC

Table 5. List of RT-qPCR primers.

Gene	Forward (5'-3')	Reverse (3'-5')
Arid1a	TGGGACTAACCCATACTCGCA	GAATCTGCTGTGCATAAGAGAGG
Arid1b	CTCCCCTGCGAGTATTCCAG	TGCCTGTCATAAAACCTCTTTCC
Arid5b	GTGATGAGTTCGCGCCAAATC	GCTGATAACTTTACCGTCACAGT
Ccl2	TTAAAAACCTGGATCGGAACCAA	GCATTAGCTTCAGATTTACGGGT
CD14	AGATTGGTCCAGCGCTTTCA	GAACTGCCCCAGATCTGCTT
CD86	GCAGCACGGACTTGAACAAC	TTGTAAATGGGCACGGCAGA
CSF-1	CAATGCTAACGCCACCGAGA	GTTGCAATCAGGCTTGGTCA

Cyp11a1	AACCTTTCCTGAGCCCTACG	TAGCCAACCATTGTCGCCAG
Cyp11b1	GCAGCCCTTTGAAGCCATAC	CGGCAACGTCACAAACACAA
Cyp11b2	TGGCATTGTGGCGGAACTAA	AGCCAGCTCAAAAAGGGTCA
Cyp17a1	TGGAGGCCACTATCCGAGAA	CACATGTGTGTCCTTCGGGA
Dusp1	GTTGTTGGATTGTCGCTCCTT	TTGGGCACGATATGCTCCAG
Gilz	ACCACCTGATGTACGCTGTG	TCTGCTCCTTTAGGACCTCCA
Il1β	TGCCACCTTTTGACAGTGATG	ATGTGCTGCTGCGAGATTTG
Il6	TAGTCCTTCCTACCCCAATTTCC	TTGGTCCTTAGCCACTCCTTC
Lcn2	GGCCAGTTCACTCTGGGAAA	TGGCGAACTGGTTGTAGTCC
Lpin1	GCCGACTGTCTCACTTTAG	CCTTGAGCTATGAGGAATGG
Mmp13	ACCTCCACAGTTGACAGGCT	AGGCACTCCACATCTTGGTTT
Mmp9	CCAGCCGACTTTTGTGGTCT	CTTCTCTCCCATCATCTGGGC
Nos2	GTTCTCAGCCCAACAATACAAGA	GTGGACGGGTCGATGTCAC
Nr3c1	AGCTCCCCCTGGTAGAGAC	GGTGAAGACGCAGAAACCTTG
Per1	ACCAGGTCATTAAGTGTGTGC	CTCTCCCGGTCTTGCTTCA
Ppib	GGAGCGCAATATGAAGGTGC	TTATCGTTGGCCACGGAGG
Rpl38	AGCAGGTACCTTTACACCCTG	AGATCCTTCACTGCCAAACCC
Smarca4	GCTCTGAACATGCCTCCAGT	CTGTTTTGCTGTCCCAAGGC
Smarcd1	CCTGCTGATGCTGGACTACC	GATCACTGGACGTGTCTGGG
Smarcd2	CCAGCGCCGAGGGTTAAAG	CTTCCTCTCGAAAGCTAAAAGA
Smarcd3	GAAAGCTGCGCCTTTATATCTCC	GCTTACTAGGATCATCCAAGAGC
Smarce1	CAAGCGACAGGTCCAGTCTT	AAGGAGTCCGTGCTTTCCAG
TNFα	CCCTCACACTCAGATCATCTTCT	GCTACGACGTGGGCTACAG
U36b4	AGCGGTTTTGCTTTTTCATC	TATGGGATTCGGTCTCTTCG

Table 6. List of small interfering RNA oligonucleotides.

Product	**Provider**	**Product number**
Arid1a – SMARTpool	Dharmacon	M-040694-01
Arid1b – SMARTpool	Dharmacon	M-053908-01
Arid5b – SMARTpool	Dharmacon	M-054678-01
Nr3c1 – SMARTpool	Dharmacon	M-045970-01
scramble – non-targeting pool	Dharmacon	D-001206-14
Smarca4 – SMARTpool	Dharmacon	M-041135-01
Smarcd1 – SMARTpool	Dharmacon	M-046893-01
Smarcd2 – SMARTpool	Dharmacon	M-048262-01
Smarcd3 – SMARTpool	Dharmacon	M-063444-01
Smarce1 – SMARTpool	Dharmacon	M-051327-00

3.2 Mice

The $GR^{\Delta Zn}$ line was generated by Cyagen US Inc. via homologous recombination in mouse ES cells. The C437G (TGC to GGC) mutation was introduced into exon 3 of *Nr3c1* via the 5' homology arm, with a LoxP flanked Neomycin cassette in the next intron. After breeding to ROSA26 Cre deleters for Neo removal, $GR^{\Delta Zn}$ mice were kept on a C57BL/6 background. Mice were housed in a controlled SPF facility with a 12 h light/dark cycle at 23 °C with constant humidity and fed *ad libitum*.

Genotyping primers of $GR^{\Delta Zn}$ mutation: 5'-AATCATGCCAAGCATAACCC-3' and 3'-AATGTCTATCATTAGTGGAC-5'. For the removal of neomycin cassette: 5'-CTATTCGGCTATGACTGGGC-3' and 3'-CACCATGATATTCGGCAAGC-5'. For presence of Rosa26Cre recombinase: 5'-ATGCCCAAGAAGAAGAGGAAGGT-3' and 5'-GAAATCAGTGCGTTCGAACGCTAGA-3'. Primers for exon 3 removal of GR^{KO} embryos: 5'-GGCATGCACATTACTGGCCTTCT-3', 5'-GTGTAGCAGCCA GCTTACAGGA-3' and 5'-CCTTCTCATTCCATGTCAGCATGT-3'. The presence of *sex determining region Y* (*Sry*) was used for embryonic gender determination. Primers for genomic *Sry* amplification: 5'-GAGAGCATGGAGGGCCAT-3' and 5'-CCACTCCTCTGTGACACT-3'.

PCR program for genotyping of $GR^{\Delta Zn}$ mutation:

95 °C	15 min	
95 °C	1 min	35x
60 °C	1 min	
72 °C	1 min	
72 °C	10 min	
10 °C	hold	

PCR product after overnight digestion with HaeIII, BSA and CutSmart at 37 °C generates the following bands; 359 bp band for WT mice and 174 bp + 185 bp for mutant mice.

PCR program for genotyping of Neomycin cassette removal, RosaCre presence, GR-null exon 3 removal and *Sry* presence in male embryos:

95 °C 5 min
95 °C 1 min ┐
56 °C 1 min ├ 35x
72 °C 1 min ┘
72 °C 10 min
10 °C hold

PCR products when Neomycin cassette is removed: WT: 341 bp, mutant: 454 bp. Presence of RosaCre generates no band for WT and a 450 bp product for Cre positive samples. Exon 3 removal in GR-null: WT: 162 bp and flox exon: 250 bp. Gender determination: males 100 bp product and no PCR product in females.

GR-null mice were generated by crossing GR-flox mice (a generous gift from J. Tuckermann, Ulm) with ROSA26 Cre deleters. Formal approval for animal experiments was obtained from the district government of Upper Bavaria (55.2-1-54-2532-33-14 and 14 and ROB-55.2-2532.Vet_02-19-43) in accordance with HMGU guidelines for the care and use of animals.

3.3 Primary cell cultures

3.3.1 Foetal liver macrophages

Livers from E13.5 embryos were washed twice with cold PBS and then homogenized. Red blood cells were lysed with AKC lysis buffer (155 mM NH_4Cl, 10 mM $KHCO_3$ and 0.1 mM EDTA) and remaining cells were kept in macrophage differentiation medium (30% L929 conditioned medium, 20% FBS, 1% Pen/Strep and high glucose DMEM supplemented with M-CSF). Macrophages were differentiated during 7 days on non-coated plates and cellular identity was validated by qRT-PCR.

3.3.2 Mouse embryonic fibroblasts

MEFs were generated from E13.5 embryos after 12 min trypsinization (0.25% Trypsin-EDTA) at 37 °C and homogenization following standard protocols. Non-immortalized cells up to passage 4 were cultured in high glucose DMEM with 10% FBS, 1% Pen/Strep at 37 °C and 5% CO_2. Dialyzed FBS was used for ligand-free samples.

3.4 Immortalised cell lines

CV-1 fibroblast cell line was used for luciferase measurements and were cultured in high glucose DMEM with 10% FBS and 1% Pen/Strep at 37 °C with 5% CO_2. Dialyzed FBS was used for ligand-free samples.

3.5 Molecular biology techniques

3.5.1 Chromatin Immunoprecipitation coupled to quantitative PCR

For MEFs and foetal liver macrophages, ChIP was performed on disuccinimidyl glutarate (DGS) and 1% methanol-free formaldehyde crosslinked chromatin as previously described (Uhlenhaut et al. 2013). In short, nuclei fraction was enriched by incubation with Fast IP buffer (150 mM $NaCl_2$, 5 mM EDTA pH 7.5, 5 mM Tris pH 7.5, 1% Triton X-100, 0.5% NP40 and protease inhibitors) and passed twice through a 24 G syringe. Chromatin was sheared on a Bioruptor from Diagenode with 30s on/30s off and high settings in shearing buffer (50 mM Tris pH 8, 10 mM EDTA pH 8, 1% SDS and protease inhibitors) into a range of 200 bp to 1 kb. Immunoprecipitation was performed with 3 µg of antibody per 2 million cells, rotating overnight at 4 °C in low DNA binding tubes. Sepharose beads were blocked with 0.5% BSA overnight at 4 °C. Next day, IPs were cleared by centrifugation and incubated with blocked beads for 2-3 h. Then, IPs were washed 5 times with IP buffer and once with TE buffer. DNA was eluted by two times 15 min incubation at room temperature at 1000 rpm with ChIP elution buffer (105 mM $NaHCO_3$, 1% SDS in H_2O). DNA was then precipitated overnight at 65 °C with 200 mM $NaCl_2$. After RNA and protein removal, samples were purified with PCR purification kit. Embryonic livers were lysed in 10 mM HEPES, 10 mM KCl, 5 mM $MgCl_2$, 0.5 mM DTT with proteinase/phosphatase inhibitors using a tissue lyser with steel beads. Hepatocytes were passed through a 70 µm cell strainer and crosslinked in 1% formaldehyde for 15 min. ChIP DNA was quantified using the Power SYBR Green Master Mix in a ViiA 7 or QuantStudio Real-Time PCR System. Primers are listed in **Table 5**. Three technical replicates for each sample were run on 384-well plates.

3.5.2 Co-Immunoprecipitation

MEFs were treated with 1 µM Dex overnight and 100 ng/µl LPS for 3 h. Protein concentration of nuclear protein extracts was determined with BCA. Per IP, 500 µg of

nuclear protein lysate were pre-cleared using α-rabbit Dynabeads for 1 h in IP buffer (20 mM Tris pH 8, 100 mM KCl, 5 mM $MgCl_2$, 0.2 mM EDTA, 20% glycerol and protease inhibitors). After pre-clearing, IPs were incubated with the antibodies for 2 h and then BSA-blocked rabbit Dynabeads were added for overnight immunoprecipitation at 4 °C. The following day, beads were washed three times with IP buffer and eluted in Lämmli buffer with DTT at 37 °C with vigorous shaking. Western Blotting was performed according to standard protocols.

3.5.3 Electrophoretic mobility shift assay

Electrophoretic mobility shift assay (EMSA), also named gel shift assays, were performed similarly to (Schauwaers et al. 2007). In short, full-length mouse GR wild type or ∆Zn was overexpressed in CV-1 cells. 24 h after transfection, cells were washed twice with ice-cold PBS and resuspended in 200 µl lysis buffer (20 mM HEPES KOH pH 7.8, 450 mM $NaCl_2$, 0.4 mM EDTA, 25% glycerol, 0.5 mM DTT and protease & phosphatase inhibitors). Cells were lysed by three freeze-thaw cycles in liquid N_2, then centrifuged at 9000 xg and the supernatant was stored at -80 °C. About 20 µg of CV-1 protein lysate were used per reaction. The following 5'-biotinylated oligos from Sigma were used: *Per1*-F 5'-AGAGAACACGATGTTCCCTA-3' and *Per1*-R 5'-TAGGGAACATCGTGTTCTCT-3'. As background, the following palindromic oligo was used: 5'-GATCGATCGATCGATCGATC-3'.

Binding reactions were performed in 20 mM HEPES KOH pH 7.9, 60 mM KCl, 5 mM $MgCl_2$, 2 mM DTT, 10% glycerol, 0.1 µg/µl Poly(dI/dC), 0.1 mg/µl BSA, 0.1 µM Dexamethasone and 1 mM $ZnCl_2$ during 20 min at room temperature. Protein:DNA complexes were run on a 6% acrylamide TBE gel from Thermo and detected using the Chemiluminescent Nucleic Acid Detection Module Kit from Thermo according to manufacturer's instructions.

3.5.4 Immunohistochemistry

MEFs were seeded onto glass cover slips and treated with vehicle, 1 µM Dex overnight and/or 100 ng/µl LPS for 3 h. Briefly, cells were fixed in 4% PFA 10 min at room temperature, permeabilized with 0.1% TritonX-100 in PBS 30 min at 4 °C and blocked with 0.1% TritonX- 100 and 1% FBS shaking 1 hour at room temperature. Primary GR antibody was diluted 1:200 in blocking buffer and incubated overnight at 4 °C with

gentle shaking. DAPI staining was performed following standard procedure. Cover slips were mounted with fluorescence mounting medium from Dako and sealed with colorless nail polish. Confocal images were taken on a Leica SP5 microscope.

3.5.5 Luciferase assays

Luciferase assays were performed in CV-1 cells treated overnight with either vehicle, 1 µM Dex or 100 ng/µl LPS, as previously described (Lim et al. 2015, Uhlenhaut et al. 2013). Relative luciferase activity was normalised to vehicle and empty vector. *Cis*-regulatory elements were cloned into pGL4.23, transfection efficiency was determined with pRL-TK renilla, and luminescence was measured using the Dual Stop & Glo kit according to manufacturer's instructions. *MMTV*, *Il6* and *Btg1* reporters are published (Uhlenhaut et al. 2013), the *Lpin1* reporter was cloned into pGL4.23 using the following primers: 5'-CGAAGCTTGATATAGGTGCCCCATTTAG-3' F and 5'-CGCTCGAGATAGAAATCACACAGAGGTC-3' R.
The human GR DBD mutants (wild type GR, C421G, F444G, F445G, I465G and C473G) were kindly provided by the Evans lab.

3.5.6 RNA isolation, complementary DNA synthesis and real-time-quantitative PCR

Total RNA was extracted with RNeasy Mini kits following manufacturer's instructions with the exception of RNA extraction from adrenal glands, where the RNeasy micro kit was used. cDNA was prepared with the QuantiTect Reverse Transcription Kit starting with 1 µg of RNA. The qPCR reaction was: 5 µl Power SYBR Green Master Mix, 0.4 µl H_2O, 0.1 µl primer mix (1µM) and 4.5 µl of cDNA. Reaction was analysed in a ViiA 7 or QuantStudio System. Gene expression values were normalised to *U36b4,* or *Rpl38* for the adrenal glands. RT-qPCR primers are listed in **Table 6**.

3.5.7 Small interfering RNA knock down

Cells were seeded in DEMEM with 10% dialyzed FBS without antibiotics to approx. 60% confluency and transfected with 10 nM siRNA oligonucleotides using Lipofectamine RNAiMAX according to the manufacturer's instructions. Next day, medium was changed to fresh DMEM with dFBS and Pen/Strep. Cells were treated 48

h after transfection with vehicle, 100 ng/µl LPS for 3 h or 1 µM Dex overnight and 100 ng/µl LPS for 3 h. Cells were collected 72 h after transfection with siRNA.

3.5.8 Western blot

Cells were lysed with RIPA buffer (50 mM Tris HCl pH 8, 150 mM $NaCl_2$, 1% NP40, 0.1% SDS and 0.5% sodium deoxycholate) supplemented with protease inhibitors. Western blotting on sonicated, snap-frozen lysates was performed according to standard protocols. Briefly, protein concentration was determined by BCA assay. Samples were prepared in Lämmli buffer with DTT and boiled for 5 min at 95 °C. Proteins were separated in precast 4-12% Bis-Tris gels from Thermo. Running buffer, ice cold transfer buffer from Thermo with 20% methanol. PVDF membranes were blocked in 5% milk in TBS-T (50 mM Tris-Cl, 150 mM $NaCl_2$ pH 7.6, 1% Tween20) and incubated overnight at 4 °C with primary antibodies in 5% milk TBS-T. Chemiluminescence was visualised in X-ray films.

3.6 Histology

Haematoxylin and Eosin (H&E) stainings of E18.5 lungs were performed on thorax sections following standard protocols. In short, the embryos were harvested, and the thoraxes were fixed in formalin at 4 °C. Then, the following methanol/PBS incubations during 8 h at 4 °C were performed: 25%, 50%, 75% and 100%. Then tissues were incubated in 50% methanol/50% isopropanol and then 100% isopropanol. After, samples were embedded in paraffin by incubation with increasing percentage of paraffin. Then 10 µM sections were cut and stained with H&E. Images were taken on a Keyence BZ-9000 microscope at a magnification of 40x and 20x.

3.7 Chromatin immunoprecipitation coupled to mass spectrometry

ChIP-MS was performed in wild type and homozygous $GR^{\Delta Zn}$ MEFs treated with 1 µM Dex overnight plus 100 ng/µl LPS for 3 h. ChIP-MS was carried out as described previously with minor modifications (Hemmer et al., 2019). Shortly, cells were lysed in IP-buffer (50 mM Tris-HCl pH 8, 100 mM $NaCl_2$, 5 mM EDTA, 0.3% SDS, 1.7% Triton X-100) and chromatin was sonicated to an average size of 200 bp. After overnight immunoprecipitation with rabbit α-GR or rabbit IgG, antibody-bait complexes were captured by protein A coupled sepharose beads, washed, eluted and analysed by

mass spectrometry. Peptide separation, chromatography and mass acquisition was performed as described with the following changes: we used an EASY-nLC 1200 ultra-high-pressure system, a gradient over 100 min, 10 data-dependent MS/MS scans (15 K resolution, 60 ms max. 20 injection time, AGC targets 1e5), an isolation window of 1.4, normalised collision energy of 27 and 30s exclusion for multiple sequencing of peptides.

Raw mass spectrometry data were analysed with MaxQuant (v1.5.3.54) and Perseus (v.1.6.0.2078) as previously reported (Hemmer et al. 2019). Protein entries referring to contaminants, identified via matches to the reverse database, or identified only via modified sites were removed, LFQ values were log2 transformed. Significant outliers were defined by permutation-controlled Student's t-test (FDR < 0.01, s0 = 1) comparing triplicate ChIP-MS samples for each antibody, requiring at least two valid values in the GR replicates. The mass spectrometry proteomics data have been deposited at the PRIDE ProteomeXchange Consortium repository (Perez-Riverol et al. 2019) with the dataset identifier PXD013772.

3.8 Next generation sequencing techniques

3.8.1 Chromatin immunoprecipitation-sequencing and data analysis

ChIP-Seq was performed on 15 million MEFs per biological replicate, treated with 1 μM Dex overnight plus 100 ng/μl LPS for 3 h as previously described with the addition of 1 h chromatin pre-clearing with α-rabbit Dynabeads before overnight IP (Uhlenhaut et al. 2013). Enrichment was quantified using the Power SYBR Green Master Mix in a ViiA 7 or QuantStudio Real-Time PCR System. ChIP DNA concentration was measured by QUBIT dsDNA HS kit from Thermo.

Libraries were prepared using the KAPA Hyperprep Kit from Kapa Biosystems. Illumina compatible adapters were used at 68 nM. DNA size selection (360-610 bp) of adapted-ligated libraries was done in 2% dye-free gels form Sage Science in a Pippin gel station. Library concentration was calculated with the KAPA Library Quantification Kit and quality was verified using the Agilent High Sensitivity DNA kit in a 2100 Bioanalyzer. Libraries were sequenced on an Illumina HiSeq4000 following standard protocols.

Reads from 2-4 replicates were merged and aligned to the mouse mm10 reference genome using BWA-MEM version 0.7.136 and duplicates were removed using Picard Tools version 2.8.3 (http://picard.sourceforge.net/). Reads were filtered for uniquely mapped read pairs with samtools7 (Li et al. 2009) and down-sampled to 12 mio read pairs for Dex+LPS. Genome browser tracks were visualized with UCSC (Kent et al. 2002) or IGB (Freese, Norris and Loraine 2016) after merging all replicates of one sample and down-sampling to 64 mio reads pairs or as individual replicates after down-sampling as mentioned above. Peaks were called using MACS2 version 2.1.1.201603099 with an FDR threshold of 0.05 in paired-end mode. The union of peaks called in all replicates per genotype and treatment was used to compare GR peaks (GR universe) and the peak overlap (min. overlap 1bp) determined after resizing peaks to 294 bp around the peak center. Genomic regions called in GR knockout MEFs, as well as blacklisted regions:
http://mitra.stanford.edu/kundaje/akundaje/release/blacklists/mm10mouse/mm10.blacklist.bed.gz were removed from the GR universe for all further analyses. Gene ontology and distance to TSS analyses were performed with GREAT version 3.0.0 (McLean et al. 2010). Motif enrichment and read distribution analysis around GR peaks were conducted with HOMER (Heinz et al. 2010). Known HOMER motifs enriched within complete peaks are displayed as position-weight matrices. Heatmaps were generated with HOMER's 'annotatePeak' function (version 4.98) and visualized with R, after log-transformation using the 'heatmap.2' function. NGS data and annotated peak files can be accessed via the NCBI's Gene Expression Omnibus Super Series accession number GSE126655.

3.8.2 RNA-sequencing and data analysis

MEFs were treated with 1 µM Dex overnight and/or 100 ng/µl LPS for 6 h. Total RNA was isolated using the RNeasy kit and quality-controlled on a 2100 Bioanalyzer. Library preparation and rRNA depletion were performed using the Illumina TruSeq mRNA Library Prep Kit v2 chemistry in an automated system from 1 µg total RNA. Libraries were sequenced on the Illumina HiSeq4000. Sequencing quality was assessed with FastQC (http://www.bioinformatics.babraham.ac.uk/projects/fastqc/). Reads were mapped to the mouse genome mm10 (Ensembl build 38.91) and reads per gene were counted using STAR version 2.4.2a2 (Dobin et al. 2013). Gene count normalization

and differential expression analysis was performed using DESeq2 (Love, Huber and Anders 2014). Genes were defined as expressed when their mean count across samples passed 200, and differentially expressed when the fold-change between treatment and reference group was greater than 1.5 at an FDR < 0.05. For gene annotation, biomaRt (Durinck et al. 2009) was used. Functional enrichment according to gene ontology was carried out using GOrilla (Eden et al. 2009). Heatmaps and volcano plots were generated in R (www.R-project.org). The heatmap was generated in R using DESeq2-normalised read counts. NGS data can be accessed via the NCBI's Gene Expression Omnibus Super Series accession number GSE126655.

3.9 Statistical analysis

For differences between 2 groups, unpaired 2-tailed Student's t-test was performed. Results are given as mean ± SEM unless otherwise specified. A p-value < 0.05 was considered significant. No statistical methods were used to predetermine sample size. The experiments were not randomized, and investigators were not blinded to allocation during experiments and analyses.

3.10 Contribution from collaborations

ChIP-MS was performed in collaboration with Dr. M. Wierer at the Max Planck Institute in Munich. All NGS analysis were performed by Dr. F. Greulich. RNA- and ChIP-Seq samples were sequenced at the Genomic Facility at Helmholtz Zentrum München by Dr. E. Graf, Dr. T. Schwarzmayr and Dr. T.M. Strom. The $GR^{\Delta Zn}$ line was designed by Prof. N.H. Uhlenhaut and Dr. F. Quagliarini. The Co-IP protocol was established together with Dr. O. García González.

4. Results

4.1 DNA binding by GR is required for survival

4.1.1 GR$^{\Delta Zn}$ mouse line generation

To investigate DNA binding dependent versus independent modes of transcriptional regulation by GR, a mouse model carrying a point mutation within the first zinc finger of the DBD of GR, named GR$^{\Delta Zn}$, was generated (**Figure 7A**). The C437G mutation was introduced into exon 3 of *Nr3c1* gene via the 5' homology arm, with a LoxP flanked Neomycin cassette in the next intron. Mutant mice were bread to ROSA26 Cre deleters for removal of the neomycin cassette (**Figure 7B**).

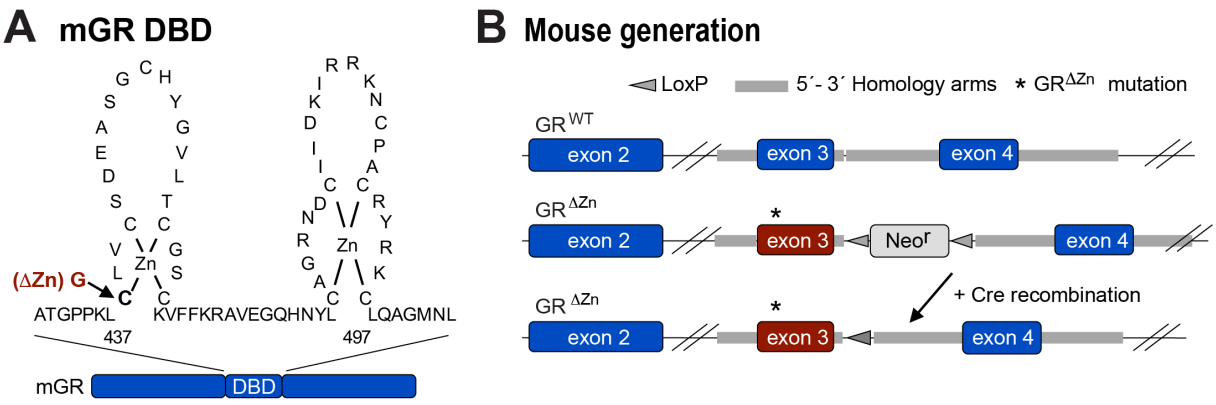

Figure 7. GR$^{\Delta Zn}$ mutation and mouse line generation.
A, GR$^{\Delta Zn}$ was generated by exchanging cysteine 437 in the first zinc finger of the DNA-binding domain (DBD) with glycine. **B**, GR$^{\Delta Zn}$ mice were generated by injection of the genomic region corresponding to exon 3 and 4 of the *Nr3c1* gene carrying the G437G mutation and followed by homology recombination of the fragment in murine embryonic stem (ES) cells and selection for neomycin resistance.

The C437G mutation where one nucleotide in the codon **T**GC (translated to a Cysteine) is mutated to **G**GC (translated to a Glycine) was verified by sequencing as shown in **Figure 8A**. This mutation generated a new HaeIII restriction site which was used for genotyping. Mouse genotyping was done by PCR amplification of exon 3 followed by HaeIII digestion as shown in **Figure 8B**.

Hollenberg and Evans showed that replacing a single amino acid, mouse cysteine 437 corresponding to human C421, with glycine abolishes direct GRE binding but leaves all other domains intact (Hollenberg and Evans 1988). Loss of GRE recognition by mouse $GR^{\Delta Zn}$ was validated *in vitro* by the traditional electrophoretic mobility shift assay (EMSA) to assess DNA-protein interactions. Protein lysates from overexpressed $GR^{\Delta Zn}$ in CV-1 cells did not bind a GRE-harbouring *Per1* DNA fragment (**Figure 8C**).

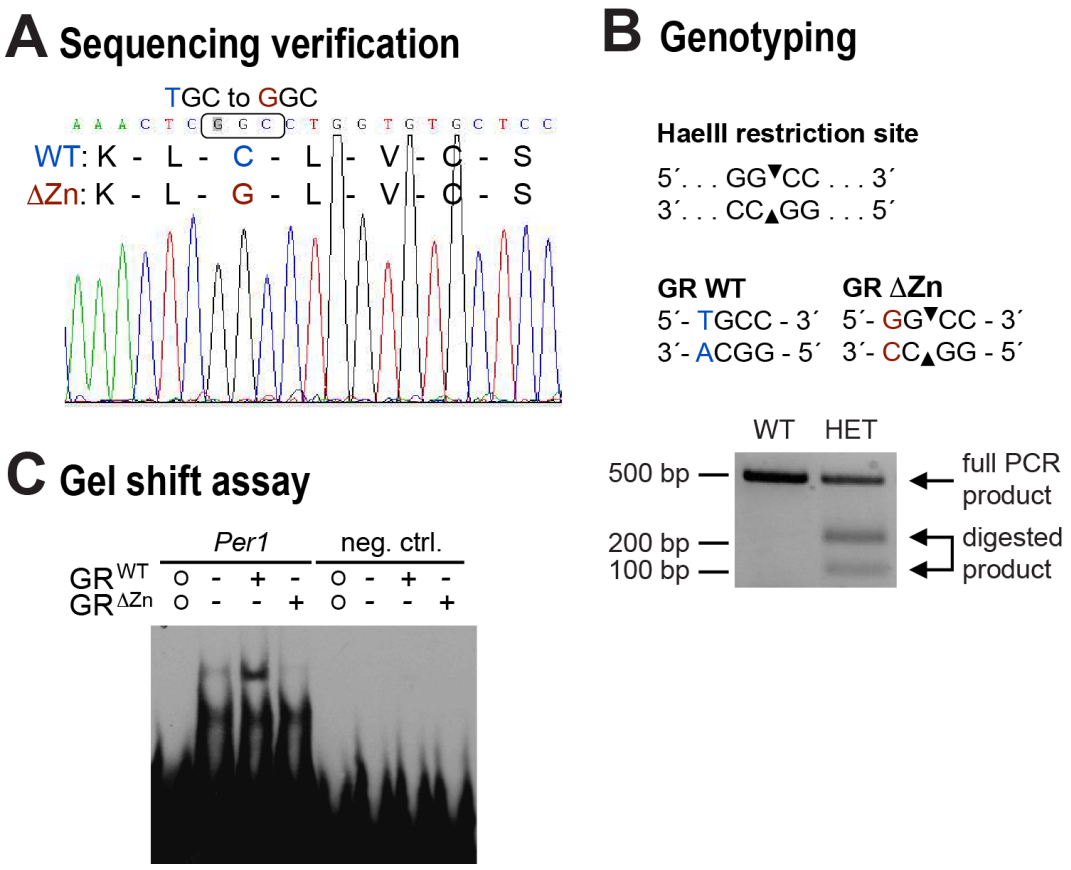

Figure 8. Genotyping of $GR^{\Delta Zn}$ mice and *in vitro* validation of the loss of DNA binding.
A, Verification of GR C437G mutation by sequencing. **B**, The zinc finger mutation generates a new HaeIII restriction site, which is used for genotyping of $GR^{\Delta Zn}$ mice. Bottom, PCR amplification of *Nr3c1* exon 3 generates an approx. 500 bp product. In the presence of the mutation, HaeIII cuts the fragment and generates two smaller fragments. **C**, EMSA with wild type or $GR^{\Delta Zn}$ protein and labelled oligos containing the *Per1* GRE sequence (neg. ctrl.: random DNA sequence negative control, o: oligo only, no protein).

In summary, $GR^{\Delta Zn}$ mice have a single DNA base pair mutated to exchange mouse cysteine 437 to glycine and the loss of GRE recognition was verified by *in vitro* gel shift assay. These results validate the $GR^{\Delta Zn}$ mice as suitable to study direct versus indirect DNA binding requirement by GR *in vivo*.

4.1.2 $GR^{\Delta Zn}$ mice die due to respiratory failure and resemble the GR null phenotype

Strikingly, the $GR^{\Delta Zn}$ mutant embryos died shortly after birth, similar to GR null mice (Cole et al. 1995). While heterozygous mutants were born with the expected Mendelian ratio, no viable homozygous $GR^{\Delta Zn}$ pups were obtained out of 119 pups born in 25 litters from more than 15 heterozygous matings (**Table 7**).

Table 7. Pups born from het. x het. matings.

Genotype	Pups	Observed	Expected
$GR^{WT/WT}$	43	36%	25%
$GR^{WT/\Delta Zn}$	76	64%	50%
$GR^{\Delta Zn/\Delta Zn}$	0	0%	25%
Total	119		

Phenocopying complete loss of GR function, $GR^{\Delta Zn}$ mice died of atelectasis and respiratory failure. To investigate the cause of impaired function of the lungs, histological analysis was performed on mice at E18.5. As shown in **Figure 9A**, lungs from $GR^{\Delta Zn}$ pups were collapsed and did not inflated as did wild type lungs. Also, $GR^{\Delta Zn}$ pups showed enlarged adrenal glands (hyperplasia) accompanied by increased expression of steroidogenic cytochrome P450 enzymes. The adrenal glands from $GR^{\Delta Zn}$ mice were enlarged and the expression of GC synthesis enzymes was up-regulated at the peak of endogenous GC levels (**Figure 9B**).

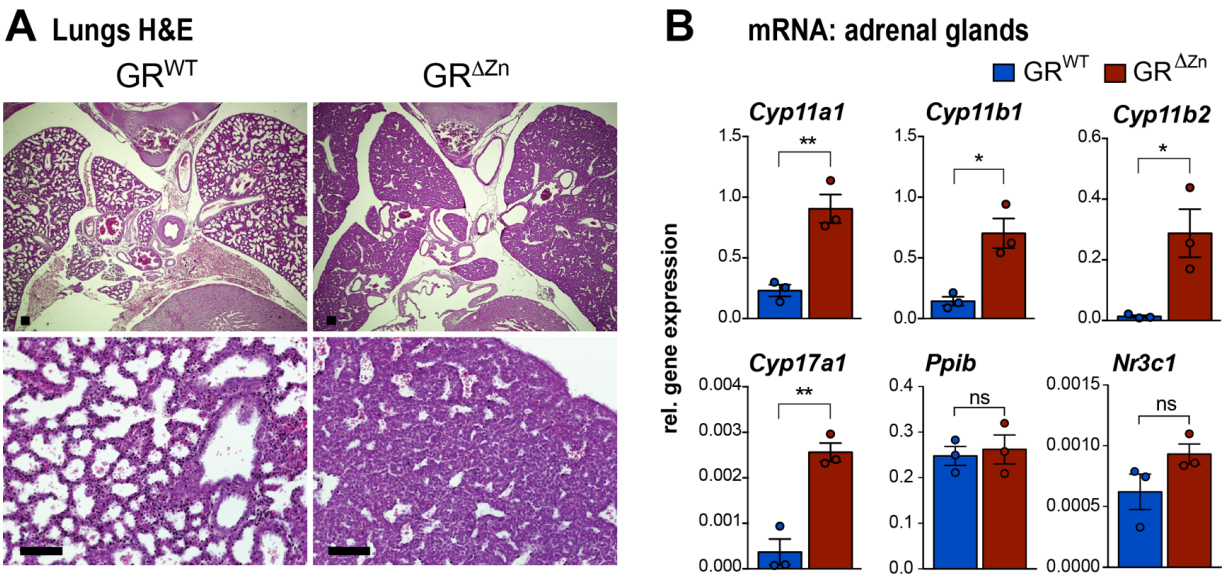

Figure 9. Homozygous $GR^{\Delta Zn}$ mice die perinatally due to respiratory failure and show upregulation of steroidogenic enzymes.
A, Lung H&E histology of wild type and homozygous $GR^{\Delta Zn}$ E18.5 embryos. Representative images from n = 3, scale bar = 100 µm. Top 4x and bottom 10x. **B**, Steroidogenic enzymes mRNA expression by qRT-PCR in the adrenal glands of E18.5 wild type and homozygous mutants. *Ppib* is a negative control gene. mRNA levels are relative to *Rpl38*. n = 3, values are mean ± SEM, * p<0.05, ** p<0.01. Student's t-test.

In conclusion, $GR^{\Delta Zn}$ mice die shortly after birth due to respiratory failure and show enlarged adrenal glands at E18.5 with increased expression of enzymes involved in the synthesis of steroid hormones. Mutating the first zinc finger of GR *in vivo* mirrored the phenotype of GR null animals, indicating that DNA binding by GR is required for viable lung development.

4.1.3 $GR^{\Delta Zn}$ mRNA, protein and phosphorylation levels are unaffected

Since mutation of the first zinc finger resulted in perinatal lethality, matings were set up to generate embryos from which MEFs and primary embryonic cells were isolated and tissues collected for further functional analyses. To rule out the possibility of $GR^{\Delta Zn}$ mRNA or protein being degraded due to instability caused by the mutation, GR mRNA and protein levels were analysed in MEFs. As shown in **Figure 10A**, $GR^{\Delta Zn}$ mRNA levels were maintained compared to wild type samples in untreated MEFs.

Importantly, no differences were observed at basal GR protein levels in untreated MEFs. Also, phosphorylation levels of GR S212 (human S203), S220 (human S211)

and S234 (human S226) were similar in wild type and $GR^{\Delta Zn}$ MEFs treated with LPS and Dex for 0-16 h. Levels of GR S212 did not change considerably after Dex addition and were similar between wild type and mutant samples. Instead, GR S220 and S234 phosphorylation marks increased upon treatment with Dex in both wild type and mutant samples. Interestingly, GR S212 is suggested to be a mark for cytoplasmic GR and not transcriptionally active GR (Wang, Frederick and Garabedian 2002). Similarly, GR S234 was proposed to increase the cytoplasmic export and degradation of GR therefore blunting the GC response (Chen et al. 2008). Conversely, GR S220 was shown to be a mark for transcriptionally active GR (Blind and Garabedian 2008) (**Figure 10B**).

Overall, a similar phosphorylation pattern between wild type and mutant GR suggests that the zinc finger mutation does not cause major alterations in the protein conformation.

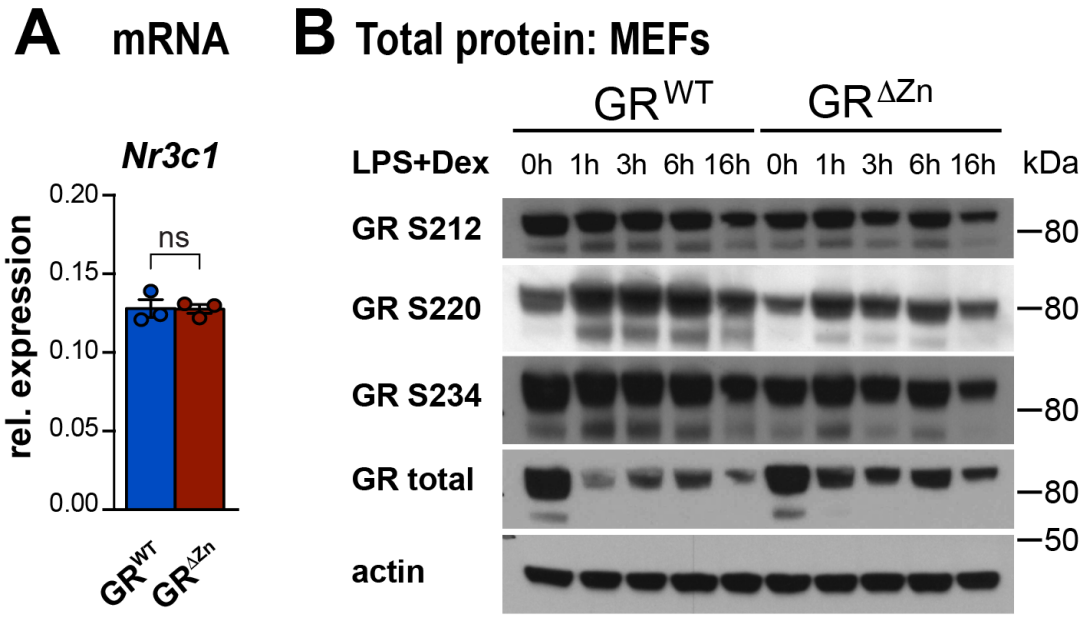

Figure 10. Total and phosphorylated GR protein levels in MEFs.
A, *Nr3c1* mRNA levels relative to *U36b4* in untreated MEFs. Values are mean ± SEM (n = 3), ns = not significant. Student's t-test. **B**, Western blot in MEFs detecting phosphorylated mouse GR S212, S220 and S234, total GR and actin as loading control. Cells were either untreated (0h) or treated with LPS and dexamethasone (Dex) for 0-16 h. Representative blot from n = 3.

4.1.4 GR nuclear translocation is unaffected in $GR^{\Delta Zn}$

Furthermore, the ability of $GR^{\Delta Zn}$ to translocate to the nucleus in the presence of the synthetic ligand dexamethasone was tested in MEFs. In the case of a misfolded $GR^{\Delta Zn}$, the nuclear translocation signals could potentially be inaccessible, causing impaired nuclear translocation. Therefore, MEFs were treated with Dex and/or LPS and GR cellular localisation was detected by immunofluorescent staining. The nuclear localisation of the receptor in response to the ligand was not impaired in MEFs expressing $GR^{\Delta Zn}$, as shown in **Figure 11**. Importantly, $GR^{\Delta Zn}$ was detected in the nucleus when cells were treated with LPS and Dex, indicating that the receptor conformation was not affected.

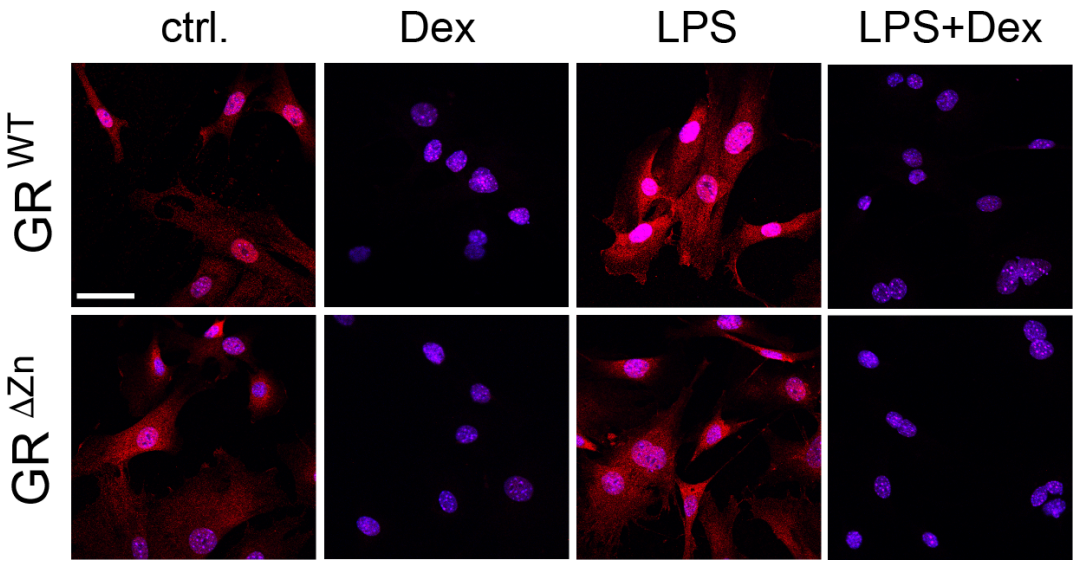

Figure 11. Nuclear localisation of $GR^{\Delta Zn}$ in Dex-treated MEFs.
Immunofluorescent detection of GR (red) nuclear localisation in MEFs treated with vehicle, 1 µM Dex for 16 h and/or LPS for 3 h. Nuclei stained with DAPI (blue). Representative images from n = 2, scale bar = 50 µm.

Taken together, GR mRNA, protein, phosphorylation levels and nuclear translocation were not affected by the zinc finger mutation. This shows that $GR^{\Delta Zn}$ is expressed and responds to ligands, suggesting that this mutation does not greatly affect the protein folding structure. Again, supporting the validity of this mouse model to study direct DNA binding and tethering functions of GR.

4.2 Non-genomic actions of GR

Phosphorylation marks of cytosolic proteins such as AKT, ERK and GSK3β have been shown to be involved in the rapid effects of GC. They could potentially be altered in $GR^{\Delta Zn}$ cells if the mutation severely affected protein folding. To test the effect of the mutation on potential non-genomic actions of GR, MEFs were briefly treated with Dex. Treatment with Dex for less than 20 min ensured that the observed effects were at the non-genomic level, since transcriptional output requires longer than 30 min. As shown in **Figure 12**, phosphorylated AKT did not change with 5, 10 or 20 min Dex in either wild type or mutant GR MEFs. In contrast, phosphorylated ERK1/2 decreased in wild type and mutant MEFs upon treatment with Dex. Surprisingly, phosphorylated GSK3β decreased in wild type and increased in mutant MEFs upon Dex addition.

These results suggest that most non-genomic actions of GR are unaffected by the zinc finger mutation, with the exception of GSK3β.

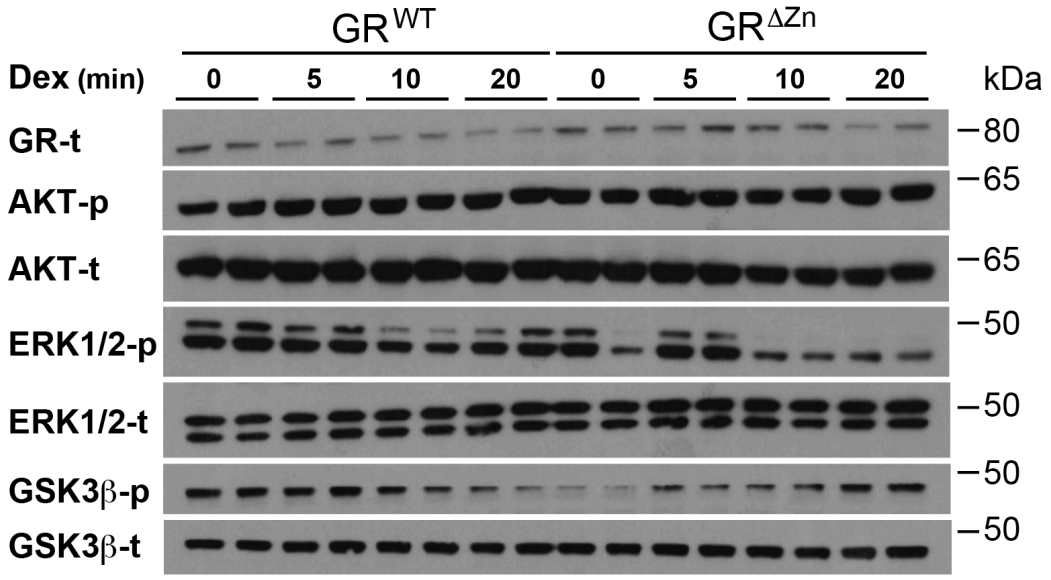

Figure 12. Non-genomic functions of GR are maintained by $GR^{\Delta Zn}$.
Western blot in short Dex-treated MEFs detecting total GR (GR-t), phospho-AKT S473 (AKT-p), total AKT (AKT-t), phospho-ERK1 T202 & Y204 and phospho-ERK2 T185 & Y187 (ERK1/2-p), total ERK1/2 (ER1/2-t), phospho-GSK3β S9 (p-GSKβ-p) and total GSK3β (GSKβ-t). Cells were untreated (0 min) or shortly treated with dexamethasone (Dex) for 5-20 min. Representative blot from n = 3.

4.3 Tethered binding sites are found near inflammatory genes in $GR^{\Delta Zn}$ MEFs

4.3.1 Genome-wide binding profiles of GR wild type and $GR^{\Delta Zn}$ in MEFs

After validation that the zinc finger mutation did not affect transcription, protein translation, phosphorylation, non-genomic actions or nuclear translocation of $GR^{\Delta Zn}$, chromatin binding was studied next. ChIP-Seq was performed for GR in wild type, mutant and knockout MEFs treated with LPS to activate inflammatory TLR4 signalling and with the GR ligand Dex to induce GR nuclear translocation and chromatin binding.

The global genomic occupancy of GR in each single biological replicate is shown in **Figure 13A**. Since the reproducibility between replicates was low, all peaks called in each set were merged to generate 'universe' lists. Peaks that were called in cells missing GR represented background DNA pulled down by the GR antibody. These background peaks were removed from the 'universe' peak lists as well as general blacklisted genomic regions. The blacklisted sets of genomic regions identified by the Encyclopedia of DNA Elements (ENCODE) have to be removed when analysing functional genomic datasets since those regions have anomalous, unstructured or high signal in NGS experiments independent of cell line or experiment. After, a total of 23,039 genomic sites were bound by GR in wild type MEFs treated with LPS and Dex. Even though $GR^{\Delta Zn}$ does not recognise GREs, genomic binding was detected at 7,932 genomic sites, in agreement with a tethering mechanism. Interestingly, 4,655 of those regions overlapped with GR peaks in wild type cells (approx. 20% of all wild type peaks) (**Figure 13B**). Protein level validation of GR^{KO} MEFs is shown in **Figure 13C.**

In summary, most GR binding sites (GBS) were lost in homozygous $GR^{\Delta Zn}$ MEFs. These results support the model where mostly GR requires direct DNA binding to bind near target genes. However, approx. 20% of GBS surprisingly maintained binding, even in cells expressing the $GR^{\Delta Zn}$ mutant with impaired DNA binding. These maintained peaks support the model of tethering for gene regulation by GR. Therefore, GR seems to mostly bind directly to DNA and tether to a small subset of sites via protein-protein interactions.

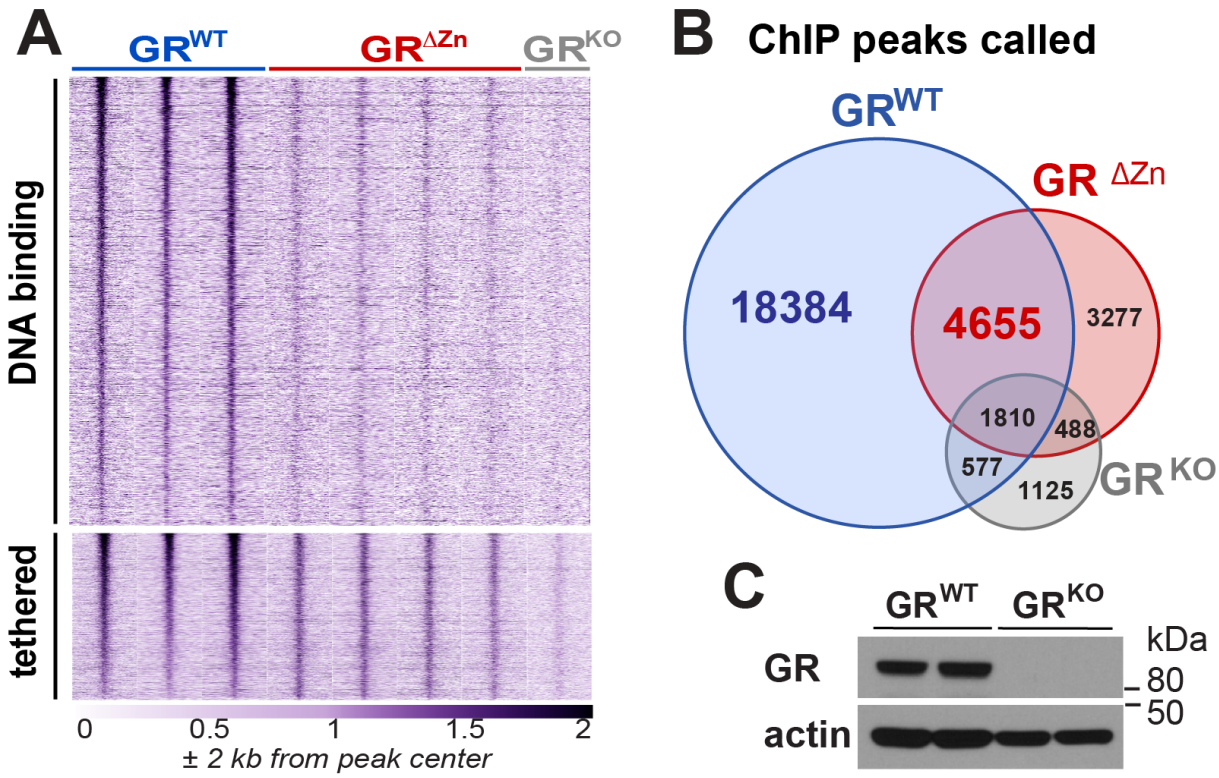

Figure 13. GR binding sites in Dex+LPS treated MEFs.
A, Heatmap of GR ChIP-Seq coverage of GR wild type (n = 3 biological replicates), homozygous $GR^{\Delta Zn}$ mutant (n = 4 biological replicates) and knockout (n = 2 biological replicates). **B**, Venn diagram showing overlap of GR wild type, homozygous $GR^{\Delta Zn}$ and knockout ChIP peaks. **A**, **B** Cells were treated 6 h with LPS and 16 h with Dex. **C**, GR western blot in wild type and GR knockout MEFs (n = 2), actin as loading control.

4.3.2 Examples of GR binding nearby target genes in wild type and $GR^{\Delta Zn}$ MEFs

In wild type MEFs, GR binding to its known targets such as the *Per1*, *Gilz*, *Ccl2* and *Il6* loci was observed, as expected. On the contrary, in $GR^{\Delta Zn}$ homozygous mutant MEFs, GR binding was almost undetectable at promoters and enhancers containing classical palindromic GREs, such as *Per1* and *Gilz*, consistent with its inability to directly bind DNA (**Figure 14A**). Importantly, ChIP-Seq revealed that only wild type GR, but not $GR^{\Delta Zn}$, bound directly to GREs near known repressed genes including *Cxcl2* or *Mmp8* (**Figure 14B**). However, a small number of maintained, tethered binding sites were observed, at the following activated target *Dusp1* and *Cp* loci

(**Figure 14C**). In addition, a significant number of maintained binding sites at the repressed targets *Ccl2*, *Ccl20, Il6* and *Vcam1* were detected, in agreement with transrepression or tethering (**Figure 14D**). The genomic positions of ChIP-Seq peaks shown in **Figure 14** are found in the **Supplementary List 1**.

In summary, most of wild type GR binding sites were lost in $GR^{\Delta Zn}$, demonstrating the importance of DNA binding by GR. However, about 20% of GBS were maintained by this mutant, showing that GR binds indirectly to DNA via tethering. In conclusion, GR seems to bind mostly directly and to a smaller extend indirectly to DNA in LPS and Dex treated MEFs.

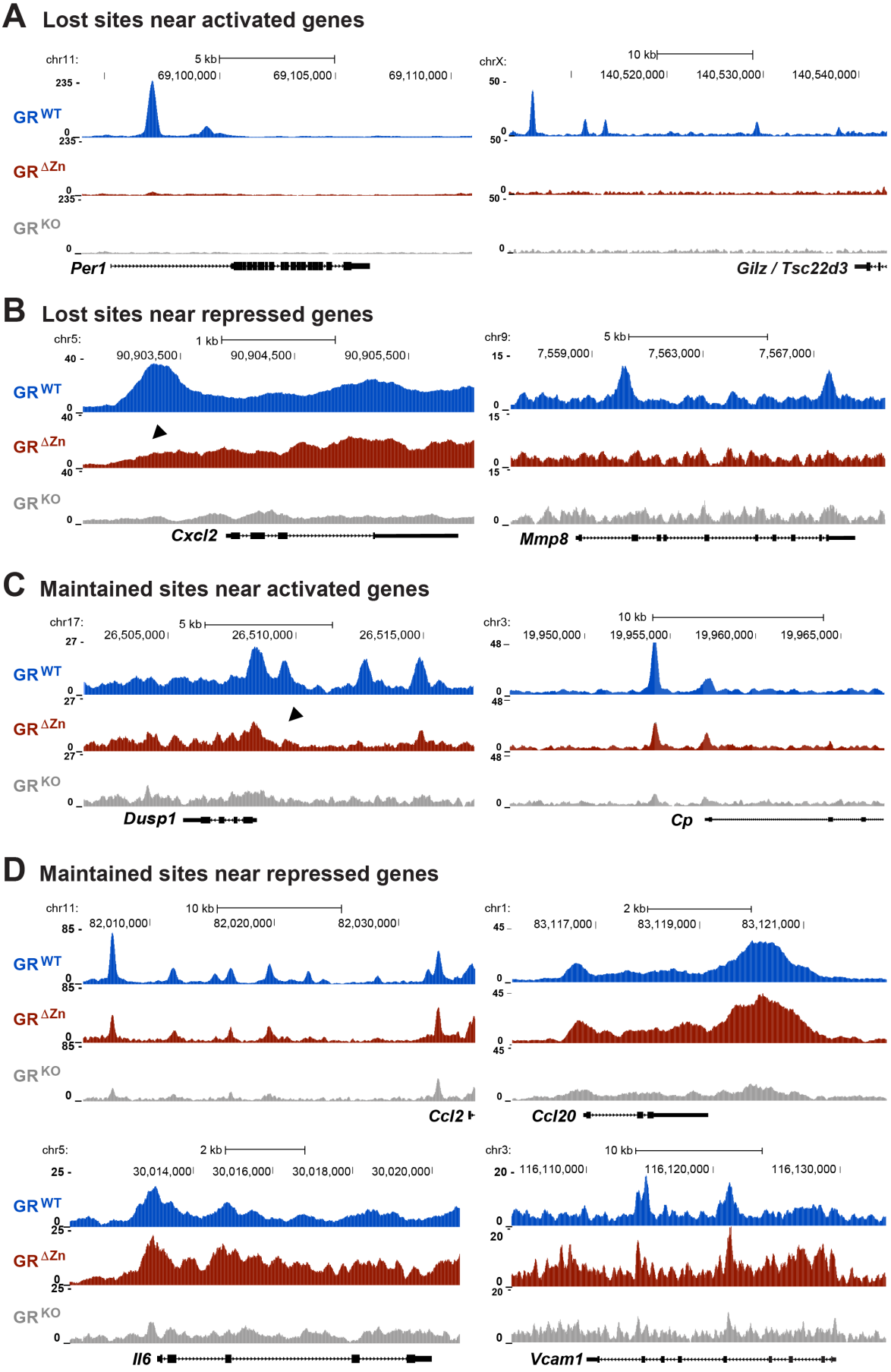
A Lost sites near activated genes
chr11:
5 kb
69,100,000
69,105,000
69,110,000
235
GR WT
GR ΔZn
GR KO
Per1
chrX:
10 kb
140,520,000
140,530,000
140,540,000
50
Gilz / Tsc22d3
B Lost sites near repressed genes
chr5:
1 kb
90,903,500
90,904,500
90,905,500
40
Cxcl2
chr9:
5 kb
7,559,000
7,563,000
7,567,000
15
Mmp8
C Maintained sites near activated genes
chr17:
5 kb
26,505,000
26,510,000
26,515,000
27
Dusp1
chr3:
10 kb
19,950,000
19,955,000
19,960,000
19,965,000
48
Cp
D Maintained sites near repressed genes
chr11:
10 kb
82,010,000
82,020,000
82,030,000
85
Ccl2
chr1:
2 kb
83,117,000
83,119,000
83,121,000
45
Ccl20
chr5:
2 kb
30,014,000
30,016,000
30,018,000
30,020,000
25
Il6
chr3:
10 kb
116,110,000
116,120,000
116,130,000
20
Vcam1

Figure 14. Representative GR binding in wild type, homozygous mutant and knockout LPS and Dex treated MEFs.
A, ChIP-Seq tracks near up-regulated target genes with lost $GR^{\Delta Zn}$ binding. **B**, ChIP-Seq tracks near down-regulated target genes with lost $GR^{\Delta Zn}$ binding. **C**, ChIP-Seq tracks near up-regulated target genes with maintained $GR^{\Delta Zn}$ binding. **D**, ChIP-Seq tracks near down-regulated target genes with maintained $GR^{\Delta Zn}$ binding. Wild type (n = 3), homozygous mutant (n = 4) and knockout (n = 2). Cells were treated with LPS for 3 h and Dex for 16 h.

4.3.3 Motif enrichment in GR ChIP-Seq peaks

HOMER bioinformatic motif analyses revealed an enrichment for GRE, AP-1, NF-κB, IRF and C/EBP consensus motifs in the GR ChIP-sequences in the wild type cistrome. Similarly, NF-κB, AP-1, interferon regulatory factor (IRF) and CCAAT-enhancer-binding protein (C/EBP) motifs were enriched among these GR ChIP-sequences obtained from $GR^{\Delta Zn}$ MEFs, while importantly GREs or half GREs were absent (**Figure 15A**). The IRF family of TF regulate transcription of interferons that modulate the innate immune response. Also, IRF can interact with CREB-binding protein (CREBBP), also known as CBP, to modulate transcription. To further analyse the ChIP-Seq peaks, enrichment of specific motifs was performed in wild type-, overlap- and mutant-specific sequences. Interestingly, GREs, Jun, AP-1 and STAT5 were significantly enriched only in wild type peaks. NF-κB (p50 and p65) was significantly enriched in tethered (overlap) peaks, indicating potential tethering of $GR^{\Delta Zn}$ with NF-κB factors rather than AP-1 or STAT5 in these cistromes. Finally, only IRF4 and the TF PU.1 were significantly present in mutant-specific peaks. The PU.1 is a tissue-specific lineage determining TF expressed in cells of the hematopoietic lineage including macrophages. Enrichment of PU.1 motif in $GR^{\Delta Zn}$ cells could be explained by $GR^{\Delta Zn}$ having a stronger preference for open chromatin marked by the PU.1 factor. This zinc finger mutant hypothetically screens chromatin and binds longer to open chromatin, marked by PU.1, by not recognising open chromatin sites with GREs.

Of note, unbiased *de novo* motif enrichment using MEME did not generate half site GREs in wild type-, overlap- or mutant-specific ChIP peaks. Therefore, $GR^{\Delta Zn}$ is unlikely to bind to half site GREs like the GR^{dim}.

In conclusion, GREs, AP-1, NF-κB, IRF, C/EBP and STAT5 motifs are enriched in wild type binding sites. At the same time, sites bound by $GR^{\Delta Zn}$ do not contain GREs, but have a strong NF-κB and IRF signature. This analysis suggests that tethering binding

sites lack GREs but are enriched for inflammatory TF motifs such as NF-κB, AP-1 and IRF.

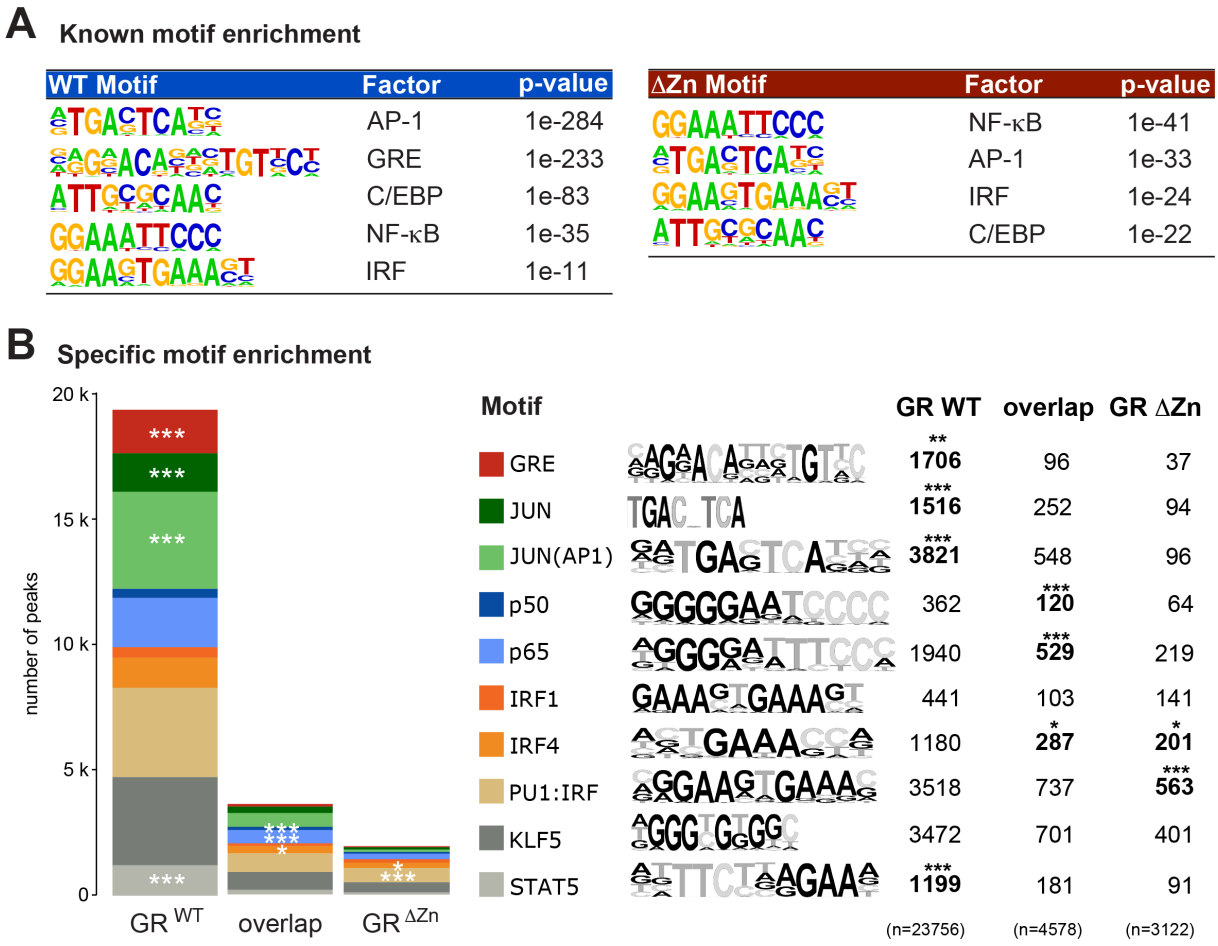

Figure 15. Motif enrichment in GR ChIP-Seq peaks.
A, Enriched known consensus motifs in GR ChIP-Seq peaks. GR peaks called in at least one biological replicate were used as the input for HOMER. Wild type (n =3) and homozygous $GR^{\Delta Zn}$ (n = 4) biological replicates. **B**, Targeted motif enrichment in GR ChIP-Seq peaks from 'universe' merged peaks. Here MEME was used to determine abundance of selected motifs generated in wild type-, mutant- or overlap-specific peaks. **A**,**B** MEFs treated with LPS for 3 h and Dex for 16 h.

4.3.4 Gene ontology for genes in the vicinity of GR ChIP peaks

Functional annotation of wild type and mutant peaks to nearby target genes showed enrichment of gene ontology (GO) terms related to inflammatory responses (**Figure 16**). These tethered binding sites could be assigned to nearby target genes involved

in inflammation, immune responses and cytokine/chemokine production, agreeing with previous reports (Cain and Cidlowski 2017, Hua et al. 2016b, Ogawa et al. 2005, Rao et al. 2011, Sacta et al. 2018).

To sum up, both wild type and mutant GR bind genomic regions near genes that are annotated with inflammatory functions. This supports the hypothesis that tethered sites are associated with the regulation of inflammatory genes and that $GR^{\Delta Zn}$ selectively distinguishes between direct GRE binding and tethering binding sites.

WT GO term	- log10(p-value)
Response to wounding	38.59
Regulation of protein phosphorylation	37.03
Regulation of immune system process	36.84
Response to biotic stimulus	32.67
Regulation of response to stress	31.66

ΔZn GO term	- log10(p-value)
Immune response	63.17
Defence response	57.35
Response to biotic stimulus	55.30
Response to cytokine stimulus	42.78
Response to stress	38.84

Figure 16. Gene ontology of wild type and $GR^{\Delta Zn}$ nearby genes.
Functional annotation of wild type (left) and mutant (right) GR ChIP peaks assigned to the nearest gene. Analysis performed in GREAT using as input all GR peaks called in at least one biological replicate. Wild type (n = 3) and mutant (n = 4) MEFs treated with LPS for 3 h and Dex for 16 h.

4.3.5 Distance distribution of GR ChIP peaks to TSS

To further characterise the cistromes, the distribution of GR ChIP peaks distance to the nearest transcription start site (TSS) in wild type and $GR^{\Delta Zn}$ was analysed with a tool called GREAT. Differences in the ChIP peak distribution could indicate a misfolded GR. Wild type GR mostly bound ± 500 to ± 50 up (+) or down (-) -stream of the nearest TSS. These sites are mostly enhancers and the binding distribution was the same in $GR^{\Delta Zn}$ (**Figure 17**). Also, GRE-containing and tethered sites had similar TSS distance distributions. There were no differences in the distribution of peaks near activated and repressed sites.

Overall, the binding pattern regarding the distance to TSS in $GR^{\Delta Zn}$ was unchanged. This suggests that $GR^{\Delta Zn}$ is a 'functional' protein in terms of the distribution of genomic binding distance to TSS.

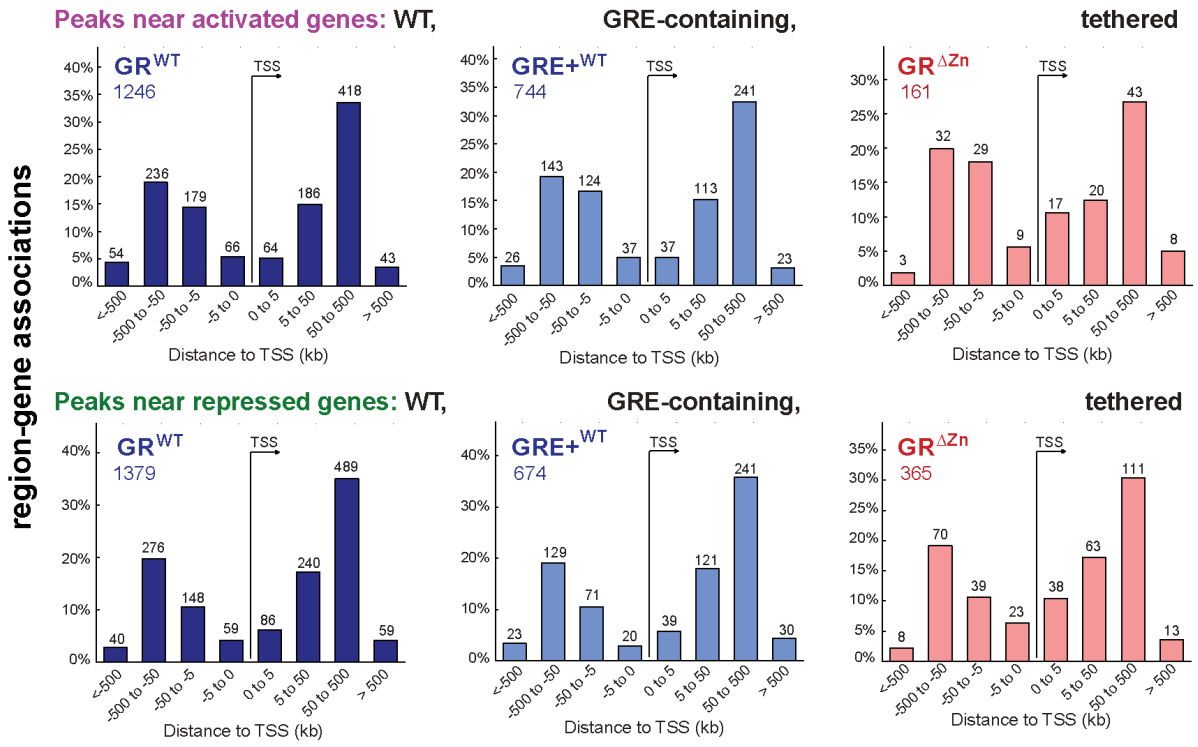

Figure 17. Distribution of peak distance to TSS of GR ChIP-Seq peaks.
Distance to nearest Transcription Start Site (TSS) of wild type-specific and tethered GR ChIP peaks. Analysis was performed in GREAT. Wild type (n = 3) and mutant (n = 4) MEFs treated with LPS for 3 h and Dex for 16 h.

4.3.6 ChIP-Seq validation and co-immunoprecipitation of GR and p65

Tethered binding near inflammatory *Ccl2* and *Il6* loci was validated by ChIP-qPCR in LPS and Dex treated wild type and $GR^{\Delta Zn}$ MEFs. Also, the loss of chromatin binding with $GR^{\Delta Zn}$ at *Per1* and *Gilz* loci was confirmed (**Figure 18A**).

To further verify that $GR^{\Delta Zn}$ retains the ability to be tethered but no longer binds directly to GREs, protein interaction experiments in both wild type and $GR^{\Delta Zn}$ MEFs were performed. GR was immunoprecipitated in nuclear extracts of LPS and Dex treated wild type and $GR^{\Delta Zn}$ MEFs and GR and p65 were detected by immunoblotting. The endogenous NF-κB subunit p65 was co-immunoprecipitated both wild type GR and $GR^{\Delta Zn}$ in nuclear protein extracts of LPS and Dex treated MEFs (**Figure 18B**). This result indicates that i) the p65 and $GR^{\Delta Zn}$ interaction is intact, which demonstrates that $GR^{\Delta Zn}$ maintained its capacity to interact with other known TF, ii) the GR and p65 interaction is likely independent of GRE-bound GR since the mutant maintained the interaction, iii) $GR^{\Delta Zn}$ seems to tether to DNA-bound p65.

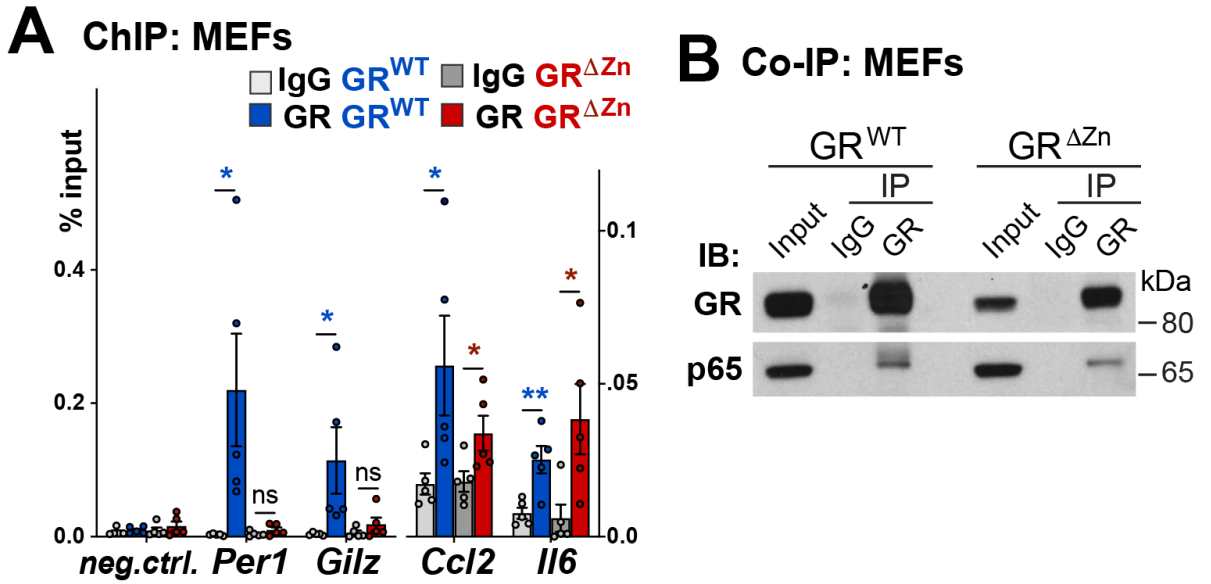

Figure 18. GR and p65 interaction and ChIP-qPCR in MEFs.
A, GR ChIP-qPCR for selected loci in MEFs treated with LPS for 3 h and with Dex for 16 h. *Per1* and *Gilz* are examples of lost binding by $GR^{\Delta Zn}$ and *Ccl2* and *Il6* are examples of maintained binding. Data presented as % input, values are mean ± SEM (n = 5), * p<0.05, ** p<0.01 and ns = not significant. Student's t-test. **B**, Endogenous GR immunoprecipitation (IP) followed by GR and p65 immunoblot (IB) of 3 h LPS and 16 h Dex treated wild type and $GR^{\Delta Zn}$ MEFs. IgG as negative IP control and 10% nuclear lysate input to control IP efficiency. Representative of n = 2 independent experiments.

Moreover, to rule out the possibility that $GR^{\Delta Zn}$ had defects such as a delayed or slower chromatin binding compared to wild type GR, time series ChIP-qPCR experiments were performed. As shown in **Figure 19**, the zinc finger mutant did not bind near *Per1* or *Gilz* at any time point between 1 to 16 h of LPS and Dex treatment. For the repressed inflammatory loci near *Ccl2* and *Il6,* the chromatin binding pattern overlaps between wild type and mutant GR with the greatest binding starting at 3 h of LPS and Dex. These results indicate that the dynamics of chromatin binding of $GR^{\Delta Zn}$ are not delayed compared to wild type GR. Furthermore, the pattern observed in the ChIP-Seq data is representative of the binding within the period of 1-16 h of LPS and Dex.

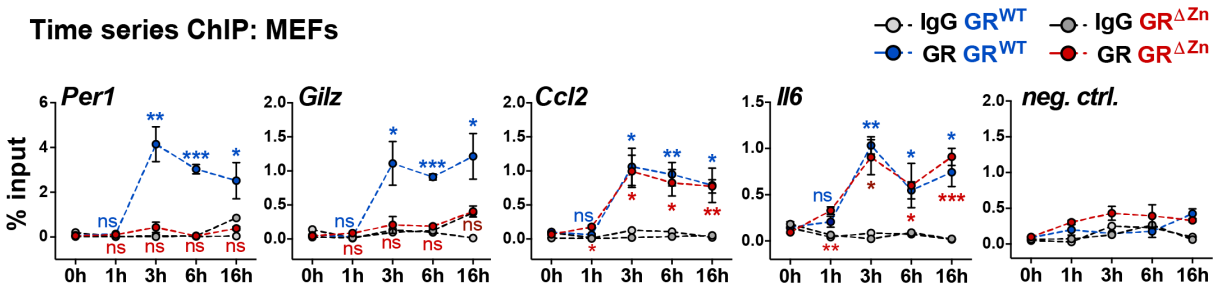

Figure 19. Chromatin binding by GR wild type and GR$^{\Delta Zn}$ over time in MEFs.
GR ChIP-qPCR for selected loci in MEFs treated with LPS and Dex for 0-16 h. t-test for each time point versus untreated control (0h). Values are mean ± SEM, ns = not significant, *p<0.05, **p<0.01, ***p<0.001. *FoxL2* locus used as the negative control.

In conclusion, GR$^{\Delta Zn}$ tethers to a subset of binding sites with NF-κB, AP-1 and IRF motifs, under inflammatory conditions. On the contrary, direct binding to GRE sequences associated with either activated or repressed targets is lost. Importantly, the p65 and GR protein-protein interaction was maintained by GR$^{\Delta Zn}$. Therefore, GR$^{\Delta Zn}$ provides a new tool to analyse the functional relationship between tethering and direct DNA binding of GR.

4.4 Target gene regulation by GR requires DNA binding

4.4.1 RNA-Seq shows no target gene regulation by GR$^{\Delta Zn}$ in response to Dex

To further study the functionality of tethered versus DNA-dependent binding sites, total RNA-Seq was performed in wild type and GR$^{\Delta Zn}$ MEFs under different conditions. Strikingly, in GR$^{\Delta Zn}$ cells, there were no significant changes in gene expression in response to Dex, which would explain the lethality of these mice. As shown in **Figure 20A**, all differentially expressed genes (DEGs) in wild type MEFs, were unchanged in GR$^{\Delta Zn}$ MEFs when comparing LPS+Dex vs. LPS or Dex alone vs. control. The list of DEGs in LPS+Dex vs LPS shown in **Supplementary List 2**. In wild type MEFs, 223 genes were differentially up-regulated and 263 were down regulated in response to Dex in LPS-treated samples. Some examples of activated genes include *Cp, Fkbp5, Gilz, Per1* and *Sgk1.* Examples of repressed genes include *Ccl2*, *Ccl20, Cxcl2, Ednra, Il6* and *Vcam1*. Remarkably, no gene significantly changed expression when comparing Dex+LPS versus LPS treated GR$^{\Delta Zn}$ MEFs.

GO analysis of the top non-redundant biological processes enriched in up- and down-regulated DEGs are displayed in **Figure 20B**. Examples of Dex-dependant up-regulated processes were signal transduction and regulation of multicellular organismal pathways. Examples of down-regulated processes are mainly inflammatory-related terms such as cellular response to LPS and chemokine-mediated signalling pathways.

In response to Dex versus untreated cells, 206 genes were up-regulated, and 114 genes were down-regulated in wild type MEFs (**Figure 20C**). Some up-regulated genes included *Fibin, Gilz*, *Lcn2, Per1* and *Saa3*. Examples of down regulated genes were *Ccl4, Cxcl12, Il6* and *Thbd*. Again, in MEFs expressing the zinc finger mutant, there was no gene differentially expressed upon Dex addition.

Taken together, these results show that $GR^{\Delta Zn}$ is unable to regulate gene expression of any target gene in Dex alone treatment nor in the inflammatory context with LPS and Dex treatment. This is a striking result because GR is widely believed to repress inflammatory genes without binding directly to GREs and the zinc finger mutant is not able to repress targets even when bound (directly or indirectly via p65) to chromatin. Also, these results suggest that the non-genomic actions of GR might potentially not contribute to transcriptional changes, at least under the conditions tested here.

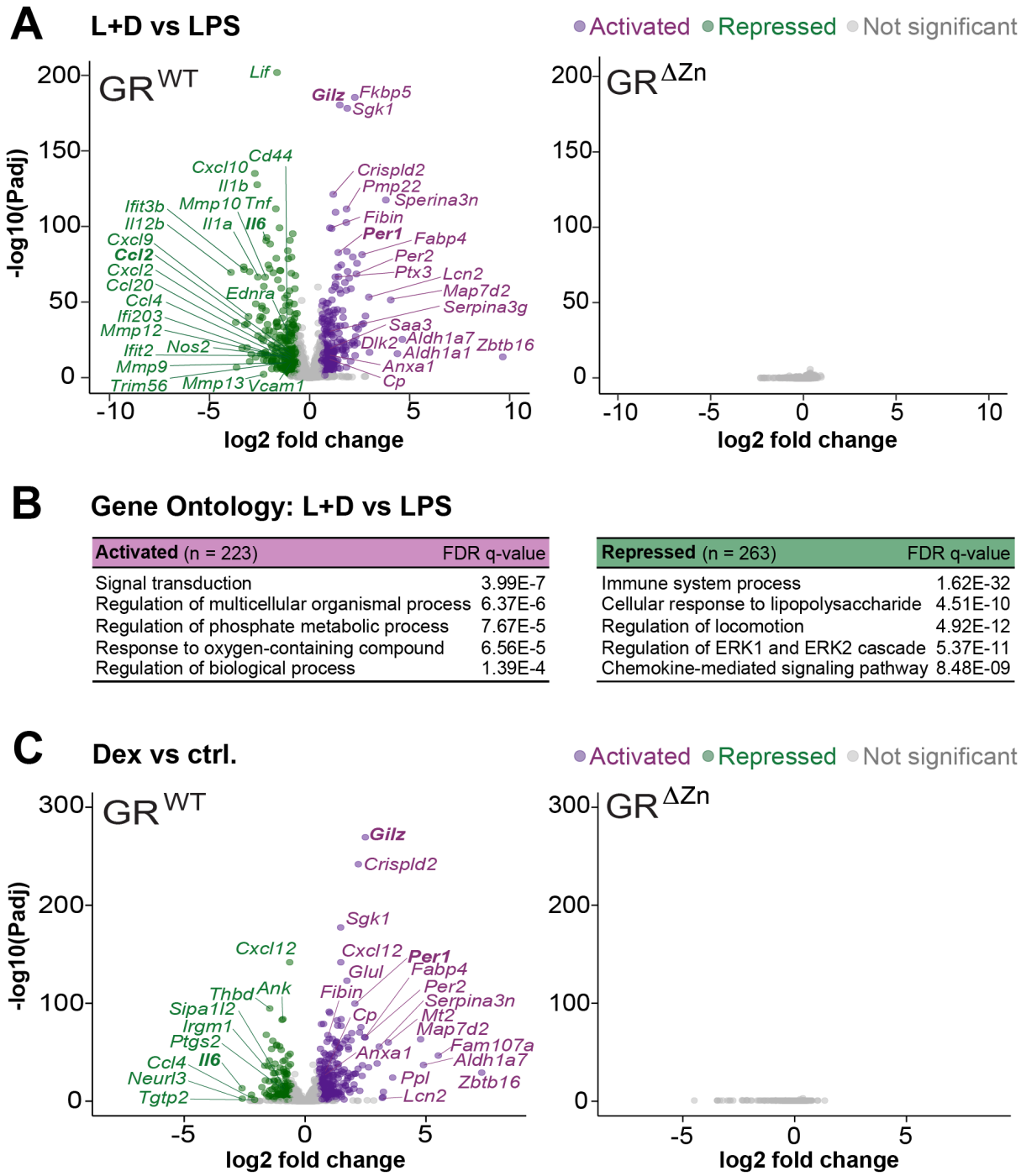

Figure 20. GR$^{\Delta Zn}$ does not regulate target gene mRNA levels in MEFs.
A, Volcano plots showing up-regulated and down-regulated transcripts in 6 h LPS + 16 h Dex (L+D) compared to 6 h LPS treated wild type and GR$^{\Delta Zn}$ MEFs. Genes regulated by wild type GR are unchanged in GR$^{\Delta Zn}$ MEFs and "log2 fold change" values are around zero. FDR < 0.05, base mean > 200, 1.5-fold change threshold, n = 3 biological replicates. L+D effect: 223 up-regulated and 263 down-regulated. **B**, Functional gene annotation from genes differentially expressed in **A**. Tool: GOrilla. **C**, same as **A** but comparison between 16 h Dex and vehicle (ctrl.) treatment. Dex effect: 206 up-regulated and 114 down-regulated.

4.4.2 Genes in the vicinity of GR tethered sites are not regulated by GR$^{\Delta Zn}$ and are enriched near repressed genes

When analysing genes harbouring a nearby tethered GR$^{\Delta Zn}$ site, again there was no difference in expression levels upon stimulation with Dex, neither in untreated nor in LPS-treated MEFs. As described in the heatmap of **Figure 21A**, mRNA levels of genes up- or down-regulated with a nearby maintained tethered GR peak did not change in cells expressing GR$^{\Delta Zn}$ in response to Dex.

The absence of a response to Dex in GR$^{\Delta Zn}$ mutants could be partially explained by the fact that approximately 80% of the binding events were lost. However, approximately 20% of tethered sites were preserved, mainly near repressed GR targets (**Figure 21B**), in agreement with previous models associating protein-protein interactions with transrepression (Desmet and De Bosscher 2017).

In summary, even if direct DNA binding by GR is not essential at tethered sites, nearby genes are not repressed by GR$^{\Delta Zn}$. This strongly suggests that DNA binding is essential for GR to up- and down-regulate target genes.

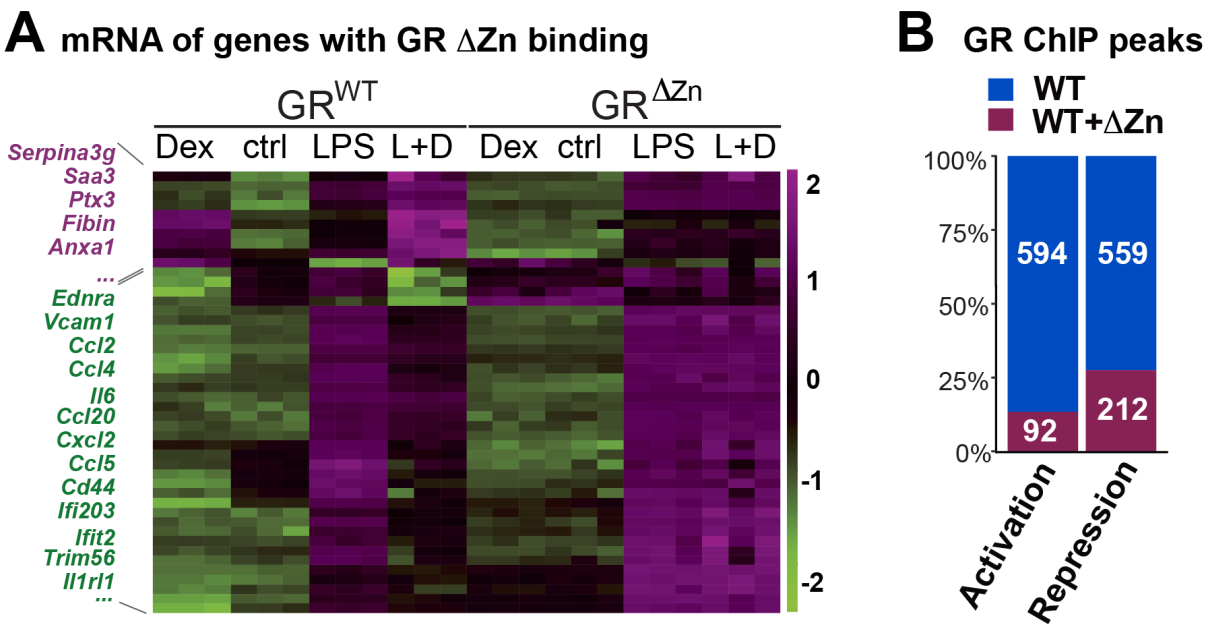

Figure 21. Tethered peaks do not regulate nearby genes and are abundant near repressed GR target genes.
A, Clustering of DESeq normalised RNA-Seq counts for transcripts near tethered sites in MEFs treated with vehicle, Dex, LPS or LPS and Dex (L+D). Values are RNA-Seq z-scores (n = 3). Up-regulated (magenta) and down-regulated (green) genes by wild type GR with a $GR^{\Delta Zn}$ peak nearby. **B**, GR ChIP-Seq peaks near activated or repressed targets, 3 h LPS + 16 h Dex treated MEFs.

4.4.3 Basal gene expression profile and PCA analysis

Importantly, there was a baseline difference in mRNA expression profiles between untreated wild type and mutant MEFs. As shown in **Figure 22A**, 249 genes were up-regulated and 277 were down-regulated in untreated mutant compared to wild type MEFs; *Ccn5*, *Aqp1*, *Lgr5* and *Grem2* were activated and *Rgs5*, *Nes*, *Pmaip1* and *Rflnb* were repressed. These results are consistent with the known role of GR in development and immunomodulation. Mutant cells showed the up-regulation of certain inflammatory genes and down-regulation of developmental genes (**Figure 22B**). Principal component analysis (PCA) is commonly used to cluster samples in a dataset in order to explain the variation between samples. $GR^{\Delta Zn}$ RNA-Seq samples clustered together regardless of treatment with Dex. LPS and Dex samples clustered with the LPS group and Dex samples with vehicle. However, mutant MEFs did respond to treatment with LPS (**Figure 22C**).

Taken together, these results show that the baseline gene profile is slightly different in $GR^{\Delta Zn}$ with up-regulation of inflammation and down-regulation of developmental genes. Also, $GR^{\Delta Zn}$ MEFs do not respond to Dex alone or in combination as LPS and Dex.

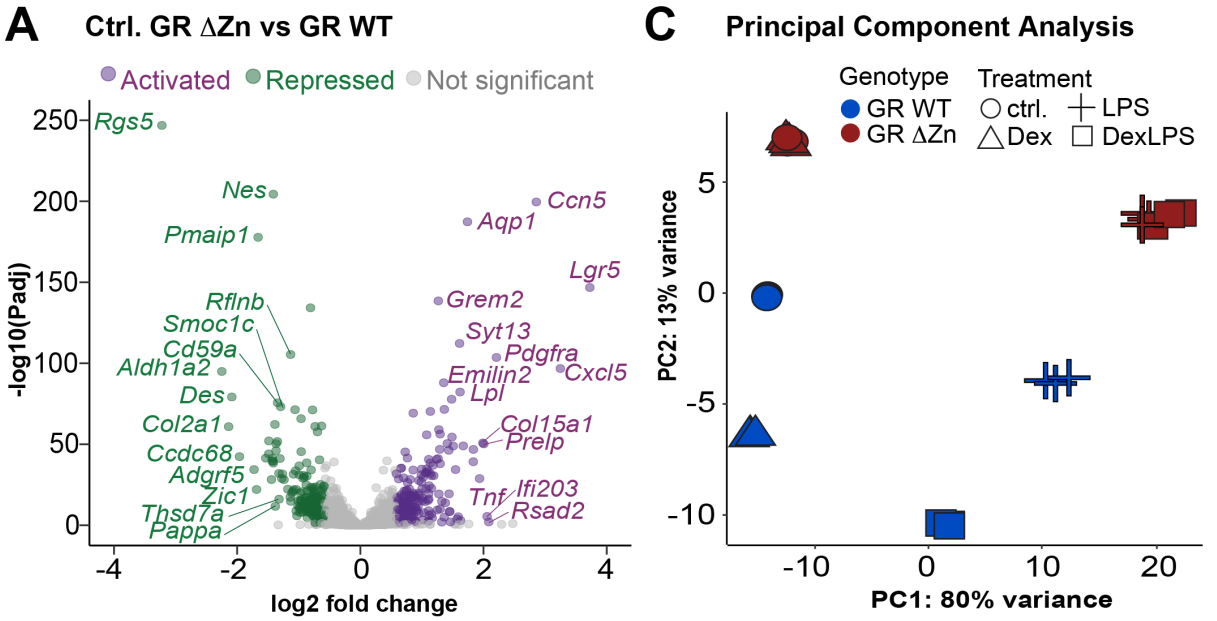

B Gene Ontology: ctrl. GR ΔZn vs WT

Activated (n = 249)	FDR q-value
Defense response	2.33E-16
Extracellular structure organization	2.21E-15
Extracellular matrix organization	1.92E-15
Taxis	6.32E-13
Response to external biotic stimulus	2.07E-12

Repressed (n = 277)	FDR q-value
Regulation of multicellular organismal process	7.16E-15
Developmental process	4.46E-13
Regulation of multicellular organismal development	4.84E-13
Multicellular organismal process	2.00E-12
Regulation of developmental process	2.63E-12

Figure 22. Baseline gene expression in untreated MEFs and PCA of RNA-Seq.
A, Volcano plots showing up-regulated and down-regulated transcripts FDR < 0.05, base mean > 200, 1.5-fold change threshold, n = 3 biological replicates. Baseline effect: 249 up-regulated and 277 down-regulated. **B**, Functional annotation of differentially regulated genes. **C**, Principal component analysis of RNA-Seq samples showing Dex treated $GR^{\Delta Zn}$ MEFs clustering with vehicle samples, indicating no effect with mutant GR (n = 3).

4.4.4 Validation of GR target genes modulation

Changes in the mRNA levels of GR targets were measured by RT-qPCR in wild type and $GR^{\Delta Zn}$ MEFs and confirmed the results of RNA-Seq, i.e. $GR^{\Delta Zn}$ did not regulate *Per1*, *Gilz*, *Ccl2*, *Il6*, *TNFα* or *Mmp9* upon the addition of Dex. GR mRNA levels (*Nr3c1*) were not different between wild type and mutant cells (**Figure 23**).

To sum up, $GR^{\Delta Zn}$ does not regulate target genes, even if it binds or tethers close to *Ccl2* and *Il6.* Losing $GR^{\Delta Zn}$ binding at *Per1*, *Gilz*, *TNFα* and *Mmp9* likely explains the lack of regulation. These results show that LPS activates inflammatory pathways in wild type and mutant MEFs, but $GR^{\Delta Zn}$ does not up- and down-regulate target genes to strongly repress inflammation, as occurs with wild type GR.

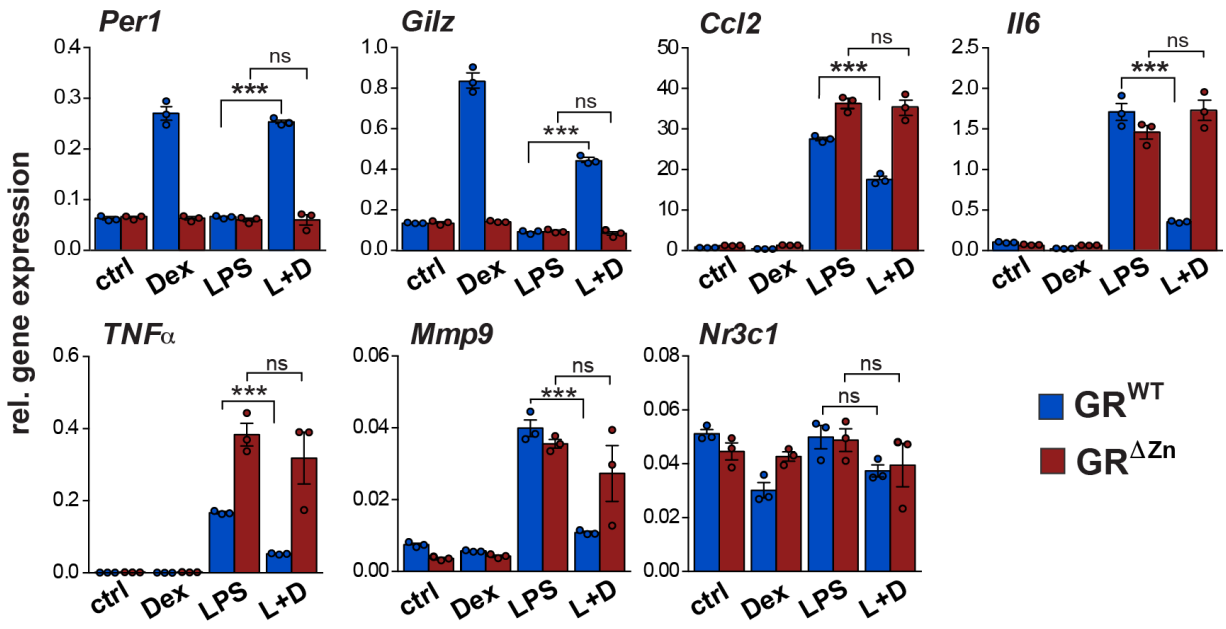

Figure 23. Validation of the RNA-Seq by qRT-PCR.
Transcript levels of GR targets measured by qRT-PCR upon treatment with vehicle (ctrl), 16 h Dex, 6 h LPS and 6 h LPS + 16 h Dex (L+D). Values are normalised to *U36b4* and represent mean ± SEM, n = 3, ***p<0.001 and ns = not significant. Student's t-test.

4.4.5 MEFs treated with TPA show no effect on target gene regulation

The same observations were confirmed in MEFs treated with 12-O-tetradecanoylphorbol-13-acetate or tetradecanoylphorbol acetate (TPA), also known as phorbol 12-myristate 13-acetate or PMA. TPA is a small molecule that activates inflammation via the signal transduction enzyme PKC (protein kinase C). The PKC pathway induces an inflammatory response, similar to LPS, but via different signalling pathways. The results again demonstrated the expected changes in gene expression of known GR targets such as *Per1*, *Gilz*, *Ccl2* or *Il6* in wild type MEFs, with no changes in $GR^{\Delta Zn}$ cells (**Figure 24**).

In conclusion, independent of LPS signalling, $GR^{\Delta Zn}$ MEFs failed to up- or down-regulate target genes when treated with Dex. Therefore, in two different stimulation pathways (LPS and TPA activators) $GR^{\Delta Zn}$ is unable to modulate target genes.

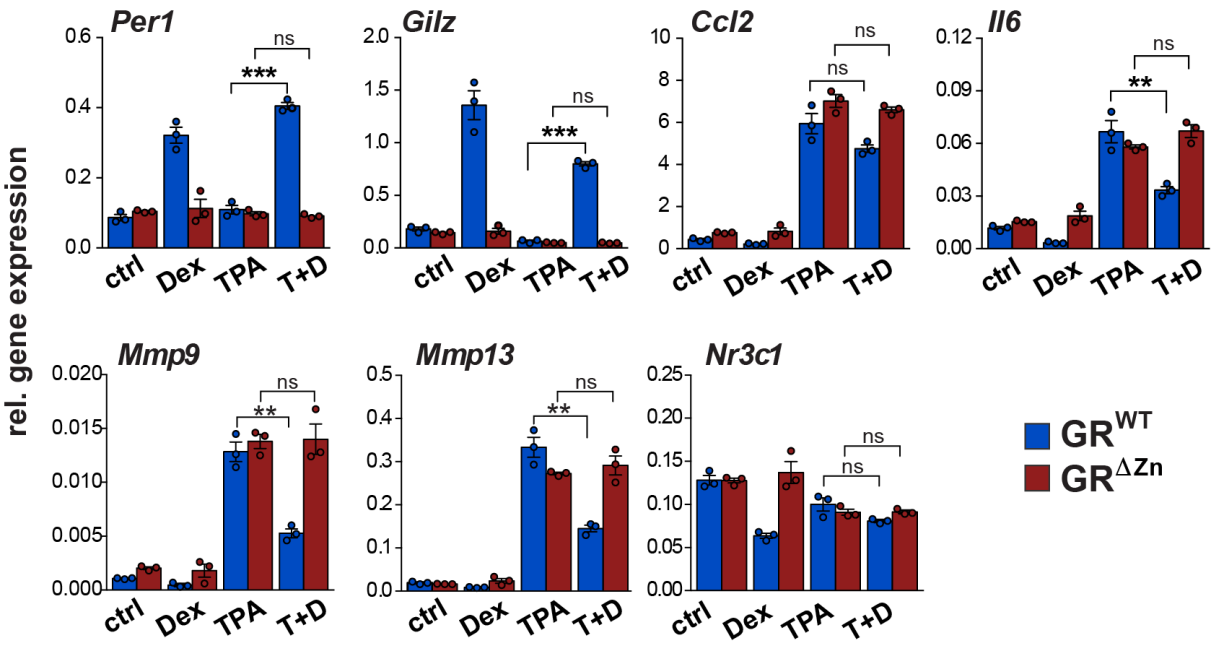

Figure 24. Gene expression of GR targets in TPA stimulated MEFs.
Transcript levels of GR targets measured by qRT-PCR upon treatment with vehicle (ctrl), 16 h Dex, 6 h TPA and 6 h TPA + 16 h Dex (T+D). Values are normalised to *U36b4* and represent mean ± SEM, n = 3, **p<0.01, ***p<0.001 and ns = not significant. Student's t-test.

4.4.6 Time series treatment with Dex alone or LPS and Dex in MEFs

The mutation in GR$^{\Delta Zn}$ cells could affect the kinetics and only delay the transcriptional response. To test this hypothesis, time series treatment where wild type or GR$^{\Delta Zn}$ MEFs were treated with Dex or LPS and Dex between 1 h and 16 h.

First, cells were treated with LPS or LPS and Dex and *Per1* and *Gilz* were activated and *Ccl2* and *Il6* were repressed, in response to Dex in wild type, but not in mutant cells, regardless of the stimulus or the time point (**Figure 25A**). Second, MEFs were treated with Dex alone over a time course and again, *Per1, Gilz, Lcn2* and *Lpin1* were strongly activated in wild type MEFs and showed no response at any time point in cells expressing GR$^{\Delta Zn}$. Importantly, GR transcript levels were the same between wild type and mutant GR at all time points (**Figure 25B**).

This data suggests that, by itself, GR tethering is not sufficient to affect gene regulation, since there were no detectable changes in mRNA expression in response to the GR ligand in GR$^{\Delta Zn}$ cells under any of the conditions tested. In summary, these findings

strongly indicate that direct DNA binding by GR is globally required for its transcriptional activity in MEFs.

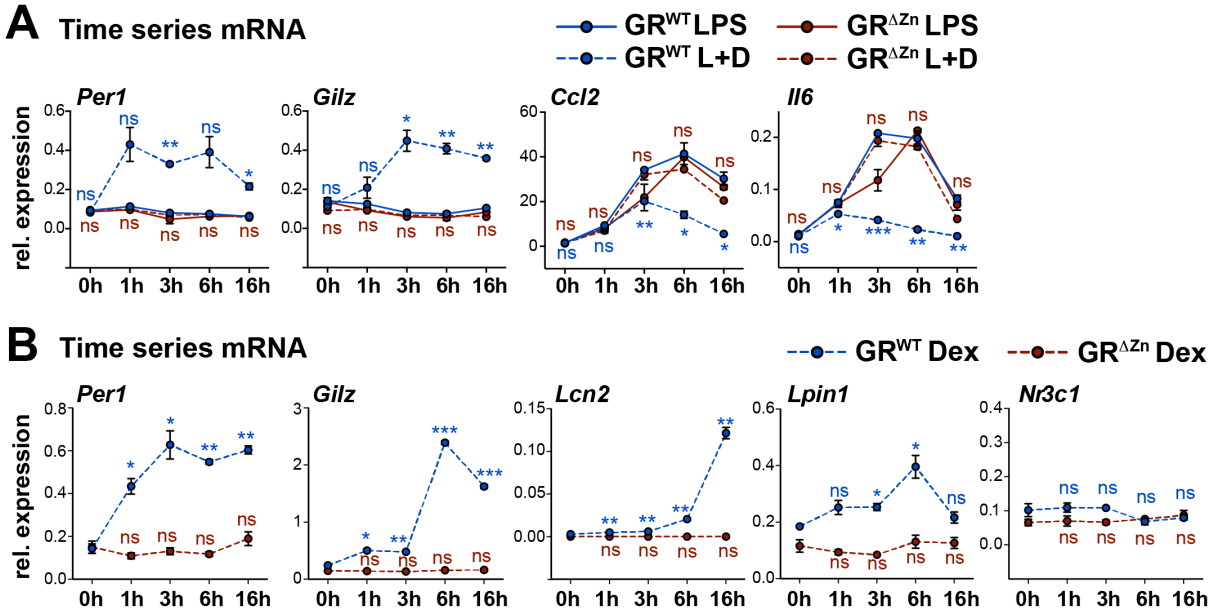

Figure 25. Time series of Dex and LPS and Dex treatment in MEFs.
A, qRT-PCR for GR target genes (normalised to *U36b4*) upon treatment with LPS or LPS+Dex (L+D) for 0-16 h. Values represent mean ± SEM, n = 3, ***p<0.001, **p<0.01, *p<0.05 and ns = not significant. Student's t-test of each time point compared to untreated (0 h). **B**, qRT-PCR for GR target genes (normalised to *U36b4*) upon treatment with Dex for 0-16 h. Values represent mean ± SEM, n = 2, *p<0.05, **p<0.01, ***p<0.001 and ns = not significant. Student's t-test of each time point compared to untreated (0 h).

4.5 GR tethering can be detected in various Dex concentrations

In order to validate the maintained tethered genomic binding with absence of transcriptional activity in $GR^{\Delta Zn}$ MEFs, ChIP- and RT-qPCR experiments with various concentrations ranging from 10 nM to 1 µM Dex were performed in MEFs (**Figure 26A**&**B**). Cells were treated with LPS and different doses of Dex for 3 h. Wild type GR bound chromatin sites and activated or repressed the expression of *Per1*, *Gilz*, *Ccl2* and *Il6* in all Dex concentrations tested. On the contrary, $GR^{\Delta Zn}$ retained occupancy

near *Ccl2* and *Il6*, but did not regulate transcriptional repression of these inflammatory genes in any of the tested conditions.

In conclusion, $GR^{\Delta Zn}$ failed to up- and down-regulate genes regardless of the time frame or Dex concentration tested, even though binding close to *Ccl2* and *Il6* was observed at all time points and ligand concentrations.

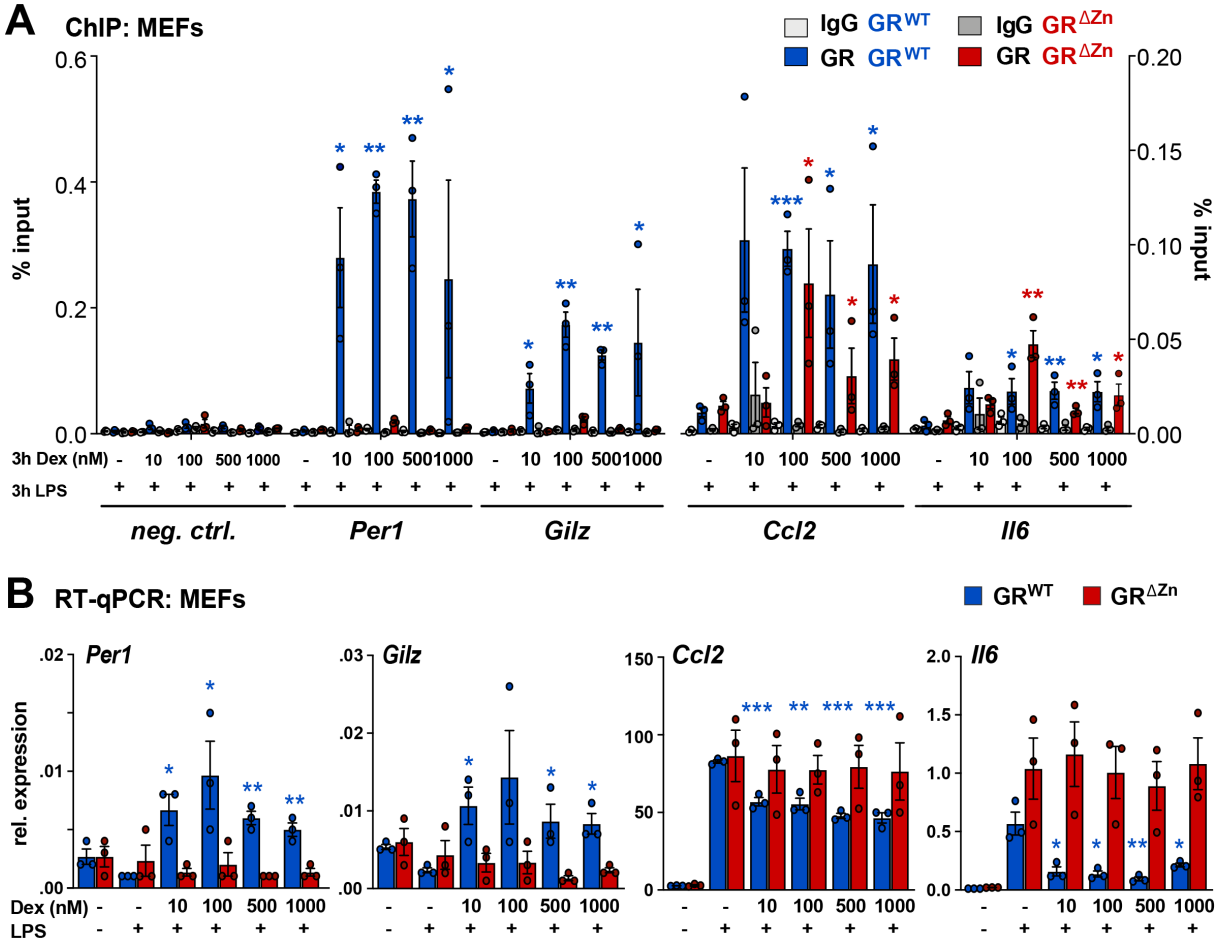

Figure 26. Tethering but no gene regulation at different Dex concentrations.
A, GR ChIP-qPCR for selected loci in MEFs treated with different concentrations between 10 nM and 1 µM Dex and LPS for 3 h (n = 3), shown as % input with t-test for GR IPs over IgG. **b**, qRT-PCR for GR target genes in MEFs treated as in **a**, normalised to *U36b4,* n = 3. t-test for different Dex concentration over LPS only. **a**, **b**, Values are mean ± SEM, ns = not significant, *p<0.05, **p<0.01, ***p<0.001.

4.6 GR binding in embryonic liver and macrophages

4.6.1 GR chromatin binding in embryonic livers at endogenous GC peak

After characterisation of the impact of the zinc finger mutation in MEFs, the importance of GR DNA binding for metabolic and inflammatory gene regulation was studied *in vivo*.

Livers from wild type and $GR^{\Delta Zn}$ E18.5 p.c. embryos were collected at the peak of endogenous ligand, without treatment with Dex, and ChIP-qPCR were performed. Genomic occupancy near the following metabolic genes was detected: *acyl-CoA oxidase 2* (*Acox2)*, *alcohol dehydrogenase 5* (*Adh5)*, *fumarylacetoacetase* (*Fah)*, *glycogen branching enzyme 1* (*Gbe1)* and *hypoxia-inducible lipid droplet-associated protein (Hilpda)*. These genes have lipid, glycogen, amino acid and bile acid metabolic hepatic functions (Rando et al. 2016) (**Figure 27**). To note, HILPDA has been shown to influence the secretion of cytokines such as IL-6 (Robinson et al. 2015). Occupancy of most of these GRE-containing sites was lost in foetal $GR^{\Delta Zn}$ livers, with the exception of the *Hilpda* locus, which appeared to be tethered and does not have a GRE motif.

In conclusion, not only in MEFs, but also in murine liver, $GR^{\Delta Zn}$ lost most genomic binding sites. These results indicate that the observations made in MEFs are also relevant in a metabolic tissue *in vivo*.

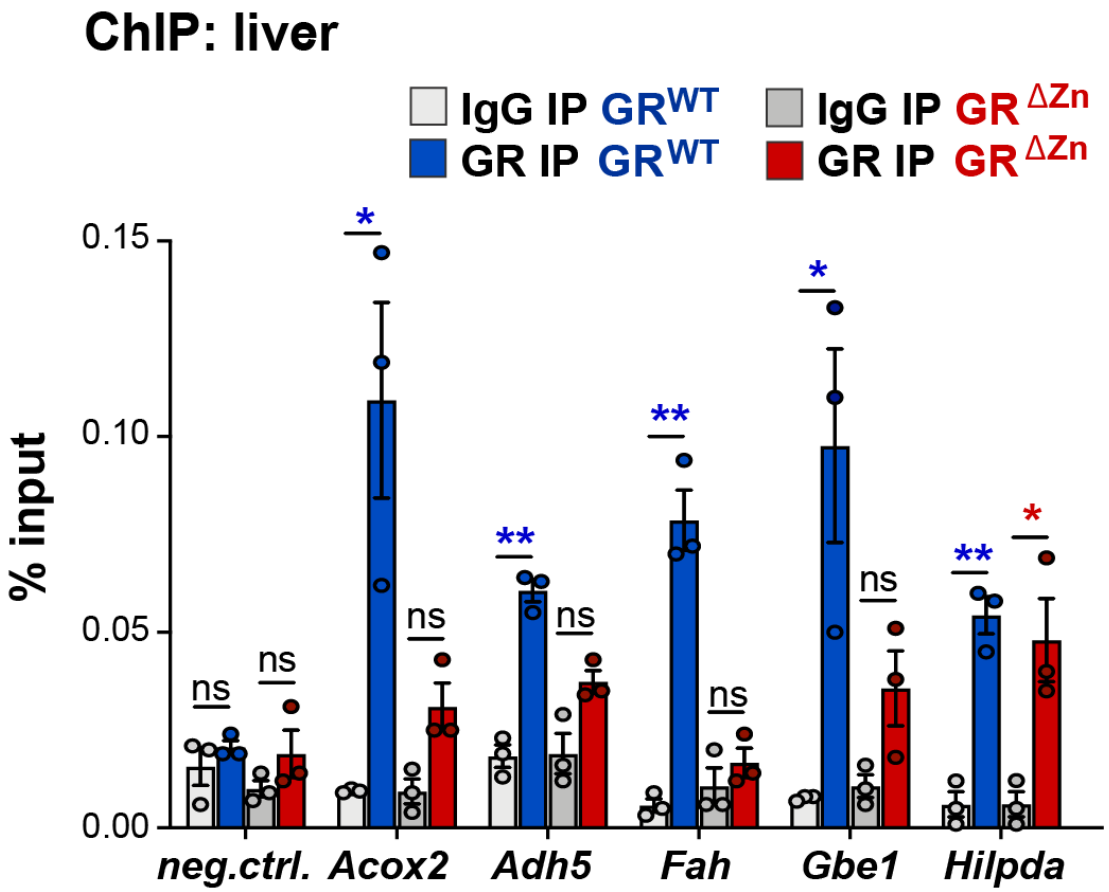

Figure 27. GR binding in embryonic livers at ZT12.
GR ChIP-qPCR in wild type and homozygous $GR^{\Delta Zn}$ E18.5 livers collected at ZT12, peak of GC in mice. *Acox2, Adh5, Fah, Gbe1* are loci with lost $GR^{\Delta Zn}$ binding, *Hilpda* is a maintained site and Neg. site is *FoxL2*. Data shown as % input, values are mean ± SEM (n = 3 embryos). * p<0.05, ** p<0.01, *** p<0.001 and ns = not significant. Student's t-test.

4.6.2 GR binding and target gene regulation in foetal liver-derived macrophages

GR occupancy was analysed in foetal liver-derived macrophages. Likewise, wild type GR was bound near *Per1*, *Dusp1*, *Nos2*, *Mmp13*, *Il1β* and *Ccl2* when analysed by ChIP-qPCR in LPS and Dex treated cells (Uhlenhaut et al. 2013) (**Figure 28**).

Per1 and *Dusp1* target genes are activated by GR. On the contrary, *Nos2*, *Mmp13*, *Il1β* and *Ccl2* are important inflammatory genes repressed by Dex. In agreement with the previous results in MEFs, GR binding at *Per1* and *Dusp1* was greatly reduced in $GR^{\Delta Zn}$ macrophages. Also, $GR^{\Delta Zn}$ binding at inflammatory *Nos2*, *Mmp13*, *Il1β* and *Ccl2* was retained regardless of the DNA-binding impaired mutation. Importantly, binding

near these repressed target genes co-occurred with NF-κB binding, as measured by ChIP-qPCR for p65 (**Figure 28**). Also, p65 binding levels were similar between wild type and mutant macrophages. Again, these results support p65 as a tethering partner for GR in its repressive functions. Also, these results complement the endogenous Co-IPs in MEFs where p65 was pulled down together with wild type and mutant GR.

In conclusion, tethering of GR to repressed sites was detected in mutant macrophages, as observed in MEFs. Also, $GR^{\Delta Zn}$ binding coincided with p65 near inflammatory genes, pointing therefore at NF-κB as a potential tethering partner.

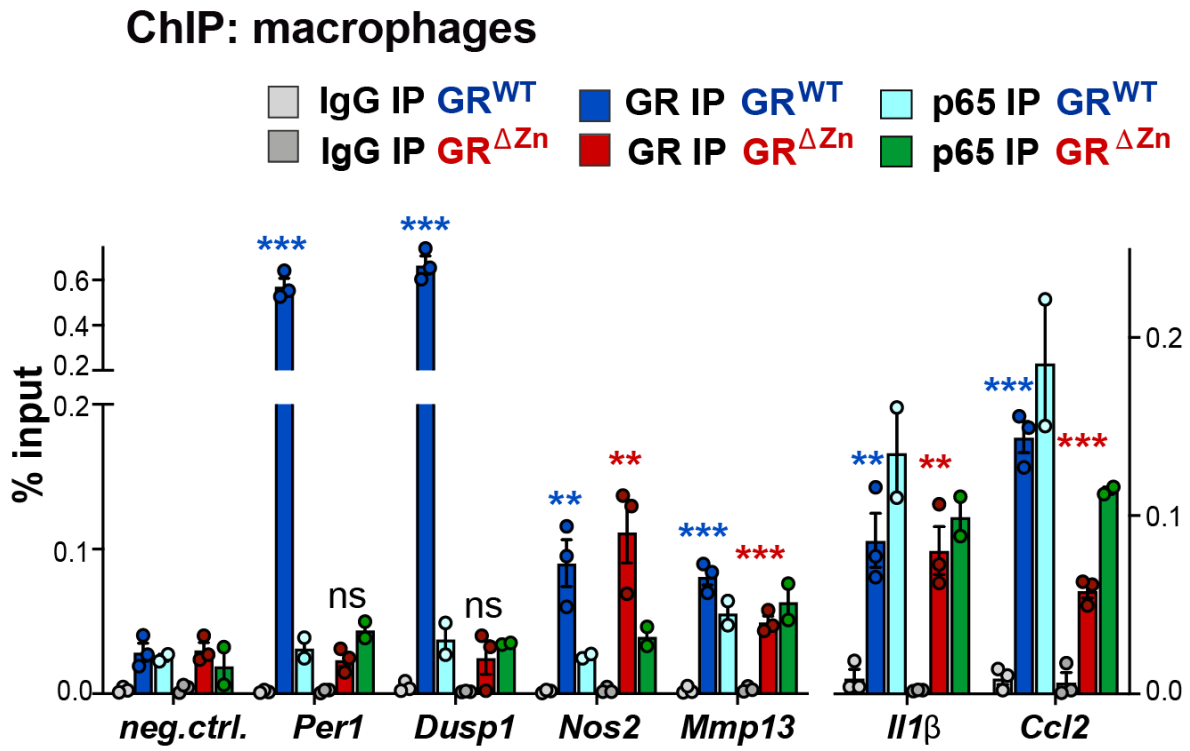

Figure 28. ChIP-qPCR in foetal liver macrophages treated with LPS and Dex.
GR and p65 ChIP-qPCR in wild type and homozygous $GR^{\Delta Zn}$ foetal macrophages. Data shown as % input, values are mean ± SEM (n = 2 biological replicates). * p<0.05, ** p<0.01, *** p<0.001 and ns = not significant. Student's t-test.

In agreement with the previous observations in MEFs, no change in the transcript levels of *Per1, Dusp1, Nos2, Mmp13, Il1β, Ccl2, Gilz* and *Lcn2* were detected in macrophages expressing $GR^{\Delta Zn}$ (**Figure 29**). Neither activation nor repression was observed in $GR^{\Delta Zn}$ macrophages. In order to verify the correct differentiation of the liver monocytes into macrophages, the mRNAs of the following macrophage markers were measured: *cluster of differentiation 14* (*Cd14*), *cluster of differentiation 86* (*Cd86*) and *colony-stimulating factor 1* (*CSF-1*), shown in **Figure 29**. From developmental stage E12 onwards, the liver is the primary site of myeloid cell production in murine embryos (Hoeffel and Ginhoux 2018). All three markers were up-regulated upon LPS treatment and *Cd86* was down-regulated in LPS and Dex treated wild type cells, but not in $GR^{\Delta Zn}$ macrophages. These results show that the monocytes isolated from foetal livers were correctly differentiated into macrophages that strongly responded to the pro-inflammatory LPS stimulus.

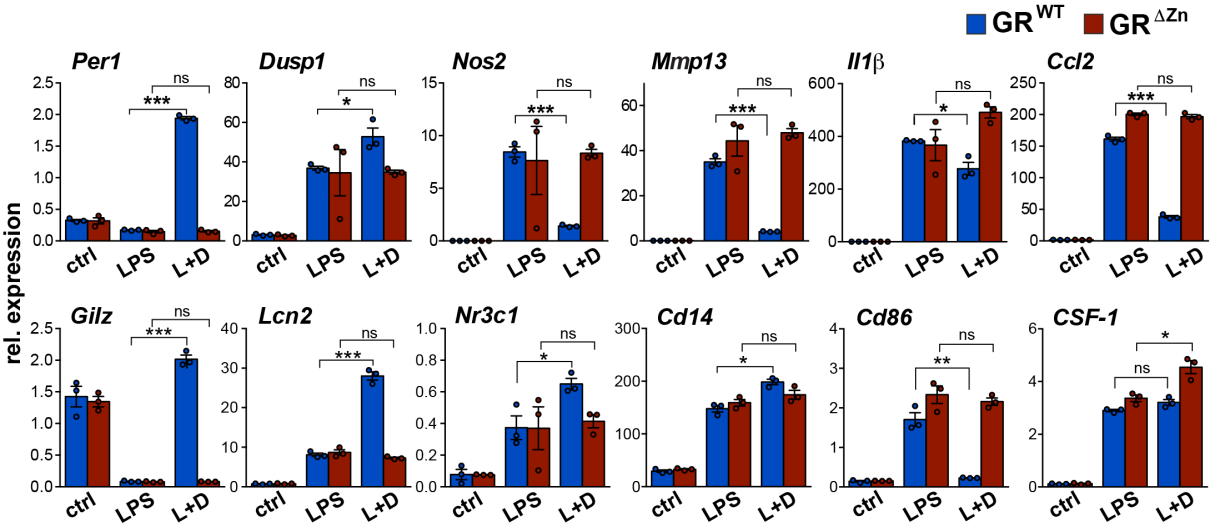

Figure 29. GR target gene and macrophage markers expression in foetal liver macrophages. qRT-PCR of target genes (normalised to *U36b4*) upon treatment with vehicle (ctrl), 16 h Dex, 6 h LPS and 6 h LPS + 16 h Dex (L+D). Wild type and $GR^{\Delta Zn}$ E13.5 liver-derived macrophages. Values represent mean ± SEM, n = 3, *p<0.05, **p<0.01, ***p<0.001 and ns = not significant. Student's t-test. *Cd14*, *Cd86* and *CSF-1* are macrophage markers.

Taken together, these results show that three different cell types, i.e. MEFs, liver and macrophages, show the same pattern of extended loss of binding and importantly, absence of regulation of all tested GR target genes. Moreover, these results underline the importance of direct DNA binding by GR for transcriptional immunomodulation.

4.7 GR DNA binding is required for the recruitment of co-regulators

4.7.1 Loss of GRIP-1 co-regulator interaction by ChIP coupled to mass spectrometry in $GR^{\Delta Zn}$

Since $GR^{\Delta Zn}$ binds a subset of loci but does not regulate nearby genes, one possibility is that the recruitment of co-regulators might be affected by the DNA-binding impairment mutation. To further characterise the assembly of transcriptional co-regulator complexes, ChIP coupled to mass spectrometry (ChIP-MS) was performed in LPS and Dex treated MEFs. Wild type and mutant GR were immunoprecipitated and proteomic analysis was performed in collaboration with Dr Michael Wierer.

Robust interactions between GR and its known co-regulators glucocorticoid receptor-interacting protein1 (GRIP-1), C/EBPβ, p300, CREB-binding protein (CBP), p65, switch/sucrose non fermentable (SWI/SNF) and others were detected in wild type MEFs (**Figure 30A**). Complete list of proteins are shown in **Supplementary List 3**.

When comparing proteins significantly enriched in wild type or $GR^{\Delta Zn}$ MEFs, interactions with NF-κB as well as many others were maintained in mutant MEFs. However, there was reduced recruitment of 1) GRIP-1, also known as nuclear receptor coactivator 2 (NCoA-2), steroid receptor coactivator 2 (SRC-2) or translation initiation factor 2 (TIF-2), 2) some components of the SWI/SNF complex, 3) the histone acetyl transferase (HAT) CBP, 4) p300, 5) C/EBPβ, 6) the co-activator transcription factor 20 (TCF20) and 7) the co-repressor transducin-like enhancer protein 3 (TLE3) (**Figure 30B**). Single peptide counts for these proteins are shown in **Figure 31A**. The biological annotations of the proteins pulled down were nuclear proteins with chromosome, chromatin and nucleosome organisation functions (**Figure 31B**).

Impaired GRIP-1 recruitment by $GR^{\Delta Zn}$, a member of the p160/SRC family, could explain the lethality and absence of transcriptional regulation. GRIP-1 plays a key role in the suppression of inflammatory responses by glucocorticoids (Chinenov et al. 2012, Uhlenhaut et al. 2013). Also, HAT complexes are often recruited by NRs to activate target genes. Therefore, loss of interaction with p300/CBP could explain the transcriptional inactivity of $GR^{\Delta Zn}$ (Uhlenhaut et al. 2013). Also, the interaction with some of the components of the SWI/SNF complex was partially lost, suggesting that SWI/SNF might play a role in transcriptional repression by GR (John et al. 2008).

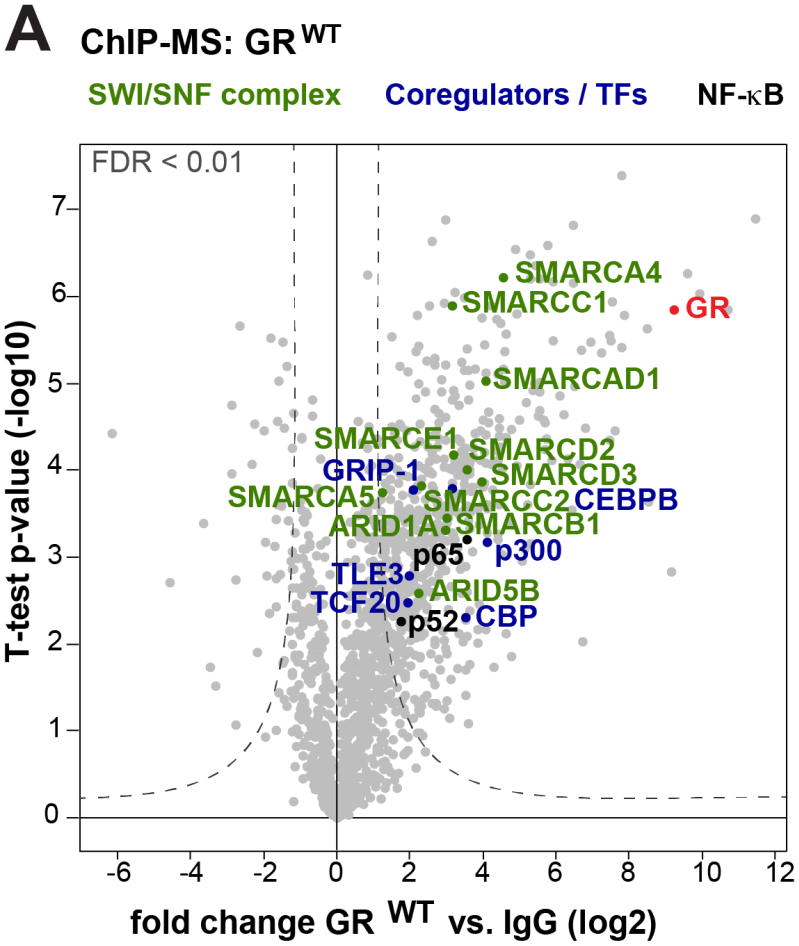
A
ChIP-MS: GR WT
SWI/SNF complex
Coregulators / TFs
NF-κB
FDR < 0.01
T-test p-value (-log10)
fold change GR WT vs. IgG (log2)
SMARCA4
SMARCC1
GR
SMARCAD1
SMARCE1
SMARCD2
GRIP-1
SMARCD3
SMARCA5
SMARCC2
CEBPB
ARID1A
SMARCB1
p65
p300
TLE3
ARID5B
TCF20
p52
CBP

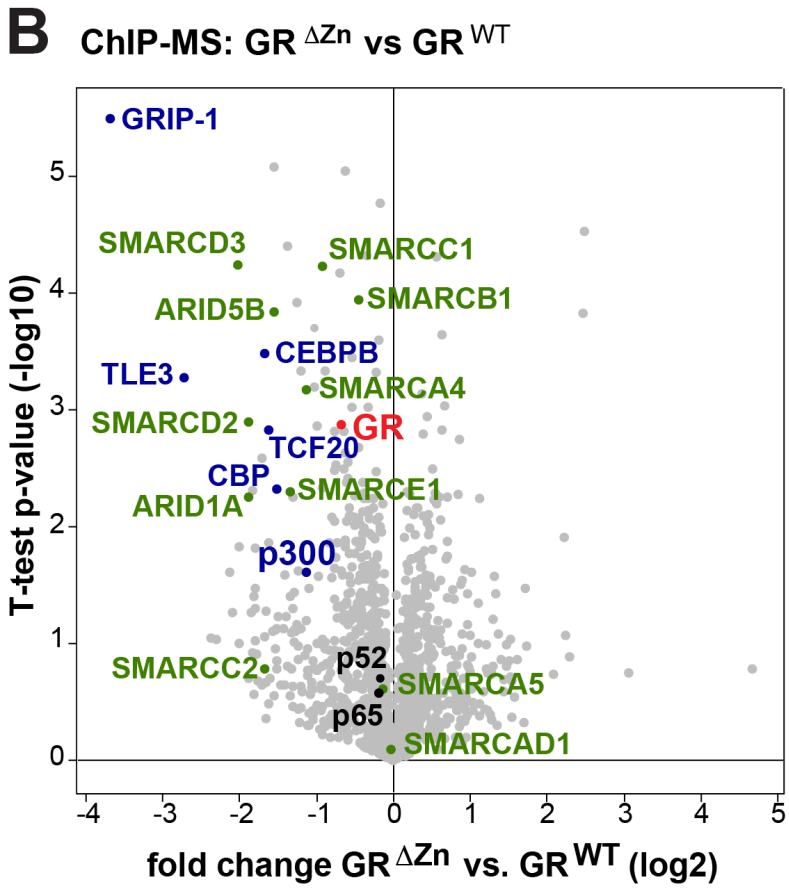
B
ChIP-MS: GR ΔZn vs GR WT
T-test p-value (-log10)
fold change GR ΔZn vs. GR WT (log2)
GRIP-1
SMARCD3
SMARCC1
SMARCB1
ARID5B
CEBPB
TLE3
SMARCA4
SMARCD2
GR
TCF20
CBP
SMARCE1
ARID1A
p300
SMARCC2
p52
SMARCA5
p65
SMARCAD1

Figure 30. Protein interactions with GR in LPS and Dex treated MEFs.
A, ChIP followed by mass spectrometry for GR in 3 h LPS + 16 h Dex treated wild type MEFs. Plot shows selected significantly enriched proteins in GR IP samples versus IgG. P-values versus the log2 fold enrichment between GR over IgG are plotted. **B**, Volcano plot showing peptides fold change in $GR^{\Delta Zn}$ IP versus wild type log2. Student's t-test with FDR<0.01, n = 3 replicates per genotype.

A Peptide counts

	GR WT1	GR WT2	GR WT3	GR ΔZn1	GR ΔZn2	GR ΔZn3
ARID1A	9	11	12	4	5	4
ARID5B	5	5	5	4	2	5
CBP/CREBPB	13	17	17	13	12	9
CEBPB	6	5	6	3	3	2
GR	39	39	38	35	39	37
GRIP-1	5	7	6	1	1	1
p300	19	19	19	9	9	11
p52 / NFKB2	7	6	7	5	7	5
p65/RelA	7	7	10	9	8	7
SMARCA4	17	22	19	12	12	13
SMARCA5	14	14	13	14	15	11
SMARCAD1	16	15	12	17	17	16
SMARCB1	7	8	8	7	9	9
SMARCC1	13	10	11	7	9	8
SMARCC2	11	12	12	1	6	7
SMARCD2	10	9	11	8	8	5
SMARCD3	8	10	10	4	4	5
SMARCE1	6	6	6	4	4	5
TCF20	28	27	28	26	25	25
TLE3	27	26	27	nd	nd	nd

B Protein functional annotation

Process description	FDR q-value
Protein-DNA complex subunit organization	1.63E-1
Chromosome organization	2.16E-1
DNA metabolic process	1.45E-1
Chromatin organization	2.23E-1
Nucleosome organization	2.32E-1

Figure 31. Peptide counts and protein functional analysis of ChIP-MS.
A, Peptide counts for selected proteins from **Figure 29** in three biological replicates, nd = not detected. **B**, Functional annotation of peptides enriched in wild type and mutant interactomes. Analysis tool: GOrilla.

In summary, our results suggest that direct DNA binding by GR is required for the assembly of a functional co-activator/co-repressor complex to regulate both transcriptional activation and repression.

4.7.2 RNA-Seq expression of the detected co-regulators

Next, loss of GRIP-1, some components of the SWI/SNF complex and the histone acetyl transferases CBP and p300 was studied in more depth. Transcript levels of the aforementioned proteins were studied to rule out the possibility of lower peptide detection due to lower expression and not an interaction with GR. **Table 8** shows the DESeq normalised counts of these factors in the LPS and Dex RNA-Seq data. No changes were detected in these factors at the mRNA level between wild type and $GR^{\Delta Zn}$ MEFs. Therefore, the transcription factors and chromatin remodellers are

equally expressed, but the interaction with GR is lost, presumably due to impaired DNA binding.

To note, the ChIP-MS method pulls down chromatin-bound GR as well as non-bound GR. Therefore, the interactions observed could theoretically also be from chromatin bound as well as 'free' GR. Also, the interaction with GR is not necessarily direct since the chromatin is crosslinked with formaldehyde.

Table 8. Average of DESeq normalised transcript levels of selected peptides from ChIP-MS.

Gene name	GR^{WT}	$GR^{\Delta Zn}$
Arid1a	2857	3058
Arid5b	2020	1754
Cbp/Crebbp	876	951
Cebpb	258	334
GR (Nr3c1)	1535	2282
Grip-1/Ncoa-2	861	769
p300	1702	1764
p52/Nfkb2	3871	6950
p54/Rela	2649	3844
Smarca4	5718	6058
Smarca5	4564	4934
Smarcad1	826	869
Smarcb1	1975	2007
Smarcc1	4701	4507
Smarcc2	2662	2660
Smarcd2	1500	1456
Smarcd3	371	187
Smarce1	2842	2857
Tcf20	2225	2429
Tle3	1507	1565

In summary, some protein interactions were maintained in $GR^{\Delta Zn}$ while other interactions (i.e. GRIP-1) were lost and, therefore, are to some extent DNA-binding dependent. Also, the changes in protein-protein interactions observed in $GR^{\Delta Zn}$ were not explained by lower expression of the selected proteins at the transcript level.

4.7.3 Validation of the loss of GRIP-1 recruitment by ChIP-qPCR

In order to validate the loss of GRIP-1 observed in the proteomics experiments, GRIP-1 ChIP-qPCR was performed in LPS and Dex treated MEFs. As shown in **Figure 32A**, wild type GR was enriched at loci near *Per1, Gilz, Ccl2, Il6, Fkbp5* and *Klf9*. At most of these sites $GR^{\Delta Zn}$ failed to recruit GRIP-1. Importantly, GRIP-1 protein levels were similar between wild type and mutant MEFs treated with LPS and Dex (**Figure 32B**). These results suggest that GRIP-1 is equally available in wild type and mutant MEFs and the recruitment to specific loci is specifically impaired.

In conclusion, GRIP-1 recruitment to chromatin-bound GR is reduced in $GR^{\Delta Zn}$, likely due to the DNA binding impairment caused by the zinc finger mutation.

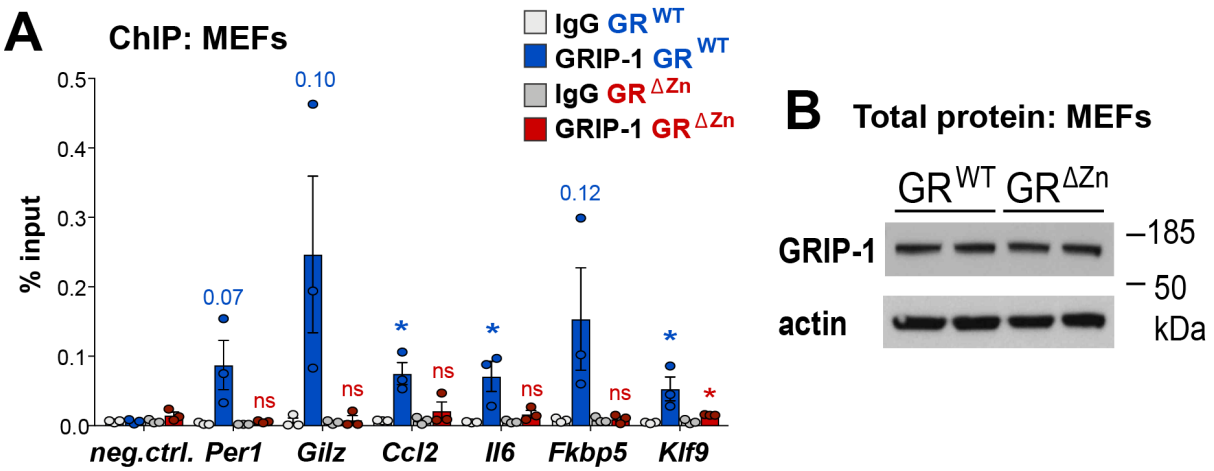

Figure 32. Validation of the loss of GRIP-1 recruitment.
A, GRIP-1 ChIP-qPCR in MEFs treated with LPS for 3 h and 16 h Dex. Values are mean ± SEM % input, from n = 3, *p<0.05. Student's t-test. **B**, Western blot showing total GRIP-1 protein levels in wild type and $GR^{\Delta Zn}$ MEFs treated with Dex for 16 h and LPS for 3 h. Representative blot from (n = 3).

4.8 SWI/SNF complex knock-down screen in MEFs

Several components of the SWI/SNF complex were pulled down together with GR in MEFs. The subunits that interact with wild type GR are: ARID1A, ARID5B, SMARCA4 (also named BRG1), SMARCA5, SMARCAD1, SMARCB1, SMARCC1, SMARCD2, SMARCD3 and SMARCE1. Surprisingly, the interaction with SMARCA5 and SMARCAD1 was maintained in $GR^{\Delta Zn}$, suggesting that it does not require DNA-bound GR. The interaction with the following subunits was slightly decreased in mutant MEFs compared to wild type: SMARCA4, SMARCB1, SMARCC1, SMARCC2 and SMARCE1. Finally, the interaction with ARID1A, ARID5B, SMARCD2 and SMARCD3 was lost in mutant GR MEFs. The gene names of SWI/SNF subunits identified by ChIP-MS and the human homologue names are shown in **Table 9**.

Table 9. Gene names of selected SWI/SNF complex homologues.

Mouse	Human
*Arid1a**	*BAF250A*
*Arid1b**	*BAF250B*
*Arid5b**	*ARID5B*
*Smarca4**	*BRG1*
Smarca5	*SMARCA5*
Smarcad1	*SMARCAD1*
Smarcb1	*BAF47*
Smarcc1	*BAF155*
Smarcc2	*BAF170*
*Smarcd1**	*BAF60A*
*Smarcd2**	*BAF60B*
*Smarcd3**	*BAF60C*
*Smarce1**	*BAF57*

* subunit tested by siRNA in MEFs

Next, the role of the SWI/SNF chromatin remodelling complex in transcriptional immunomodulation by GR was further investigated. Therefore, siRNA knock-down experiments were performed in wild type MEFs. Eight subunits of the complex were independently silenced, cells were stimulated with control, LPS or LPS and Dex and target gene expression was measured.

Overall, the effect of single knock down of SWI/SNF components was surprisingly modest. However, as shown in **Figure 33A**, decreased *Smarca4* transcript levels lead to strong activation of *Per1* and *Gilz* upon treatment with LPS and Dex. The knock-down efficiencies were greater than 70% and is shown for each subunit in **Figure 33B**. The strong induction of *Per1* and *Gilz* was significantly greater than in wild type MEFs. Regarding gene repression, siRNA against *Smarca4* had no effect on the down-regulation of *Ccl2* and *Il6.* Opposite results were obtained when *Arid1b* was knocked down. Activation of *Per1* and *Gilz* was unaffected. However, the repression of *Ccl2* and *Il6* was affected by silencing of *Arid1b. Il6* repression was down to 35% (normalised to 100% LPS induction) in the presence of Dex in scramble cells and went down to only 57% in si-*Arid1b*. These results hint at ARID1B playing a role in the repression of inflammatory genes and SMARCA4 in activation. An example for a knocked down subunit, *Smarcd1,* with no effect on activated or repressed genes is shown in **Figure 33A**&**B**, for comparison.

The following subunits were tested but had no effect either in activated or repressed GR target genes: *Arid1a, Arid5b, Smarcd2, Smarcd3* and *Smarce1.* Results including knock-down efficiencies are shown in **Supplementary Figure S1**. The double and triple knock-down for *Smarcd* subunits was performed with no significant changes compared to scramble samples: *Smarcd1* + *Smarcd2*, *Smarcd1* + *Smarcd3, Smarcd2* + *Smarcd3* and *Smarcd1* + *Smarcd2* + *Smarcd3* (data not shown). None of the combinations had an effect on *Per1, Gilz*, *Ccl2* or *Il6*.

In conclusion, the SWI/SNF chromatin remodelling complex seems to play a role in the repression of inflammatory genes by GR. This molecular mechanism is complex since it is subunit- and locus-specific. The crosstalk between GR and SWI/SNF under inflammatory conditions is still largely unexplored.

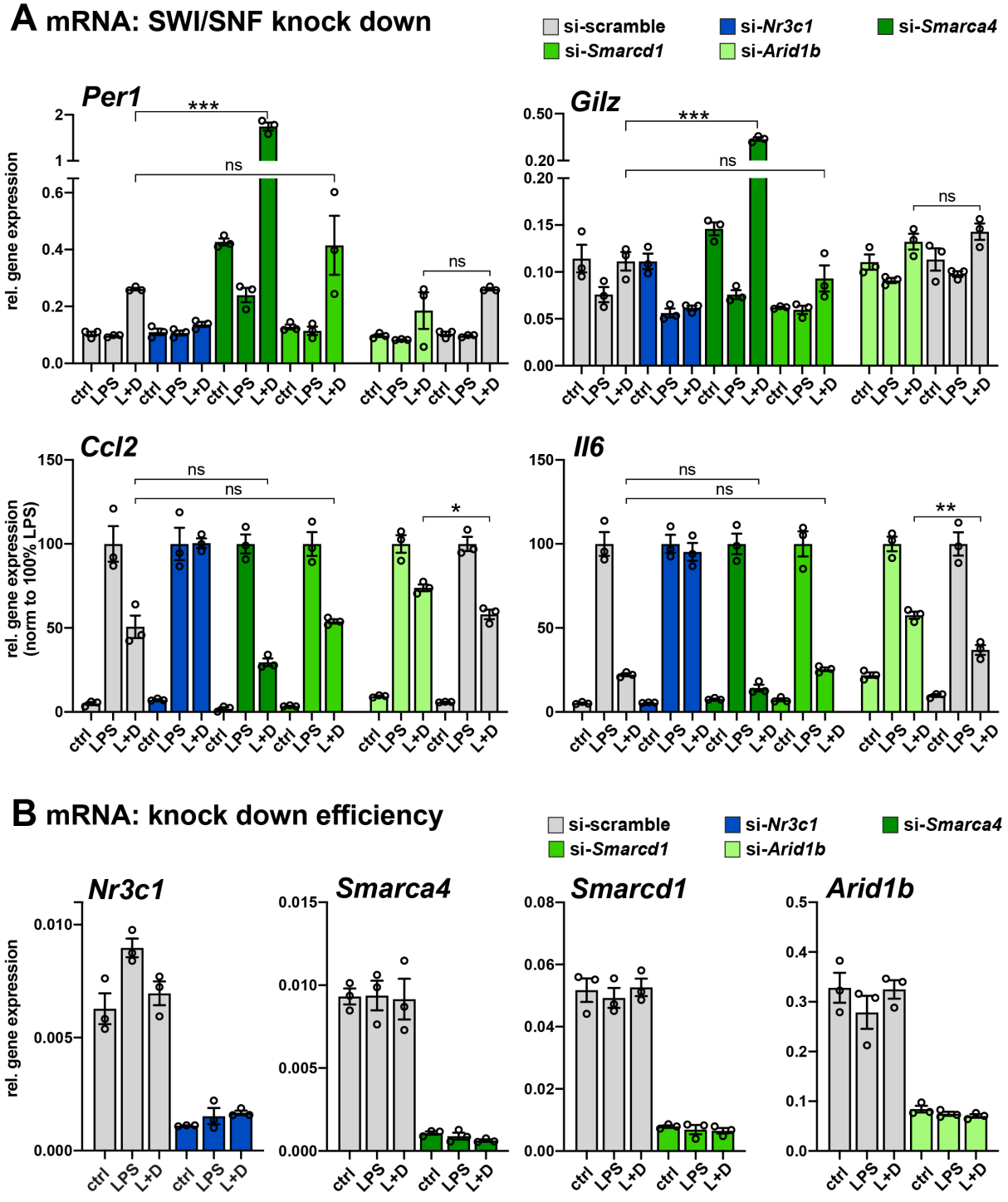

Figure 33. SWI/SNF complex knock down with siRNA in MEFs.
A, qRT-PCR of target genes (normalised to *U36b4*) upon treatment with vehicle (ctrl), 16 h Dex, 6 h LPS and 6 h LPS + 16 h Dex (L+D). Wild type GR MEFs with non-targeted siRNA (scramble), siRNA against *Nr3c1*, *Smarca4*, *Smarcd1* or *Arid1b*. Values represent mean ± SEM, n = 3, *p<0.05, **p<0.01, ***p<0.001 and ns = not significant. Student's t-test. **B**, qRT-PCR to validate knock down efficiency (normalised to *U36b4*).

4.9 Regulation of functional enhancers requires sequence recognition by GR

Next, the functionality of $GR^{\Delta Zn}$ regarding transcriptional activation and repression was investigated using *in vitro* in luciferase assays. GRE-containing *cis*-regulatory elements from activated and repressed genes were analysed. CV-1 cells were transiently transfected with promoter and enhancer reporter constructs regulated by GR. CV-1 cells are non-steroidogenic monkey kidney-derived fibroblasts. Cells were cultured in medium supplemented with vehicle, Dex, LPS or LPS+Dex. Luciferase activity was measured and normalised to Renilla activity for transfection efficiency. Indeed, all the transcriptional effects of wild type GR in presence of Dex were absent in the $GR^{\Delta Zn}$ expression constructs in either positive or negative genomic fragments (**Figure 34A**).

Furthermore, four other single point human GR mutants where the cysteine zinc finger structure is unchanged also failed to activate or repress the GRE-containing reporter sequences *Lpin1*, *Btg1* and *Il6*. Those mutants were previously shown to abolish GR DNA binding (Hollenberg and Evans 1988) (**Figure 34B**&**C**).

To sum up, the results obtained in MEFs were confirmed in the liver, macrophages and using luciferase reporter assays. Both murine and human $GR^{\Delta Zn}$ fail to activate or repress *cis*-regulatory elements. Importantly, other GR DBD single mutations show similar effects even when the four-cysteine zinc fingers are unmodified. This suggests that not only the zinc fingers but the whole DBD is likely required for activation and repression. However, the respective mouse mutants would need to be generated to evaluate the effect of each amino acid *in vivo*.

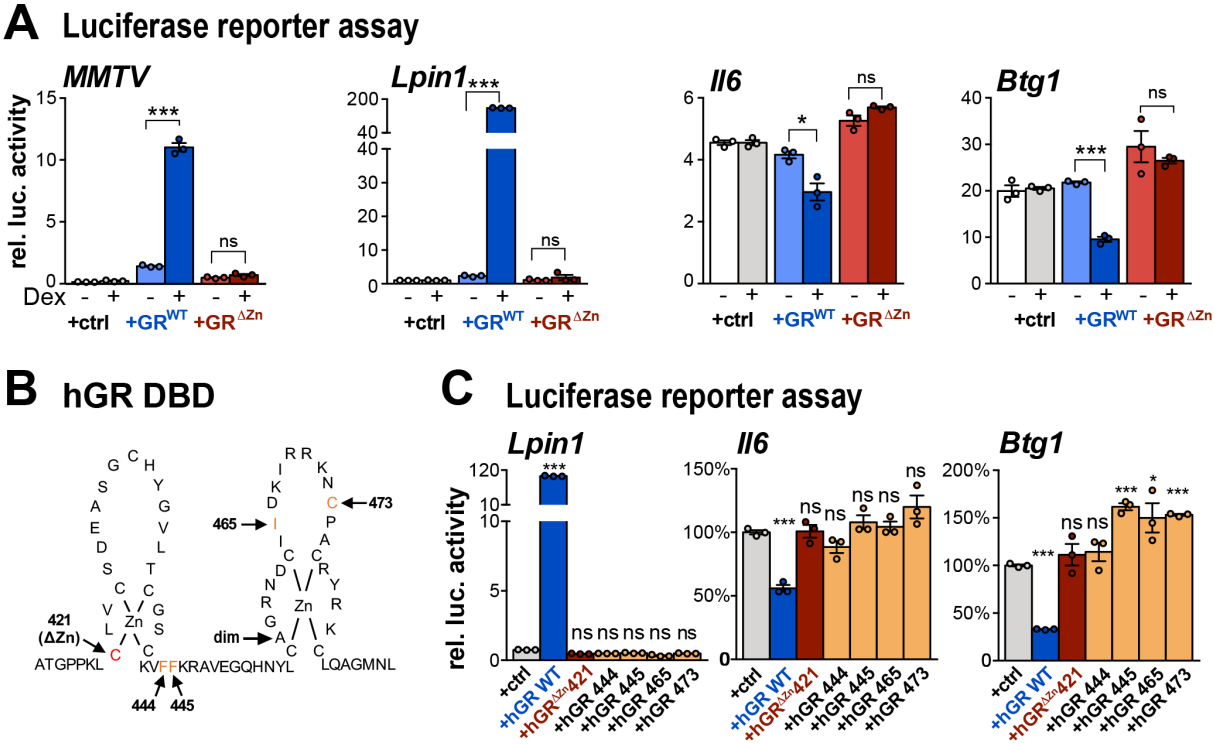

Figure 34. Luciferase reporter assay with wild type and GR$^{\Delta Zn}$ and human GR DBD mutants.
A, Luciferase activity relative to Renilla in CV-1 cells overexpressing empty vector (+ctrl), wild type murine GR or ΔZn mutant and *MMTV*, *Lpin1*, *Il6* or *Btg1* reporters. For *MMTV* and *Lpin1* cells were treated with vehicle or Dex for 16 h. For *Il6* and *Btg1* cells were treated with either with LPS or LPS+Dex for 16 h (n = 3 biological replicates). **B**, Human GR DNA binding domain (DBD) showing the mutations from **C. C**, Luciferase activity relative to Renilla in CV-1 cells overexpressing empty vector (+ctrl), human GR wild type, ΔZn (hGR C421G), F444G, F445G, I465G and C473G mutants. For *Lpin1* cells were treated with Dex for 16 h. For *Il6* and *Btg1* cells were treated with either with LPS+Dex for 16 h. **A**&**B** Values represent mean ± SEM, n = 3, ***p<0.001, *p<0.05 and ns = not significant. Student's t-test.

5. Discussion

The aim of this project was to study direct DNA binding by GR as a mechanism for immunomodulation of target genes *in vivo*. With this purpose, the $GR^{\Delta Zn}$ mouse line, which is deficient in the recognition of GREs, was generated.

The main conclusion of this work is that direct DNA binding by GR is absolutely required for both transcriptional activation and, importantly, the repression of inflammatory genes. $GR^{\Delta Zn}$ mice and cells showed no response to glucocorticoids in any of the tested conditions, despite the fact that ligand binding, nuclear localisation, protein expression, protein-protein interactions and tethering to chromatin-bound factors were preserved.

This discovery has important implications for the development of novel glucocorticoid receptor agonists or modulators with reduced side effect profiles (Sundahl et al. 2015), and has deepened our understanding of transcriptional regulation by GR.

5.1 DNA binding by GR is required for survival

Generally, GR is thought to dimerise and bind GREs to activate target genes. On the other hand, indirect interaction of GR with chromatin by tethering, for example by binding AP-1 or NF-κB proteins instead of GRE sequences, is proposed to mediate negative regulation (Cain and Cidlowski 2017, Greulich et al. 2016, Sundahl et al. 2015). Many mechanistic studies on the suppression of inflammatory responses by GR have therefore focused on protein-protein interactions with transcription factors such as AP-1 or NF-κB (Schule et al. 1990, Reichardt et al. 1998, Ogawa et al. 2005, Cain and Cidlowski 2017).

Initially, the GR^{dim} mouse was designed to assess the relative importance of DNA binding-dependent versus -independent mechanisms *in vivo*. With this purpose, a GR mutation (human A458T, mouse A465T, rat A477T) was introduced that impairs dimerisation of the receptor. The concept was that gene activation requires dimerisation of the receptor via recognition of a classical GRE motif. However, transrepression occurs potentially via monomeric GR tethering to DNA-bound transcription factors such as AP-1 or NF-κB. Thus, dimerisation-defective GR^{dim} mice were generated to study the DNA-independent functions of GR. Intriguingly, mice born

with this mutation survived on certain backgrounds (Reichardt et al. 1998), and simple inflammatory models, such as phorbol ester-induced skin irritation, responded to GC treatment in these animals. These mice had normal lungs and adrenal glands but decreased up-regulation and maintained down-regulation of some target genes. Therefore, it was concluded that the GR monomer and thus transrepression by tethering might be sufficient to reduce inflammation. However, for most other inflammatory models, GC failed to have an effect in GR^{dim} mice (Vandevyver et al. 2012, Silverman et al. 2013, Kleiman et al. 2012). Analyses of GR^{dim} mutants initially supported the tethering model, but in the meantime GR was found to actually bind DNA, calling for re-interpretation and re-analysis (Reichardt et al. 1998, Presman et al. 2014, Lim et al. 2015). Taken together, these observations strongly suggest that GR^{dim} is a relevant model to study the monomeric actions of the receptor. However, other models might be more suitable to study DNA-binding independent mechanisms of repression, for example the $GR^{\Delta Zn}$ mouse line reported here, in which GR does not bind GREs but retains protein interactions with NF-κB.

Later on, characterisation of GR binding sites in BMDM, associated with repressed inflammatory target genes, surprisingly revealed GREs to be significantly enriched. This observation underlined the potential role of direct DNA binding as a mechanism of inflammatory gene repression (Uhlenhaut et al. 2013, Hemmer et al. 2019).

Over the past three decades, numerous studies have investigated the effects of mutations in GR and transcriptional output *in vitro.* In particular, Hollenberg and Evans characterised the effect of several hGR DBD point mutations in transcriptional activation by CAT reporter assays as well as DNA binding by gel shift assays. The authors dissected the trans-activation properties of hGR and identified eight conserved cysteines as well as amino acids in the first half of the interfinger region to be critical for DNA binding. Overall, a high correlation between DNA binding and transcriptional activation was observed in hGR DBD mutants, indicating the importance of DNA binding for GR transcriptional regulation (Hollenberg and Evans 1988).

Based on these *in vitro* results, the hGR C421G (mouse C437G) mutation was selected for this study because it abolishes GRE binding as well as gene regulation. In this project, the effect of the GR C437G mutation in transcriptional regulation was investigated *in vivo*. First, the loss of DNA binding in murine GR C437G was validated

by the gel shift assay. Then, the $GR^{\Delta Zn}$ mouse line was generated by traditional embryonic stem (ES) cell targeting, and heterozygous breeding was set up (**Figure 7&8**). Contrary to GR^{dim} mice, homozygous $GR^{\Delta Zn}$ were not viable and died shortly after birth due to atelectasis and respiratory failure. Furthermore, embryonic adrenal glands were enlarged and presented increased expression of steroidogenic cytochrome P450 enzymes. Remarkably, the phenotype of $GR^{\Delta Zn}$ resembled that of the GR global knockout phenotype, as GR is required to promote surfactant synthesis in alveolar epithelial cells and the development of adrenal chromaffin cells (Cole et al. 1995, Mendelson and Boggaram 1991) (**Figure 9**).

To put into perspective the relevance of the fact that DNA-binding deficient $GR^{\Delta Zn}$ mice are not viable, it should be mentioned that other steroid hormone receptor global knockout mice such as progesterone (PR^{KO} (Lydon et al. 1996)), androgen (AR^{KO} (Yeh et al. 2002)) or oestrogen receptor knock out (ER^{KO} (Antonson et al. 2012)) mice can live, with various severe reproductive impairments, and similar to GR^{KO} mice, mineralocorticoid MR^{KO} are not viable. Pups die several days after birth due to impaired renal sodium reabsorption (Berger et al. 1998).

Several GR mutant mouse models have been studied, for example GR K293R (human K310) sumoylation-deficient mice. Treatment with Dex was shown to not efficiently reduce TPA-induced skin inflammation in GR K310R mice. Also, the NCoR1/SMRT co-repressor complex formation to tethered transrepression sites was reduced in GR K310R mice (Hua et al. 2016a, Hua et al. 2016b). Another knockin mouse line solely expressing the GR-C3 isoform was generated by Cidlowski and colleagues. GR-C3 mice died at birth and were hypersensitive to LPS administration, suggesting that the GR-C3 isoform plays a role in the repression of inflammatory genes (Oakley et al. 2018).

Since homozygous $GR^{\Delta Zn}$ mice are not viable, primary MEFs were used to further dissect the mechanisms of gene repression. Importantly, mRNA, protein and phosphorylation levels were unchanged in $GR^{\Delta Zn}$ MEFs (**Figure 10-12**). This indicates that the protein functionality was unaffected by the mutation, in terms of full length transcript translation and the protein conformation (Chen et al. 2008, Blind and Garabedian 2008, Webster et al. 1997). Moreover, the phosphorylation of AKT and ERK1/2 in response to short treatment with Dex were maintained, suggesting that

potential non-genomic actions including crosstalk with the MAPK signalling pathway were preserved (Matthews et al. 2008). Also, the nuclear translocation after treatment with Dex was maintained in $GR^{\Delta Zn}$ MEFs. These results suggest that the protein conformation, interactions with cytoplasmic proteins and ligand binding were not strongly affected by the DBD mutation.

In summary, the first part of this work shoed that DNA binding-deficient $GR^{\Delta Zn}$ mice die due to respiratory failure and present a GR^{KO}-like phenotype, including enlarged adrenal glands and up-regulation of CGs synthesis enzymes. The mutant $GR^{\Delta Zn}$ protein is expressed, phosphorylated and translocates to the nucleus in the presence of a ligand.

5.2 Tethered binding sites are found near inflammatory genes, but gene regulation by GR requires DNA binding

ChIP-Seq for GR was performed in wild type and mutant MEFs treated with LPS and Dex to study the binding across the genome (**Figure 13**&**14**). Intriguingly, out of the 23,039 sites bound by wild type GR, only 20% were retained in $GR^{\Delta Zn}$ expressing MEFs. This new observation suggests that an intact DBD domain is required for binding to about 80% of sites. The top known non-repetitive motifs enriched in the GR wild type cistrome were AP-1, C/EBP, GRE, NF-κB and IRF, while for the GR mutant they were AP-1, C/EBP, NF-κB and IRF (**Figure 15**). Importantly, GREs or half GREs were not enriched in the mutant cistrome, indicating that $GR^{\Delta Zn}$ does not recognise GREs. Also, the distribution of peak distance to the nearest TSS of the $GR^{\Delta Zn}$ cistrome was similar to that of wild type GR. In line with previous studies, tethered binding sites were more abundant near repressed target genes than activated genes (**Figure 16**&**17**).

Depending on the cell type and context, GR can tether to different factors for transcription regulation, for example AP-1, NF-κB or STAT3 (Scheschowitsch et al. 2017, Ray and Prefontaine 1994, Langlais et al. 2012). In line with these previous observations, the NF-κB subunit p65 was detected by western blot when pulled down together with both wild type and mutant GR in endogenous Co-IPs (**Figure 18**). It should be noted that tethering to AP-1 or other factors cannot be ruled out.

Perhaps the most striking observation was the fact that no gene was differentially regulated upon treatment with Dex alone or in combination with LPS in $GR^{\Delta Zn}$ MEFs. Genes with a nearby tethered site were surprisingly not regulated. These results directly challenge the model of repression of inflammatory genes via transrepression. Various ligand concentrations and times were examined, with the same result of binding at inflammatory *Ccl2* and *Il6* genes with absence of transcriptional regulation (**Figure 19**-**21**).

Cell type-specific gene regulation depends on the exposure of binding sites through open chromatin state, which is largely dependent on chromatin accessibility (John et al. 2011). The pro-inflammatory TFs, AP-1 and NF-κB co-localise in a large subset of binding sites with GR. Also, AP-1 seems to be critical for the recruitment of GR to regulatory sites as well as to prime open chromatin (Biddie et al. 2011). Similarly, the crosstalk between p65 and GR goes in both directions. Chromatin occupancy by GR was altered by p65 activation and vice versa (Rao et al. 2011). Importantly, the observations made in MEFs were also true in other cell types, such as the metabolic organ foetal liver as well as foetal macrophages. In both cases, the majority of chromatin binding was lost in $GR^{\Delta Zn}$, with the exception of *Hilpda* in the liver and *Il1β* and *Ccl2* in macrophages (**Figure 27**-**29**). In the liver, GR is known to regulate glucose and lipid metabolism. Interestingly, GREs were found near both activated and repressed genes regulated by GR in liver tissue (Hemmer et al. 2019, Quagliarini et al. 2019).

The exact DNA motif recognised and bound by GR is another key component of the transcriptional regulation by GR. An intriguing concept is the 'negative GRE' (nGRE), a GRE motif in the promoter or close to a GR-repressed gene. The definition of nGRE, however, has not yet reached a consensus. Nowadays, an imperfect GRE motif near a repressed gene is sometimes also called an nGRE. Similarly, the nGRE variation 'inverted repeat' (IR) nGRE has been described to play a role in GR-mediated repression (Surjit et al. 2011). Interestingly, the $GR^{\Delta Zn}$ cistrome did not present significantly enriched GREs, half GREs or GRE-like motifs. Also, overlapping motifs or 'composite' elements between GR and other TFs could explain the absence of perfect GREs in GR binding sites near regulated genes, for example the pIfG element at the promoter of the *proliferin* gene, which contains overlapping AP-1 and GR consensus

motifs (Mordacq and Linzer 1989, Miner and Yamamoto 1992). The characterisation of overlapping motifs is challenging due to the high complexity and endless combinations possible. The exact motif sequence might influence transcriptional regulation as well, i.e. a novel GR binding site (AATTT) inside the NF-κB consensus motif. Crystal structures of the human GR DBD have been reported to directly bind to the promoter regions of the *Ccl2*, *Il8*, *Plau*, *Relb* and *Icam1* genes harbouring this conserved AATTT sequence (Hudson et al. 2018). Therefore, even though our observations suggest that tethering is not sufficient for the anti-inflammatory actions of GR, it might be required for a specific conformational change or to strengthen interactions required for repression. Also, additional requirements for GREs, half sites or cryptic motifs with the tethered peak or a nearby ChIP-Seq peak might be necessary for gene repression.

In the future, more refined bioinformatic tools such as machine learning or deep learning might help decipher novel motifs and/or new key factors of *cis*-regulatory elements (Zhou et al. 2018). Furthermore, the crystal structure of $GR^{\Delta Zn}$ DBD bound (or not) to different DNA fragments harbouring NF-κB, AP-1, STAT3 and/or other motifs would elucidate whether binding is dependent on tethering TFs or is direct tethering-facilitated DNA binding to unknown motifs by $GR^{\Delta Zn}$.

Importantly, other NR mouse mutants have been shown to dissociate DNA binding-dependent and independent actions. In particular, deletion of the DBD of the transcriptional repressor Rev-Erbα showed modulation of a subset of metabolic genes by the recruitment of HDAC3 via tethering to cell type-specific TFs. On the contrary, regulation of circadian physiology requires direct DNA binding by Rev-erbα (Zhang et al. 2015). Likewise, a point mutation in the second zinc finger of peroxisome proliferator-activated receptor alpha (PPARα) abrogated metabolic gene activation while anti-inflammatory actions were maintained. Liver-specific expression of this PPARα mutant lacking DNA-binding-dependent activities was found to inhibit hepatic inflammatory responses by transrepression or tethering (Pawlak et al. 2014). On the contrary, the $GR^{\Delta Zn}$ mutant does not separate between activation and repression actions. Transcriptional regulation by GR was lost when DNA binding was impaired which is a particular characteristic that distinguishes it from other groups of NR.

The addition of 3D genomic techniques such as Hi-C and 4C can study the dynamics of enhancer promoter looping interaction modulation in the presence of a ligand in the context of immunomodulation by GR (Kempfer and Pombo 2020). It is unclear to what extent the 3D chromatin landscape plays a role in transcription regulation by GR. Promisingly, a recent study found that 7% of chromatin interactions change in response to Dex in human epithelial cells (D'Ippolito et al. 2018). In combination with 3D techniques, higher resolution ChIP techniques (e.g. ChIP-exo and ChIP-nexus) could add another layer of complexity and potentially help to better understand the mechanisms of transcriptional repression (Starick et al. 2015, Lim et al. 2015).

5.3 Recruitment of GRIP-1 and other co-regulators is modulated by chromatin-bound GR

In order to characterise the protein interactome and identify potential new co-regulators, ChIP-MS was performed in MEFs (**Figure 30**&**31**). A graphical summary of the ChIP-MS results is shown in **Figure 35**. The interaction with the NF-κB components p65 and p52, together with other proteins, was maintained in $GR^{\Delta Zn}$ MEFs.

The interaction between GR and NF-κB was described long ago (Ray and Prefontaine 1994). Also, inflammatory suppression by GR is widely believed to happen via tethering to p65. However, GR was shown to be recruited directly to NF-κB response elements, in the absence of p65, arguing against the tethering mechanism (Hudson et al. 2018). Also, the GR cistrome increases in the presence of LPS, suggesting that LPS signalling influences GR binding (Uhlenhaut et al. 2013). Overall, the interaction between GR and p65 seems to be conserved between cell types and retained in $GR^{\Delta Zn}$ MEFs.

The interaction with some subunits of the SWI/SNF chromatin remodelling complex was lost while other subunits were detected. Recruitment of the SWI/SNF complex induces ATP-dependent reorganisation of nucleosomes, which consequently facilitates binding of other TFs. This complex is comprised of two mutually exclusive catalytic subunits, BRG1 (also known as SMARCA4) and BRM. Also, 10 or more BRM/BRG1-associated factors (BAF) proteins form the complex. Importantly,

mutations in the SWI/SNF complex have been identified in approximately 20% of all human cancers (Kadoch et al. 2013, Shain and Pollack 2013). The crosstalk between the SWI/SNF complex and GR in an inflammatory context has not yet been fully studied. However, GR has been shown to directly interact with BAF57, BAF60A and BAF250 (Hsiao et al. 2003, Nie et al. 2000). Importantly, BRG1 has been shown to be required for the recruitment of pioneer factors by GR and proper transcriptional response in human breast cancer cells (Hoffman et al. 2018). Moreover, Dex-induced GR binding was shown to occur with increased recruitment of BRG1 in murine cancer cells (Johnson et al. 2018). Knock down of *Smarca4* and *Arid1b* modestly affected the activation of *Per1* and *Gilz* and repression of *Ccl2* and *Il6, respectively.* However, the knock down of *Arid1a*, *Arid5b*, *Smarcd1*, *Smarcd2*, *Smarcd3* and *Smarce1* had no effect on the transcriptional regulation of *Per1*, *Gilz*, *Ccl2* or *Il6* in MEFs treated with LPS and Dex (**Figure 33**&**S1**).

Surprisingly, the interaction with GRIP-1 was lost in mutant MEFs (**Figure 30**&**32**). This observation was validated by ChIP-qPCR. Also, the total GRIP-1 protein levels were similar between wild type and mutant MEFs. GRIP-1 is also known as SRC-2, NCoA-2 or TIF-2 and belongs to the p160 family, which includes the co-regulators SRC-1, SRC-2 and SRC-3. These factors have been implicated in the regulation of a number of physiological processes, from reproduction and uterine function to energy metabolism and thermogenesis (York and O'Malley 2010). The SRC family of co-activators bind to NRs and facilitate transcription by serving as binding platforms for additional cofactors with chromatin-modifying and remodelling activities. GRIP-1 null mice were described as having serious fertility impairment in both male and female mice, in contrast to SRC-1 or SRC-3 knockout mice (Gehin et al. 2002). Macrophage-specific conditional GRIP-1 depletion dampened the repression of NF-κB target genes by GR. Also, GRIP-1-deficient mice developed signs of LPS-induced shock sooner than wild type mice. Thus, these observations support the model of GRIP-1 serving as a co-repressor of GR anti-inflammatory effects *in vivo* (Chinenov et al. 2012). Moreover, CDK9-mediated phosphorylation of GRIP-1 at specific GC-induced sites was shown to associate with GRIP-1 co-activator, but not co-repressor properties (Rollins et al. 2017). In summary, the exact mechanisms of how GRIP-1 acts as a co-activator or co-repressor remain unknown. However, the recruitment by GR seems to be DNA-dependent, at least in MEFs and under the conditions tested here.

CBP, also known as CREBBP or KAT3A, is a HAT that has been shown to interact with a variety of TFs, including both GR and NF-κB (McKay and Cidlowski 2000). HATs regulate transcription by transferring an acetyl group to a lysine histone residue. Chromatin acetylation is a key mark for transcription regulation. CBP can function both as a co-activator and as a central 'integrator/platform' that assembles multiple TFs on DNA (Kamei et al. 1996). The interaction with the CBP homologue p300, also known as Ep300 or KAT3B, was decreased in $GR^{\Delta Zn}$ MEFs. According to these results, the zinc finger mutation in $GR^{\Delta Zn}$ influences the interaction between GR and CBP/p300.

C/EBPβ is a leucine zipper TF that mediates the acute-phase immune reaction and inflammatory responses, among other processes (Ramji and Foka 2002, Tengku-Muhammad et al. 2000). Importantly, C/EBPβ has been reported to prime chromatin accessibility and GR recruitment in the liver after glucocorticoid injection in adrenalectomised mice (Grontved et al. 2013). The interaction between $GR^{\Delta Zn}$ and C/EBPβ was decreased compared to wild type GR in MEFs, suggesting that recruitment likely depends on direct DNA-bound GR.

The interaction with the transcriptional co-repressor transducin-like enhancer protein 3 (TLE3) and the co-activator transcription factor 20 (TCF20) in $GR^{\Delta Zn}$ MEFs was lost and decreased, respectively. Interestingly, the interaction between these two co-regulators and GR in the context of inflammation has not yet been studied. Therefore, TCF20 and TLE3 represent potential candidates to further study co-regulator crosstalk with GR, for example by performing knock-down experiments in primary macrophages, protein-protein studies by Co-IP and/or the generation of CRISPR/Cas9 knockout lines. Although few studies have focused on the TCF20 co-regulator, the TLE3 co-regulator has been identified to interact with GR in human cells in a Dex-dependent manner by proximity mapping (Lempiainen et al. 2017). TLE3 regulates embryonic development and, when knocked out, embryos die before day E15.5 (Gasperowicz et al. 2013). Further characterisation of the role of TCF20 and TLE3 in the transcriptional immunomodulation of GR might improve our understanding of the immunosuppressive effects of GC.

Several GR DBD mutants, where the cysteines forming the zinc fingers were not affected, also failed to repress in the luciferase reporter assays (**Figure 34**). This observation suggests that the whole DBD is important for transcriptional regulation,

and the other non-cysteine DBD mutations could potentially have the same effects as $GR^{\Delta Zn}$. An interesting experiment would be to exchange the GR DBD for another NR DBD (i.e. testicular receptor 4, TR4) that does not recognise GREs and study transcriptional repression. In that way, one could elucidate whether the recognition of GREs is essential for gene regulation. Alternatively, genomic GRE deletions with CRISPR/Cas9 could show the requirement of GREs in inflammatory repression by GR. However, the usage of CRISPR/Cas9 technology comes with potential off-target effects, making interpretation difficult.

Competition for limited co-factors, also named 'squelching', has been proposed to mediate gene repression by NRs. Whether co-factors are present in limited amounts in a particular cell is controversial. However, in the case of co-factors being indeed limited, the reduced residence time on chromatin or in the nucleus together with failure to recruit GRIP-1 by $GR^{\Delta Zn}$, could affect squelching or the sequestration of co-factors (Schmidt et al. 2016, Clauss et al. 2017). Some studies have reported the redistribution of co-activators consistent with a cofactor squelching model, for example p300 redistribution after treatment with oestrogen in breast cancer cells or p65-mediated cofactor squelching from super enhancers or hotspots to repress cell identity genes (Guertin et al. 2014, Schmidt et al. 2015). However, the physiological relevance of this phenomenon is unclear as well as controversial.

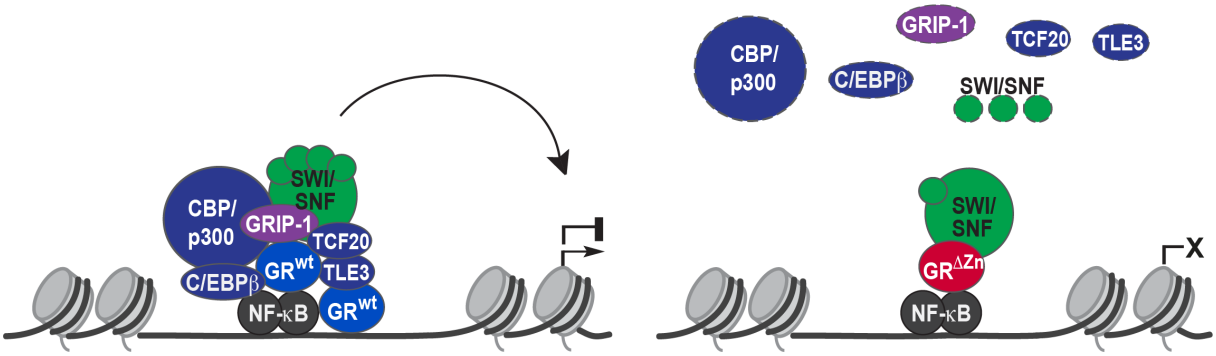

Figure 35. Graphical summary of proteomic results.
Protein interactions were analysed by ChIP followed by mass spectrometry in Dex+LPS-treated MEFs. The interaction with NF-κB some subunits of the SWI/SNF chromatin remodelling complex were maintained. Interaction with GRIP-1, CBP, p300, C/EBPβ, TCF20, TLE3 and some SWI/SNF components was strongly decreased in $GR^{\Delta Zn}$ MEFs.

A phase separation model was proposed to partially explain the formation of super-enhancers and transcriptional control. Like nucleoli, Cajal bodies or other membraneless organelles, super enhancers were proposed to control transcription (Hnisz et al. 2017). Later on, the activation domain (AD) of TFs were reported to form phase-separated condensates with the co-activator Mediator. Also, oestrogen was found to stimulate the formation of droplets in stem cells (Boija et al. 2018, Sabari et al. 2018). Globally, phase separation condensates with high-affinity interactions with Mediator have been proposed to be a general mechanism for gene activation. However, the role of phase separation condensates in gene repression remains unstudied.

5.4 Therapeutic relevance of DNA binding requirement for GR's immunomodulation actions

Selective glucocorticoid receptor agonists (SEGRAs) or selective glucocorticoid receptor modulators (SEGRMs) are novel compounds designed and/or developed to favour the transrepression/tethering actions of GR, but not transactivation, with the argument that GR activates genes by directly binding to DNA and repression occurs via protein-protein interactions. Pharmaceutical companies have developed dissociated ligands favouring GR monomer-dependent beneficial anti-inflammatory effects and reducing undesired GR dimer activation action (Schacke et al. 2007, De Bosscher, Beck and Haegeman 2010). Various selective GR agonists (SEGRAs), such as RU24858 and RU24782, and non-steroidal ligands (LDG552, ZK216348, Compound A), have been studied for desired anti-inflammatory effects with fewer side effects (De Bosscher et al. 2010, Hubner et al. 2015). However, these programs led to only a few novel compounds with promising results in preclinical trials (Vandevyver et al. 2013). The limited success in the translation of SEGRAs to clinical trials warrants for re-interpretation of the basic understanding of transcriptional regulation by GR (Hartmann et al. 2016, Lim et al. 2015, Clark and Belvisi 2012, Schone et al. 2016, Desmet and De Bosscher 2017, Souffriau et al. 2018).

The $GR^{\Delta Zn}$ mouse can separate the direct from the indirect DNA actions of GR. Importantly, $GR^{\Delta Zn}$ mice die, unlike the GR^{dim} mice, highlighting the importance of the direct DNA binding functions of GR. The mutant protein is expressed, translocates to the nucleus upon ligand addition and also tethers to about 20% of genomic binding

sites in an inflammatory context. However, since GRE recognition is impaired, $GR^{\Delta Zn}$ does not regulate any target gene. Moreover, the recruitment of GRIP-1 is impaired in $GR^{\Delta Zn}$ MEFs. This explains, at least partially, the failure to regulate transcription in $GR^{\Delta Zn}$ MEFs. Co-factor squelching or sequestration, chromatin 3D conformation, phase separation or unknown motifs might also play a role, together with tethering in the transcriptional regulation by GR and should be further studied (**Figure 36**).

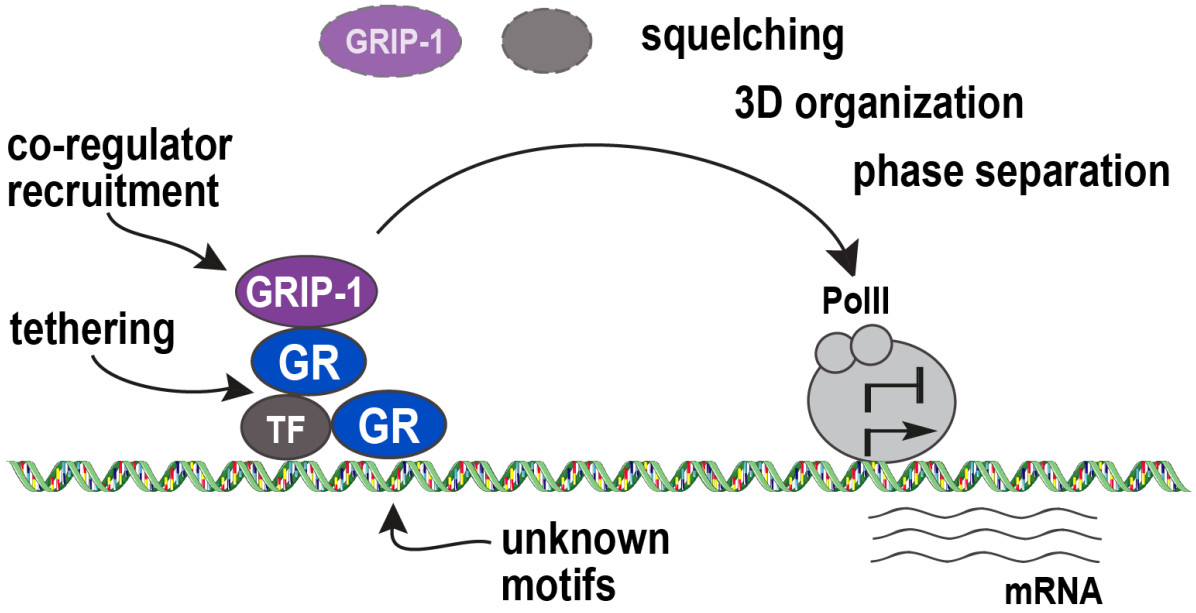

Figure 36. Graphical abstract and proposed mechanism.
GR binding to DNA leads to the recruitment of GRIP-1 and other co-regulators to activate or repress transcription. While tethering still occurs in $GR^{\Delta Zn}$ mice, it is not sufficient to regulate gene expression either positively or negatively. The transcriptional inactivity of $GR^{\Delta Zn}$ mutants could be explained by the failure to recruit co-regulators, or by other mechanisms such as squelching, novel GR binding motifs, 3-dimensional (3D) chromatin organisation and phase separation.

Taken together, these findings emphasise the importance of direct DNA binding for GR for both the activation and repression of inflammatory gene regulation. The observations reported here have important implications for the development of novel glucocorticoid receptor agonists or modulators with reduced side effect profiles, and for the understanding of transcriptional regulation by GR.

References

Abraham, S. M., T. Lawrence, A. Kleiman, P. Warden, M. Medghalchi, J. Tuckermann, J. Saklatvala & A. R. Clark (2006) Antiinflammatory effects of dexamethasone are partly dependent on induction of dual specificity phosphatase 1. *J Exp Med,* 203, 1883-9.

Alnemri, E. S., T. F. Fernandes, S. Haldar, C. M. Croce & G. Litwack (1992) Involvement of BCL-2 in glucocorticoid-induced apoptosis of human pre-B-leukemias. *Cancer Res,* 52, 491-5.

Antonson, P., Y. Omoto, P. Humire & J. A. Gustafsson (2012) Generation of ERalpha-floxed and knockout mice using the Cre/LoxP system. *Biochem Biophys Res Commun,* 424, 710-6.

Aslam, F., V. Shalhoub, A. J. van Wijnen, C. Banerjee, R. Bortell, A. R. Shakoori, G. Litwack, J. L. Stein, G. S. Stein & J. B. Lian (1995) Contributions of distal and proximal promoter elements to glucocorticoid regulation of osteocalcin gene transcription. *Mol Endocrinol,* 9, 679-90.

Auphan, N., J. A. DiDonato, C. Rosette, A. Helmberg & M. Karin (1995) Immunosuppression by glucocorticoids: inhibition of NF-kappa B activity through induction of I kappa B synthesis. *Science,* 270, 286-90.

Balsalobre, A., S. A. Brown, L. Marcacci, F. Tronche, C. Kellendonk, H. M. Reichardt, G. Schutz & U. Schibler (2000) Resetting of circadian time in peripheral tissues by glucocorticoid signaling. *Science,* 289, 2344-7.

Bartholome, B., C. M. Spies, T. Gaber, S. Schuchmann, T. Berki, D. Kunkel, M. Bienert, A. Radbruch, G. R. Burmester, R. Lauster, A. Scheffold & F. Buttgereit (2004) Membrane glucocorticoid receptors (mGCR) are expressed in normal human peripheral blood mononuclear cells and up-regulated after in vitro stimulation and in patients with rheumatoid arthritis. *FASEB J,* 18, 70-80.

Baschant, U., L. Frappart, U. Rauchhaus, L. Bruns, H. M. Reichardt, T. Kamradt, R. Brauer & J. P. Tuckermann (2011) Glucocorticoid therapy of antigen-induced arthritis depends on the dimerized glucocorticoid receptor in T cells. *Proc Natl Acad Sci U S A,* 108, 19317-22.

Beck, I. M., K. De Bosscher & G. Haegeman (2011) Glucocorticoid receptor mutants: man-made tools for functional research. *Trends Endocrinol Metab,* 22, 295-310.

Beck, I. M., W. Vanden Berghe, L. Vermeulen, N. Bougarne, B. Vander Cruyssen, G. Haegeman & K. De Bosscher (2008) Altered subcellular distribution of MSK1 induced by glucocorticoids contributes to NF-kappaB inhibition. *EMBO J,* 27, 1682-93.

Berger, S., M. Bleich, W. Schmid, T. J. Cole, J. Peters, H. Watanabe, W. Kriz, R. Warth, R. Greger & G. Schutz (1998) Mineralocorticoid receptor knockout mice: pathophysiology of Na+ metabolism. *Proc Natl Acad Sci U S A,* 95, 9424-9.

Berrebi, D., S. Bruscoli, N. Cohen, A. Foussat, G. Migliorati, L. Bouchet-Delbos, M. C. Maillot, A. Portier, J. Couderc, P. Galanaud, M. Peuchmaur, C. Riccardi & D. Emilie (2003) Synthesis of glucocorticoid-induced leucine zipper (GILZ) by

macrophages: an anti-inflammatory and immunosuppressive mechanism shared by glucocorticoids and IL-10. *Blood,* 101, 729-38.

Biddie, S. C., B. L. Conway-Campbell & S. L. Lightman (2012) Dynamic regulation of glucocorticoid signalling in health and disease. *Rheumatology (Oxford),* 51, 403-12.

Biddie, S. C., S. John, P. J. Sabo, R. E. Thurman, T. A. Johnson, R. L. Schiltz, T. B. Miranda, M. H. Sung, S. Trump, S. L. Lightman, C. Vinson, J. A. Stamatoyannopoulos & G. L. Hager (2011) Transcription factor AP1 potentiates chromatin accessibility and glucocorticoid receptor binding. *Mol Cell,* 43, 145-55.

Bladh, L. G., J. Liden, K. Dahlman-Wright, M. Reimers, S. Nilsson & S. Okret (2005) Identification of endogenous glucocorticoid repressed genes differentially regulated by a glucocorticoid receptor mutant able to separate between nuclear factor-kappaB and activator protein-1 repression. *Mol Pharmacol,* 67, 815-26.

Blind, R. D. & M. J. Garabedian (2008) Differential recruitment of glucocorticoid receptor phospho-isoforms to glucocorticoid-induced genes. *J Steroid Biochem Mol Biol,* 109, 150-7.

Boija, A., I. A. Klein, B. R. Sabari, A. Dall'Agnese, E. L. Coffey, A. V. Zamudio, C. H. Li, K. Shrinivas, J. C. Manteiga, N. M. Hannett, B. J. Abraham, L. K. Afeyan, Y. E. Guo, J. K. Rimel, C. B. Fant, J. Schuijers, T. I. Lee, D. J. Taatjes & R. A. Young (2018) Transcription factors activate genes through the phase-separation capacity of their activation domains. *Cell,* 175, 1842-1855 e16.

Buttgereit, F., J. A. da Silva, M. Boers, G. R. Burmester, M. Cutolo, J. Jacobs, J. Kirwan, L. Kohler, P. Van Riel, T. Vischer & J. W. Bijlsma (2002) Standardised nomenclature for glucocorticoid dosages and glucocorticoid treatment regimens: current questions and tentative answers in rheumatology. *Ann Rheum Dis,* 61, 718-22.

Buttgereit, F. & A. Scheffold (2002) Rapid glucocorticoid effects on immune cells. *Steroids,* 67, 529-34.

Cain, D. W. & J. A. Cidlowski (2017) Immune regulation by glucocorticoids. *Nat Rev Immunol,* 17, 233-247.

Cao, Y., I. K. Bender, A. K. Konstantinidis, S. C. Shin, C. M. Jewell, J. A. Cidlowski, R. P. Schleimer & N. Z. Lu (2013) Glucocorticoid receptor translational isoforms underlie maturational stage-specific glucocorticoid sensitivities of dendritic cells in mice and humans. *Blood,* 121, 1553-62.

Chen, W., T. Dang, R. D. Blind, Z. Wang, C. N. Cavasotto, A. B. Hittelman, I. Rogatsky, S. K. Logan & M. J. Garabedian (2008) Glucocorticoid receptor phosphorylation differentially affects target gene expression. *Mol Endocrinol,* 22, 1754-66.

Chinenov, Y., R. Gupte, J. Dobrovolna, J. R. Flammer, B. Liu, F. E. Michelassi & I. Rogatsky (2012) Role of transcriptional coregulator GRIP1 in the anti-inflammatory actions of glucocorticoids. *Proc Natl Acad Sci U S A,* 109, 11776-81.

Clark, A. R. & M. G. Belvisi (2012) Maps and legends: the quest for dissociated ligands of the glucocorticoid receptor. *Pharmacol Ther,* 134, 54-67.

Clauss, K., A. P. Popp, L. Schulze, J. Hettich, M. Reisser, L. Escoter Torres, N. H. Uhlenhaut & J. C. M. Gebhardt (2017) DNA residence time is a regulatory factor of transcription repression. *Nucleic Acids Res,* 45, 11121-11130.

Cole, T. J., J. A. Blendy, A. P. Monaghan, K. Krieglstein, W. Schmid, A. Aguzzi, G. Fantuzzi, E. Hummler, K. Unsicker & G. Schutz (1995) Targeted disruption of the glucocorticoid receptor gene blocks adrenergic chromaffin cell development and severely retards lung maturation. *Genes Dev,* 9, 1608-21.

D'Ippolito, A. M., I. C. McDowell, A. Barrera, L. K. Hong, S. M. Leichter, L. C. Bartelt, C. M. Vockley, W. H. Majoros, A. Safi, L. Song, C. A. Gersbach, G. E. Crawford & T. E. Reddy (2018) Pre-established chromatin interactions mediate the genomic response to glucocorticoids. *Cell Syst,* 7, 146-160 e7.

De Bosscher, K., I. M. Beck & G. Haegeman (2010) Classic glucocorticoids versus non-steroidal glucocorticoid receptor modulators: survival of the fittest regulator of the immune system? *Brain Behav Immun,* 24, 1035-42.

De Lucena, D. D. & E. B. Rangel (2018) Glucocorticoids use in kidney transplant setting. *Expert Opin Drug Metab Toxicol,* 14, 1023-1041.

Deroo, B. J., C. Rentsch, S. Sampath, J. Young, D. B. DeFranco & T. K. Archer (2002) Proteasomal inhibition enhances glucocorticoid receptor transactivation and alters its subnuclear trafficking. *Mol Cell Biol,* 22, 4113-23.

Desmet, S. J. & K. De Bosscher (2017) Glucocorticoid receptors: finding the middle ground. *J Clin Invest,* 127, 1136-1145.

Dobin, A., C. A. Davis, F. Schlesinger, J. Drenkow, C. Zaleski, S. Jha, P. Batut, M. Chaisson & T. R. Gingeras (2013) STAR: ultrafast universal RNA-seq aligner. *Bioinformatics,* 29, 15-21.

Drouin, J., M. A. Trifiro, R. K. Plante, M. Nemer, P. Eriksson & O. Wrange (1989) Glucocorticoid receptor binding to a specific DNA sequence is required for hormone-dependent repression of pro-opiomelanocortin gene transcription. *Mol Cell Biol,* 9, 5305-14.

Druker, J., A. C. Liberman, M. Antunica-Noguerol, J. Gerez, M. Paez-Pereda, T. Rein, J. A. Iniguez-Lluhi, F. Holsboer & E. Arzt (2013) RSUME enhances glucocorticoid receptor SUMOylation and transcriptional activity. *Mol Cell Biol,* 33, 2116-27.

Durinck, S., P. T. Spellman, E. Birney & W. Huber (2009) Mapping identifiers for the integration of genomic datasets with the R/Bioconductor package biomaRt. *Nat Protoc,* 4, 1184-91.

Eden, E., R. Navon, I. Steinfeld, D. Lipson & Z. Yakhini (2009) GOrilla: a tool for discovery and visualization of enriched GO terms in ranked gene lists. *BMC Bioinformatics,* 10, 48.

Ehrchen, J. M., J. Roth & K. Barczyk-Kahlert (2019) More than suppression: glucocorticoid action on monocytes and macrophages. *Front Immunol,* 10, 2028.

Escoter-Torres, L., G. Caratti, A. Mechtidou, J. Tuckermann, N. H. Uhlenhaut & S. Vettorazzi (2019) Fighting the fire: mechanisms of inflammatory gene regulation by the glucocorticoid receptor. *Front Immunol,* 10, 1859.

Farley, E. K., K. M. Olson, W. Zhang, D. S. Rokhsar & M. S. Levine (2016) Syntax compensates for poor binding sites to encode tissue specificity of developmental enhancers. *Proc Natl Acad Sci U S A,* 113, 6508-13.

Freese, N. H., D. C. Norris & A. E. Loraine (2016) Integrated genome browser: visual analytics platform for genomics. *Bioinformatics,* 32, 2089-95.

Galliher-Beckley, A. J. & J. A. Cidlowski (2009) Emerging roles of glucocorticoid receptor phosphorylation in modulating glucocorticoid hormone action in health and disease. *IUBMB Life,* 61, 979-86.

Gasperowicz, M., C. Surmann-Schmitt, Y. Hamada, F. Otto & J. C. Cross (2013) The transcriptional co-repressor TLE3 regulates development of trophoblast giant cells lining maternal blood spaces in the mouse placenta. *Dev Biol,* 382, 1-14.

Gebhardt, J. C., D. M. Suter, R. Roy, Z. W. Zhao, A. R. Chapman, S. Basu, T. Maniatis & X. S. Xie (2013) Single-molecule imaging of transcription factor binding to DNA in live mammalian cells. *Nat Methods,* 10, 421-6.

Gehin, M., M. Mark, C. Dennefeld, A. Dierich, H. Gronemeyer & P. Chambon (2002) The function of TIF2/GRIP1 in mouse reproduction is distinct from those of SRC-1 and p/CIP. *Mol Cell Biol,* 22, 5923-37.

Giguere, V., S. M. Hollenberg, M. G. Rosenfeld & R. M. Evans (1986) Functional domains of the human glucocorticoid receptor. *Cell,* 46, 645-52.

Gjerstad, J. K., S. L. Lightman & F. Spiga (2018) Role of glucocorticoid negative feedback in the regulation of HPA axis pulsatility. *Stress,* 21, 403-416.

Glass, C. K. & K. Saijo (2010) Nuclear receptor transrepression pathways that regulate inflammation in macrophages and T cells. *Nat Rev Immunol,* 10, 365-76.

Goossens, S. & P. Van Vlierberghe (2016) Overcoming steroid resistance in T cell acute lymphoblastic leukemia. *PLoS Med,* 13, e1002208.

Gordon, S. (2003) Alternative activation of macrophages. *Nat Rev Immunol,* 3, 23-35.

Greulich, F., M. C. Hemmer, D. A. Rollins, I. Rogatsky & N. H. Uhlenhaut (2016) There goes the neighborhood: Assembly of transcriptional complexes during the regulation of metabolism and inflammation by the glucocorticoid receptor. *Steroids,* 114, 7-15.

Grontved, L., S. John, S. Baek, Y. Liu, J. R. Buckley, C. Vinson, G. Aguilera & G. L. Hager (2013) C/EBP maintains chromatin accessibility in liver and facilitates glucocorticoid receptor recruitment to steroid response elements. *EMBO J,* 32, 1568-83.

Guertin, M. J., X. Zhang, S. A. Coonrod & G. L. Hager (2014) Transient estrogen receptor binding and p300 redistribution support a squelching mechanism for estradiol-repressed genes. *Mol Endocrinol,* 28, 1522-33.

Hardy, R. S., K. Raza & M. S. Cooper (2020) Therapeutic glucocorticoids: mechanisms of actions in rheumatic diseases. *Nat Rev Rheumatol,* 16, 133-144.

Hartmann, K., M. Koenen, S. Schauer, S. Wittig-Blaich, M. Ahmad, U. Baschant & J. P. Tuckermann (2016) Molecular actions of glucocorticoids in cartilage and bone during health, disease, and steroid therapy. *Physiol Rev,* 96, 409-47.

Hayden, M. S. & S. Ghosh (2004) Signaling to NF-kappaB. *Genes Dev,* 18, 2195-224.

Heinz, S., C. Benner, N. Spann, E. Bertolino, Y. C. Lin, P. Laslo, J. X. Cheng, C. Murre, H. Singh & C. K. Glass (2010) Simple combinations of lineage-determining transcription factors prime cis-regulatory elements required for macrophage and B cell identities. *Mol Cell,* 38, 576-89.

Hemmer, M. C., M. Wierer, K. Schachtrup, M. Downes, N. Hubner, R. M. Evans & N. H. Uhlenhaut (2019) E47 modulates hepatic glucocorticoid action. *Nat Commun,* 10, 306.

Hench, P. S. (1952) The reversibility of certain rheumatic and nonrheumatic conditions by the use of cortisone or of the pituitary adrenocotropic hormone. *Ann Intern Med,* 36, 1-38.

Hench, P. S., E. C. Kendall & et al. (1949) The effect of a hormone of the adrenal cortex (17-hydroxy-11-dehydrocorticosterone; compound E) and of pituitary adrenocorticotropic hormone on rheumatoid arthritis. *Proc Staff Meet Mayo Clin,* 24, 181-97.

Herman, J. P., J. M. McKlveen, S. Ghosal, B. Kopp, A. Wulsin, R. Makinson, J. Scheimann & B. Myers (2016) Regulation of the hypothalamic-pituitary-adrenocortical stress response. *Compr Physiol,* 6, 603-21.

Hillmer, E. J., H. Zhang, H. S. Li & S. S. Watowich (2016) STAT3 signaling in immunity. *Cytokine Growth Factor Rev,* 31, 1-15.

Hirayama, D., T. Iida & H. Nakase (2017) The phagocytic function of macrophage-enforcing innate immunity and tissue homeostasis. *Int J Mol Sci,* 19.

Hnisz, D., K. Shrinivas, R. A. Young, A. K. Chakraborty & P. A. Sharp (2017) A phase separation model for transcriptional control. *Cell,* 169, 13-23.

Hoeffel, G. & F. Ginhoux (2018) Fetal monocytes and the origins of tissue-resident macrophages. *Cell Immunol,* 330, 5-15.

Hoffman, J. A., K. W. Trotter, J. M. Ward & T. K. Archer (2018) BRG1 governs glucocorticoid receptor interactions with chromatin and pioneer factors across the genome. *Elife,* 7.

Holland, E. J., M. Fingeret & F. S. Mah (2019) Use of Topical steroids in conjunctivitis: a review of the evidence. *Cornea,* 38, 1062-1067.

Hollenberg, S. M. & R. M. Evans (1988) Multiple and cooperative trans-activation domains of the human glucocorticoid receptor. *Cell,* 55, 899-906.

Hsiao, P. W., C. J. Fryer, K. W. Trotter, W. Wang & T. K. Archer (2003) BAF60a mediates critical interactions between nuclear receptors and the BRG1 chromatin-remodeling complex for transactivation. *Mol Cell Biol,* 23, 6210-20.

Hua, G., K. P. Ganti & P. Chambon (2016a) Glucocorticoid-induced tethered transrepression requires SUMOylation of GR and formation of a SUMO-SMRT/NCoR1-HDAC3 repressing complex. *Proc Natl Acad Sci U S A,* 113, E635-43.

Hua, G., L. Paulen & P. Chambon (2016b) GR SUMOylation and formation of an SUMO-SMRT/NCoR1-HDAC3 repressing complex is mandatory for GC-induced IR nGRE-mediated transrepression. *Proc Natl Acad Sci U S A,* 113, E626-34.

Hubner, S., L. Dejager, C. Libert & J. P. Tuckermann (2015) The glucocorticoid receptor in inflammatory processes: transrepression is not enough. *Biol Chem,* 396, 1223-31.

Hudson, W. H., I. M. S. Vera, J. C. Nwachukwu, E. R. Weikum, A. G. Herbst, Q. Yang, D. L. Bain, K. W. Nettles, D. J. Kojetin & E. A. Ortlund (2018) Cryptic glucocorticoid receptor-binding sites pervade genomic NF-kappaB response elements. *Nat Commun,* 9, 1337.

Itani, O. A., K. Z. Liu, K. L. Cornish, J. R. Campbell & C. P. Thomas (2002) Glucocorticoids stimulate human sgk1 gene expression by activation of a GRE in its 5'-flanking region. *Am J Physiol Endocrinol Metab,* 283, E971-9.

John, S., P. J. Sabo, T. A. Johnson, M. H. Sung, S. C. Biddie, S. L. Lightman, T. C. Voss, S. R. Davis, P. S. Meltzer, J. A. Stamatoyannopoulos & G. L. Hager (2008) Interaction of the glucocorticoid receptor with the chromatin landscape. *Mol Cell,* 29, 611-24.

John, S., P. J. Sabo, R. E. Thurman, M. H. Sung, S. C. Biddie, T. A. Johnson, G. L. Hager & J. A. Stamatoyannopoulos (2011) Chromatin accessibility pre-determines glucocorticoid receptor binding patterns. *Nat Genet,* 43, 264-8.

Johnson, T. A., R. V. Chereji, D. A. Stavreva, S. A. Morris, G. L. Hager & D. J. Clark (2018) Conventional and pioneer modes of glucocorticoid receptor interaction with enhancer chromatin in vivo. *Nucleic Acids Res,* 46, 203-214.

Jonat, C., H. J. Rahmsdorf, K. K. Park, A. C. Cato, S. Gebel, H. Ponta & P. Herrlich (1990) Antitumor promotion and antiinflammation: down-modulation of AP-1 (Fos/Jun) activity by glucocorticoid hormone. *Cell,* 62, 1189-204.

Kadmiel, M. & J. A. Cidlowski (2013) Glucocorticoid receptor signaling in health and disease. *Trends Pharmacol Sci,* 34, 518-30.

Kadoch, C., D. C. Hargreaves, C. Hodges, L. Elias, L. Ho, J. Ranish & G. R. Crabtree (2013) Proteomic and bioinformatic analysis of mammalian SWI/SNF complexes identifies extensive roles in human malignancy. *Nat Genet,* 45, 592-601.

Kamei, Y., L. Xu, T. Heinzel, J. Torchia, R. Kurokawa, B. Gloss, S. C. Lin, R. A. Heyman, D. W. Rose, C. K. Glass & M. G. Rosenfeld (1996) A CBP integrator complex mediates transcriptional activation and AP-1 inhibition by nuclear receptors. *Cell,* 85, 403-14.

Kempfer, R. & A. Pombo (2020) Methods for mapping 3D chromosome architecture. *Nat Rev Genet,* 21, 207-226.

Kendall, E. C. (1949) Some observations on the hormone of the adrenal cortex designated compound E. *Proc Staff Meet Mayo Clin,* 24, 298-301.

Kent, W. J., C. W. Sugnet, T. S. Furey, K. M. Roskin, T. H. Pringle, A. M. Zahler & D. Haussler (2002) The human genome browser at UCSC. *Genome Res,* 12, 996-1006.

Kino, T., Y. A. Su & G. P. Chrousos (2009) Human glucocorticoid receptor isoform beta: recent understanding of its potential implications in physiology and pathophysiology. *Cell Mol Life Sci,* 66, 3435-48.

Klassen, C., A. Karabinskaya, L. Dejager, S. Vettorazzi, J. Van Moorleghem, F. Luhder, S. H. Meijsing, J. P. Tuckermann, H. Bohnenberger, C. Libert & H. M. Reichardt (2017) Airway epithelial cells are crucial targets of glucocorticoids in a mouse model of allergic asthma. *J Immunol,* 199, 48-61.

Kleiman, A., S. Hubner, J. M. Rodriguez Parkitna, A. Neumann, S. Hofer, M. A. Weigand, M. Bauer, W. Schmid, G. Schutz, C. Libert, H. M. Reichardt & J. P. Tuckermann (2012) Glucocorticoid receptor dimerization is required for survival in septic shock via suppression of interleukin-1 in macrophages. *FASEB J,* 26, 722-9.

Kuo, T., A. McQueen, T. C. Chen & J. C. Wang (2015) Regulation of glucose homeostasis by glucocorticoids. *Adv Exp Med Biol,* 872, 99-126.

Langlais, D., C. Couture, A. Balsalobre & J. Drouin (2012) The Stat3/GR interaction code: predictive value of direct/indirect DNA recruitment for transcription outcome. *Mol Cell,* 47, 38-49.

Lempiainen, J. K., E. A. Niskanen, K. M. Vuoti, R. E. Lampinen, H. Goos, M. Varjosalo & J. J. Palvimo (2017) Agonist-specific protein interactomes of glucocorticoid and androgen receptor as revealed by proximity mapping. *Mol Cell Proteomics,* 16, 1462-1474.

Li, H., B. Handsaker, A. Wysoker, T. Fennell, J. Ruan, N. Homer, G. Marth, G. Abecasis, R. Durbin & S. Genome Project Data Processing (2009) The Sequence Alignment/Map format and SAMtools. *Bioinformatics,* 25, 2078-9.

Liden, J., F. Delaunay, I. Rafter, J. Gustafsson & S. Okret (1997) A new function for the C-terminal zinc finger of the glucocorticoid receptor. Repression of RelA transactivation. *J Biol Chem,* 272, 21467-72.

Lim, H. W., N. H. Uhlenhaut, A. Rauch, J. Weiner, S. Hubner, N. Hubner, K. J. Won, M. A. Lazar, J. Tuckermann & D. J. Steger (2015) Genomic redistribution of GR monomers and dimers mediates transcriptional response to exogenous glucocorticoid in vivo. *Genome Res,* 25, 836-44.

Long, F., Y. X. Wang, L. Liu, J. Zhou, R. Y. Cui & C. L. Jiang (2005) Rapid nongenomic inhibitory effects of glucocorticoids on phagocytosis and superoxide anion production by macrophages. *Steroids,* 70, 55-61.

Love, M. I., W. Huber & S. Anders (2014) Moderated estimation of fold change and dispersion for RNA-seq data with DESeq2. *Genome Biol,* 15, 550.

Lowenberg, M., A. P. Verhaar, J. Bilderbeek, J. Marle, F. Buttgereit, M. P. Peppelenbosch, S. J. van Deventer & D. W. Hommes (2006) Glucocorticoids cause rapid dissociation of a T-cell-receptor-associated protein complex containing LCK and FYN. *EMBO Rep,* 7, 1023-9.

Lu, N. Z. & J. A. Cidlowski (2005) Translational regulatory mechanisms generate N-terminal glucocorticoid receptor isoforms with unique transcriptional target genes. *Mol Cell,* 18, 331-42.

Lydon, J. P., F. J. DeMayo, O. M. Conneely & B. W. O'Malley (1996) Reproductive phenotpes of the progesterone receptor null mutant mouse. *J Steroid Biochem Mol Biol,* 56, 67-77.

Ma, W., K. Gee, W. Lim, K. Chambers, J. B. Angel, M. Kozlowski & A. Kumar (2004) Dexamethasone inhibits IL-12p40 production in lipopolysaccharide-stimulated human monocytic cells by down-regulating the activity of c-Jun N-terminal kinase, the activation protein-1, and NF-kappa B transcription factors. *J Immunol,* 172, 318-30.

Martinez, F. O. & S. Gordon (2014) The M1 and M2 paradigm of macrophage activation: time for reassessment. *F1000Prime Rep,* 6, 13.

Matthews, L., A. Berry, V. Ohanian, J. Ohanian, H. Garside & D. Ray (2008) Caveolin mediates rapid glucocorticoid effects and couples glucocorticoid action to the antiproliferative program. *Mol Endocrinol,* 22, 1320-30.

Matyszak, M. K., S. Citterio, M. Rescigno & P. Ricciardi-Castagnoli (2000) Differential effects of corticosteroids during different stages of dendritic cell maturation. *Eur J Immunol,* 30, 1233-42.

McDonough, A. K., J. R. Curtis & K. G. Saag (2008) The epidemiology of glucocorticoid-associated adverse events. *Curr Opin Rheumatol,* 20, 131-7.

McKay, L. I. & J. A. Cidlowski (2000) CBP (CREB binding protein) integrates NF-kappaB (nuclear factor-kappaB) and glucocorticoid receptor physical interactions and antagonism. *Mol Endocrinol,* 14, 1222-34.

McLean, C. Y., D. Bristor, M. Hiller, S. L. Clarke, B. T. Schaar, C. B. Lowe, A. M. Wenger & G. Bejerano (2010) GREAT improves functional interpretation of cis-regulatory regions. *Nat Biotechnol,* 28, 495-501.

Medzhitov, R. & T. Horng (2009) Transcriptional control of the inflammatory response. *Nat Rev Immunol,* 9, 692-703.

Meijsing, S. H., M. A. Pufall, A. Y. So, D. L. Bates, L. Chen & K. R. Yamamoto (2009) DNA binding site sequence directs glucocorticoid receptor structure and activity. *Science,* 324, 407-10.

Mendelson, C. R. & V. Boggaram (1991) Hormonal control of the surfactant system in fetal lung. *Annu Rev Physiol,* 53, 415-40.

Miner, J. N. & K. R. Yamamoto (1992) The basic region of AP-1 specifies glucocorticoid receptor activity at a composite response element. *Genes Dev,* 6, 2491-501.

Mordacq, J. C. & D. I. Linzer (1989) Co-localization of elements required for phorbol ester stimulation and glucocorticoid repression of proliferin gene expression. *Genes Dev,* 3, 760-9.

Muller, M. B. & F. Holsboer (2006) Mice with mutations in the HPA-system as models for symptoms of depression. *Biol Psychiatry,* 59, 1104-15.

Nie, Z., Y. Xue, D. Yang, S. Zhou, B. J. Deroo, T. K. Archer & W. Wang (2000) A specificity and targeting subunit of a human SWI/SNF family-related chromatin-remodeling complex. *Mol Cell Biol,* 20, 8879-88.

Oakley, R. H. & J. A. Cidlowski (2013) The biology of the glucocorticoid receptor: new signaling mechanisms in health and disease. *J Allergy Clin Immunol,* 132, 1033-44.

Oakley, R. H., S. Ramamoorthy, J. F. Foley, J. T. Busada, N. Z. Lu & J. A. Cidlowski (2018) Glucocorticoid receptor isoform-specific regulation of development, circadian rhythm, and inflammation in mice. *FASEB J,* 32, 5258-5271.

Oeckinghaus, A. & S. Ghosh (2009) The NF-kappaB family of transcription factors and its regulation. *Cold Spring Harb Perspect Biol,* 1, a000034.

Ogawa, S., J. Lozach, C. Benner, G. Pascual, R. K. Tangirala, S. Westin, A. Hoffmann, S. Subramaniam, M. David, M. G. Rosenfeld & C. K. Glass (2005) Molecular determinants of crosstalk between nuclear receptors and toll-like receptors. *Cell,* 122, 707-21.

Olaloko, O., R. Mohammed & U. Ojha (2018) Evaluating the use of corticosteroids in preventing and treating bronchopulmonary dysplasia in preterm neonates. *Int J Gen Med,* 11, 265-274.

Paakinaho, V., D. M. Presman, D. A. Ball, T. A. Johnson, R. L. Schiltz, P. Levitt, D. Mazza, T. Morisaki, T. S. Karpova & G. L. Hager (2017) Single-molecule analysis of steroid receptor and cofactor action in living cells. *Nat Commun,* 8, 15896.

Pawlak, M., E. Bauge, W. Bourguet, K. De Bosscher, F. Lalloyer, A. Tailleux, C. Lebherz, P. Lefebvre & B. Staels (2014) The transrepressive activity of peroxisome proliferator-activated receptor alpha is necessary and sufficient to prevent liver fibrosis in mice. *Hepatology,* 60, 1593-606.

Payvar, F., D. DeFranco, G. L. Firestone, B. Edgar, O. Wrange, S. Okret, J. A. Gustafsson & K. R. Yamamoto (1983) Sequence-specific binding of glucocorticoid receptor to MTV DNA at sites within and upstream of the transcribed region. *Cell,* 35, 381-92.

Perez-Riverol, Y., A. Csordas, J. Bai, M. Bernal-Llinares, S. Hewapathirana, D. J. Kundu, A. Inuganti, J. Griss, G. Mayer, M. Eisenacher, E. Perez, J. Uszkoreit, J. Pfeuffer, T. Sachsenberg, S. Yilmaz, S. Tiwary, J. Cox, E. Audain, M. Walzer, A. F. Jarnuczak, T. Ternent, A. Brazma & J. A. Vizcaino (2019) The PRIDE database and related tools and resources in 2019: improving support for quantification data. *Nucleic Acids Res,* 47, D442-D450.

Pimenta, E., M. Wolley & M. Stowasser (2012) Adverse cardiovascular outcomes of corticosteroid excess. *Endocrinology,* 153, 5137-42.

Pratt, W. B. & D. O. Toft (2003) Regulation of signaling protein function and trafficking by the hsp90/hsp70-based chaperone machinery. *Exp Biol Med (Maywood),* 228, 111-33.

Presman, D. M., S. Ganguly, R. L. Schiltz, T. A. Johnson, T. S. Karpova & G. L. Hager (2016) DNA binding triggers tetramerization of the glucocorticoid receptor in live cells. *Proc Natl Acad Sci U S A,* 113, 8236-41.

Presman, D. M., M. F. Ogara, M. Stortz, L. D. Alvarez, J. R. Pooley, R. L. Schiltz, L. Grontved, T. A. Johnson, P. R. Mittelstadt, J. D. Ashwell, S. Ganesan, G. Burton, V. Levi, G. L. Hager & A. Pecci (2014) Live cell imaging unveils multiple domain requirements for in vivo dimerization of the glucocorticoid receptor. *PLoS Biol,* 12, e1001813.

Proven, A., S. E. Gabriel, C. Orces, W. M. O'Fallon & G. G. Hunder (2003) Glucocorticoid therapy in giant cell arteritis: duration and adverse outcomes. *Arthritis Rheum,* 49, 703-8.

Quagliarini, F., A. A. Mir, K. Balazs, M. Wierer, K. A. Dyar, C. Jouffe, K. Makris, J. Hawe, M. Heinig, F. V. Filipp, G. D. Barish & N. H. Uhlenhaut (2019) Cistromic reprogramming of the diurnal glucocorticoid hormone response by high-fat diet. *Mol Cell,* 76, 531-545 e5.

Radoja, N., M. Komine, S. H. Jho, M. Blumenberg & M. Tomic-Canic (2000) Novel mechanism of steroid action in skin through glucocorticoid receptor monomers. *Mol Cell Biol,* 20, 4328-39.

Raff, H. & T. Carroll (2015) Cushing's syndrome: from physiological principles to diagnosis and clinical care. *J Physiol,* 593, 493-506.

Ramamoorthy, S. & J. A. Cidlowski (2016) Corticosteroids: mechanisms of action in health and disease. *Rheum Dis Clin North Am,* 42, 15-31, vii.

Ramji, D. P. & P. Foka (2002) CCAAT/enhancer-binding proteins: structure, function and regulation. *Biochem J,* 365, 561-75.

Rando, G., C. K. Tan, N. Khaled, A. Montagner, N. Leuenberger, J. Bertrand-Michel, E. Paramalingam, H. Guillou & W. Wahli (2016) Glucocorticoid receptor-PPARalpha axis in fetal mouse liver prepares neonates for milk lipid catabolism. *Elife,* 5.

Rao, N. A., M. T. McCalman, P. Moulos, K. J. Francoijs, A. Chatziioannou, F. N. Kolisis, M. N. Alexis, D. J. Mitsiou & H. G. Stunnenberg (2011) Coactivation of GR and NFKB alters the repertoire of their binding sites and target genes. *Genome Res,* 21, 1404-16.

Ray, A. & K. E. Prefontaine (1994) Physical association and functional antagonism between the p65 subunit of transcription factor NF-kappa B and the glucocorticoid receptor. *Proc Natl Acad Sci U S A,* 91, 752-6.

Reichardt, H. M., K. H. Kaestner, J. Tuckermann, O. Kretz, O. Wessely, R. Bock, P. Gass, W. Schmid, P. Herrlich, P. Angel & G. Schutz (1998) DNA binding of the glucocorticoid receptor is not essential for survival. *Cell,* 93, 531-41.

Reichardt, H. M., J. P. Tuckermann, M. Gottlicher, M. Vujic, F. Weih, P. Angel, P. Herrlich & G. Schutz (2001) Repression of inflammatory responses in the absence of DNA binding by the glucocorticoid receptor. *EMBO J,* 20, 7168-73.

Robinson, M. B., D. A. Deshpande, J. Chou, W. Cui, S. Smith, C. Langefeld, A. T. Hastie, E. R. Bleecker & G. A. Hawkins (2015) IL-6 trans-signaling increases expression of airways disease genes in airway smooth muscle. *Am J Physiol Lung Cell Mol Physiol,* 309, L129-38.

Rogatsky, I., C. L. Waase & M. J. Garabedian (1998) Phosphorylation and inhibition of rat glucocorticoid receptor transcriptional activation by glycogen synthase kinase-3 (GSK-3). Species-specific differences between human and rat glucocorticoid receptor signaling as revealed through GSK-3 phosphorylation. *J Biol Chem,* 273, 14315-21.

Roh, J. S. & D. H. Sohn (2018) Damage-associated molecular patterns in inflammatory diseases. *Immune Netw,* 18, e27.

Rollins, D. A., J. B. Kharlyngdoh, M. Coppo, B. Tharmalingam, S. Mimouna, Z. Guo, M. A. Sacta, M. A. Pufall, R. P. Fisher, X. Hu, Y. Chinenov & I. Rogatsky (2017) Glucocorticoid-induced phosphorylation by CDK9 modulates the coactivator

functions of transcriptional cofactor GRIP1 in macrophages. *Nat Commun,* 8, 1739.

Sabari, B. R., A. Dall'Agnese, A. Boija, I. A. Klein, E. L. Coffey, K. Shrinivas, B. J. Abraham, N. M. Hannett, A. V. Zamudio, J. C. Manteiga, C. H. Li, Y. E. Guo, D. S. Day, J. Schuijers, E. Vasile, S. Malik, D. Hnisz, T. I. Lee, Cisse, II, R. G. Roeder, P. A. Sharp, A. K. Chakraborty & R. A. Young (2018) Coactivator condensation at super-enhancers links phase separation and gene control. *Science,* 361.

Sacta, M. A., B. Tharmalingam, M. Coppo, D. A. Rollins, D. K. Deochand, B. Benjamin, L. Yu, B. Zhang, X. Hu, R. Li, Y. Chinenov & I. Rogatsky (2018) Gene-specific mechanisms direct glucocorticoid-receptor-driven repression of inflammatory response genes in macrophages. *Elife,* 7.

Sarett, L. H. (1946) Partial synthesis of pregnene-4-triol-17(beta), 20(beta), 21-dione-3,11 and pregnene-4-diol-17(beta), 21-trione-3,11,20 monoacetate. *J Biol Chem,* 162, 601-31.

Sasse, S. K., C. M. Mailloux, A. J. Barczak, Q. Wang, M. O. Altonsy, M. K. Jain, S. M. Haldar & A. N. Gerber (2013) The glucocorticoid receptor and KLF15 regulate gene expression dynamics and integrate signals through feed-forward circuitry. *Mol Cell Biol,* 33, 2104-15.

Schacke, H., M. Berger, H. Rehwinkel & K. Asadullah (2007) Selective glucocorticoid receptor agonists (SEGRAs): novel ligands with an improved therapeutic index. *Mol Cell Endocrinol,* 275, 109-17.

Schauwaers, K., K. De Gendt, P. T. Saunders, N. Atanassova, A. Haelens, L. Callewaert, U. Moehren, J. V. Swinnen, G. Verhoeven, G. Verrijdt & F. Claessens (2007) Loss of androgen receptor binding to selective androgen response elements causes a reproductive phenotype in a knockin mouse model. *Proc Natl Acad Sci U S A,* 104, 4961-6.

Scheschowitsch, K., J. A. Leite & J. Assreuy (2017) New insights in glucocorticoid receptor signaling-more than just a ligand-binding receptor. *Front Endocrinol (Lausanne),* 8, 16.

Schleimer, R. P. (2004) Glucocorticoids suppress inflammation but spare innate immune responses in airway epithelium. *Proc Am Thorac Soc,* 1, 222-30.

Schmidt, S. F., B. D. Larsen, A. Loft & S. Mandrup (2016) Cofactor squelching: artifact or fact? *Bioessays,* 38, 618-26.

Schmidt, S. F., B. D. Larsen, A. Loft, R. Nielsen, J. G. Madsen & S. Mandrup (2015) Acute TNF-induced repression of cell identity genes is mediated by NFkappaB-directed redistribution of cofactors from super-enhancers. *Genome Res,* 25, 1281-94.

Schone, S., M. Bothe, E. Einfeldt, M. Borschiwer, P. Benner, M. Vingron, M. Thomas-Chollier & S. H. Meijsing (2018) Synthetic STARR-seq reveals how DNA shape and sequence modulate transcriptional output and noise. *PLoS Genet,* 14, e1007793.

Schone, S., M. Jurk, M. B. Helabad, I. Dror, I. Lebars, B. Kieffer, P. Imhof, R. Rohs, M. Vingron, M. Thomas-Chollier & S. H. Meijsing (2016) Sequences flanking the

core-binding site modulate glucocorticoid receptor structure and activity. *Nat Commun,* 7, 12621.

Schule, R., P. Rangarajan, S. Kliewer, L. J. Ransone, J. Bolado, N. Yang, I. M. Verma & R. M. Evans. 1990. Functional antagonism between oncoprotein c-Jun and the glucocorticoid receptor. In *Cell*, 1217-26. United States.

Sevilla, L. M. & P. Perez (2018) Roles of the Glucocorticoid and Mineralocorticoid Receptors in Skin Pathophysiology. *Int J Mol Sci,* 19.

Shain, A. H. & J. R. Pollack (2013) The spectrum of SWI/SNF mutations, ubiquitous in human cancers. *PLoS One,* 8, e55119.

Siersbaek, R., R. Nielsen, S. John, M. H. Sung, S. Baek, A. Loft, G. L. Hager & S. Mandrup (2011) Extensive chromatin remodelling and establishment of transcription factor 'hotspots' during early adipogenesis. *EMBO J,* 30, 1459-72.

Silverman, M. N., P. Mukhopadhyay, E. Belyavskaya, L. H. Tonelli, B. D. Revenis, J. H. Doran, B. E. Ballard, J. Tam, P. Pacher & E. M. Sternberg (2013) Glucocorticoid receptor dimerization is required for proper recovery of LPS-induced inflammation, sickness behavior and metabolism in mice. *Mol Psychiatry,* 18, 1006-17.

Souffriau, J., M. Eggermont, S. Van Ryckeghem, K. Van Looveren, L. Van Wyngene, E. Van Hamme, M. Vuylsteke, R. Beyaert, K. De Bosscher & C. Libert (2018) A screening assay for Selective Dimerizing Glucocorticoid Receptor Agonists and Modulators (SEDIGRAM) that are effective against acute inflammation. *Sci Rep,* 8, 12894.

Spies, C. M., D. H. Schaumann, T. Berki, K. Mayer, M. Jakstadt, D. Huscher, C. Wunder, G. R. Burmester, A. Radbruch, R. Lauster, A. Scheffold & F. Buttgereit (2006) Membrane glucocorticoid receptors are down regulated by glucocorticoids in patients with systemic lupus erythematosus and use a caveolin-1-independent expression pathway. *Ann Rheum Dis,* 65, 1139-46.

Starick, S. R., J. Ibn-Salem, M. Jurk, C. Hernandez, M. I. Love, H. R. Chung, M. Vingron, M. Thomas-Chollier & S. H. Meijsing (2015) ChIP-exo signal associated with DNA-binding motifs provides insight into the genomic binding of the glucocorticoid receptor and cooperating transcription factors. *Genome Res,* 25, 825-35.

Strehl, C., L. Ehlers, T. Gaber & F. Buttgereit (2019) Glucocorticoids-all-rounders tackling the versatile players of the immune system. *Front Immunol,* 10, 1744.

Subramaniam, N., W. Cairns & S. Okret (1997) Studies on the mechanism of glucocorticoid-mediated repression from a negative glucocorticoid response element from the bovine prolactin gene. *DNA Cell Biol,* 16, 153-63.

Sundahl, N., J. Bridelance, C. Libert, K. De Bosscher & I. M. Beck (2015) Selective glucocorticoid receptor modulation: New directions with non-steroidal scaffolds. *Pharmacol Ther,* 152, 28-41.

Surjit, M., K. P. Ganti, A. Mukherji, T. Ye, G. Hua, D. Metzger, M. Li & P. Chambon (2011) Widespread negative response elements mediate direct repression by agonist-liganded glucocorticoid receptor. *Cell,* 145, 224-41.

Swinstead, E. E., T. B. Miranda, V. Paakinaho, S. Baek, I. Goldstein, M. Hawkins, T. S. Karpova, D. Ball, D. Mazza, L. D. Lavis, J. B. Grimm, T. Morisaki, L. Grontved, D. M. Presman & G. L. Hager (2016) Steroid receptors reprogram FoxA1 occupancy through dynamic chromatin transitions. *Cell,* 165, 593-605.

Tengku-Muhammad, T. S., T. R. Hughes, H. Ranki, A. Cryer & D. P. Ramji (2000) Differential regulation of macrophage CCAAT-enhancer binding protein isoforms by lipopolysaccharide and cytokines. *Cytokine,* 12, 1430-6.

Thormann, V., L. V. Glaser, M. C. Rothkegel, M. Borschiwer, M. Bothe, A. Fuchs & S. H. Meijsing (2019) Expanding the repertoire of glucocorticoid receptor target genes by engineering genomic response elements. *Life Sci Alliance,* 2.

Tsai, S. Y., J. Carlstedt-Duke, N. L. Weigel, K. Dahlman, J. A. Gustafsson, M. J. Tsai & B. W. O'Malley (1988) Molecular interactions of steroid hormone receptor with its enhancer element: evidence for receptor dimer formation. *Cell,* 55, 361-9.

Tuckermann, J. P., A. Kleiman, K. G. McPherson & H. M. Reichardt (2005) Molecular mechanisms of glucocorticoids in the control of inflammation and lymphocyte apoptosis. *Crit Rev Clin Lab Sci,* 42, 71-104.

Tuckermann, J. P., A. Kleiman, R. Moriggl, R. Spanbroek, A. Neumann, A. Illing, B. E. Clausen, B. Stride, I. Forster, A. J. Habenicht, H. M. Reichardt, F. Tronche, W. Schmid & G. Schutz (2007) Macrophages and neutrophils are the targets for immune suppression by glucocorticoids in contact allergy. *J Clin Invest,* 117, 1381-90.

Uhlenhaut, N. H., G. D. Barish, R. T. Yu, M. Downes, M. Karunasiri, C. Liddle, P. Schwalie, N. Hubner & R. M. Evans (2013) Insights into negative regulation by the glucocorticoid receptor from genome-wide profiling of inflammatory cistromes. *Mol Cell,* 49, 158-71.

Vandevyver, S., L. Dejager, J. Tuckermann & C. Libert (2013) New insights into the anti-inflammatory mechanisms of glucocorticoids: an emerging role for glucocorticoid-receptor-mediated transactivation. *Endocrinology,* 154, 993-1007.

Vandevyver, S., L. Dejager, T. Van Bogaert, A. Kleyman, Y. Liu, J. Tuckermann & C. Libert (2012) Glucocorticoid receptor dimerization induces MKP1 to protect against TNF-induced inflammation. *J Clin Invest,* 122, 2130-40.

Vettorazzi, S., C. Bode, L. Dejager, L. Frappart, E. Shelest, C. Klassen, A. Tasdogan, H. M. Reichardt, C. Libert, M. Schneider, F. Weih, N. Henriette Uhlenhaut, J. P. David, M. Graler, A. Kleiman & J. P. Tuckermann (2015) Glucocorticoids limit acute lung inflammation in concert with inflammatory stimuli by induction of SphK1. *Nat Commun,* 6, 7796.

Wang, Z., J. Frederick & M. J. Garabedian (2002) Deciphering the phosphorylation "code" of the glucocorticoid receptor in vivo. *J Biol Chem,* 277, 26573-80.

Wang, Z., M. H. Malone, H. He, K. S. McColl & C. W. Distelhorst (2003) Microarray analysis uncovers the induction of the proapoptotic BH3-only protein Bim in multiple models of glucocorticoid-induced apoptosis. *J Biol Chem,* 278, 23861-7.

Webster, J. C., C. M. Jewell, J. E. Bodwell, A. Munck, M. Sar & J. A. Cidlowski (1997) Mouse glucocorticoid receptor phosphorylation status influences multiple functions of the receptor protein. *J Biol Chem,* 272, 9287-93.

Wrange, O., J. Carlstedt-Duke & J. A. Gustafsson (1986) Stoichiometric analysis of the specific interaction of the glucocorticoid receptor with DNA. *J Biol Chem,* 261, 11770-8.

Wrange, O., P. Eriksson & T. Perlmann (1989) The purified activated glucocorticoid receptor is a homodimer. *J Biol Chem,* 264, 5253-9.

Yang-Yen, H. F., J. C. Chambard, Y. L. Sun, T. Smeal, T. J. Schmidt, J. Drouin & M. Karin (1990) Transcriptional interference between c-Jun and the glucocorticoid receptor: mutual inhibition of DNA binding due to direct protein-protein interaction. *Cell,* 62, 1205-15.

Yeh, S., M. Y. Tsai, Q. Xu, X. M. Mu, H. Lardy, K. E. Huang, H. Lin, S. D. Yeh, S. Altuwaijri, X. Zhou, L. Xing, B. F. Boyce, M. C. Hung, S. Zhang, L. Gan & C. Chang (2002) Generation and characterization of androgen receptor knockout (ARKO) mice: an in vivo model for the study of androgen functions in selective tissues. *Proc Natl Acad Sci U S A,* 99, 13498-503.

York, B. & B. W. O'Malley (2010) Steroid receptor coactivator (SRC) family: masters of systems biology. *J Biol Chem,* 285, 38743-50.

Zenz, R., R. Eferl, C. Scheinecker, K. Redlich, J. Smolen, H. B. Schonthaler, L. Kenner, E. Tschachler & E. F. Wagner (2008) Activator protein 1 (Fos/Jun) functions in inflammatory bone and skin disease. *Arthritis Res Ther,* 10, 201.

Zhang, G., L. Zhang & G. W. Duff (1997) A negative regulatory region containing a glucocorticosteroid response element (nGRE) in the human interleukin-1beta gene. *DNA Cell Biol,* 16, 145-52.

Zhang, Y., B. Fang, M. J. Emmett, M. Damle, Z. Sun, D. Feng, S. M. Armour, J. R. Remsberg, J. Jager, R. E. Soccio, D. J. Steger & M. A. Lazar (2015) Discrete functions of nuclear receptor Rev-erbalpha couple metabolism to the clock. *Science,* 348, 1488-92.

Zhang, Z., P. E. Burch, A. J. Cooney, R. B. Lanz, F. A. Pereira, J. Wu, R. A. Gibbs, G. Weinstock & D. A. Wheeler (2004) Genomic analysis of the nuclear receptor family: new insights into structure, regulation, and evolution from the rat genome. *Genome Res,* 14, 580-90.

Zhou, J., C. L. Theesfeld, K. Yao, K. M. Chen, A. K. Wong & O. G. Troyanskaya (2018) Deep learning sequence-based ab initio prediction of variant effects on expression and disease risk. *Nat Genet,* 50, 1171-1179.

Supplementary data

Supplementary figure 1. SWI/SNF subunits knock down with no effect on GR target genes in MEFs.

Supplementary list 1. Selected GR ChIP-Seq peaks.

Supplementary list 2. Differentially expressed genes LPS vs LPS and Dex.

Supplementary list 3. Peptide counts from ChIP-MS.

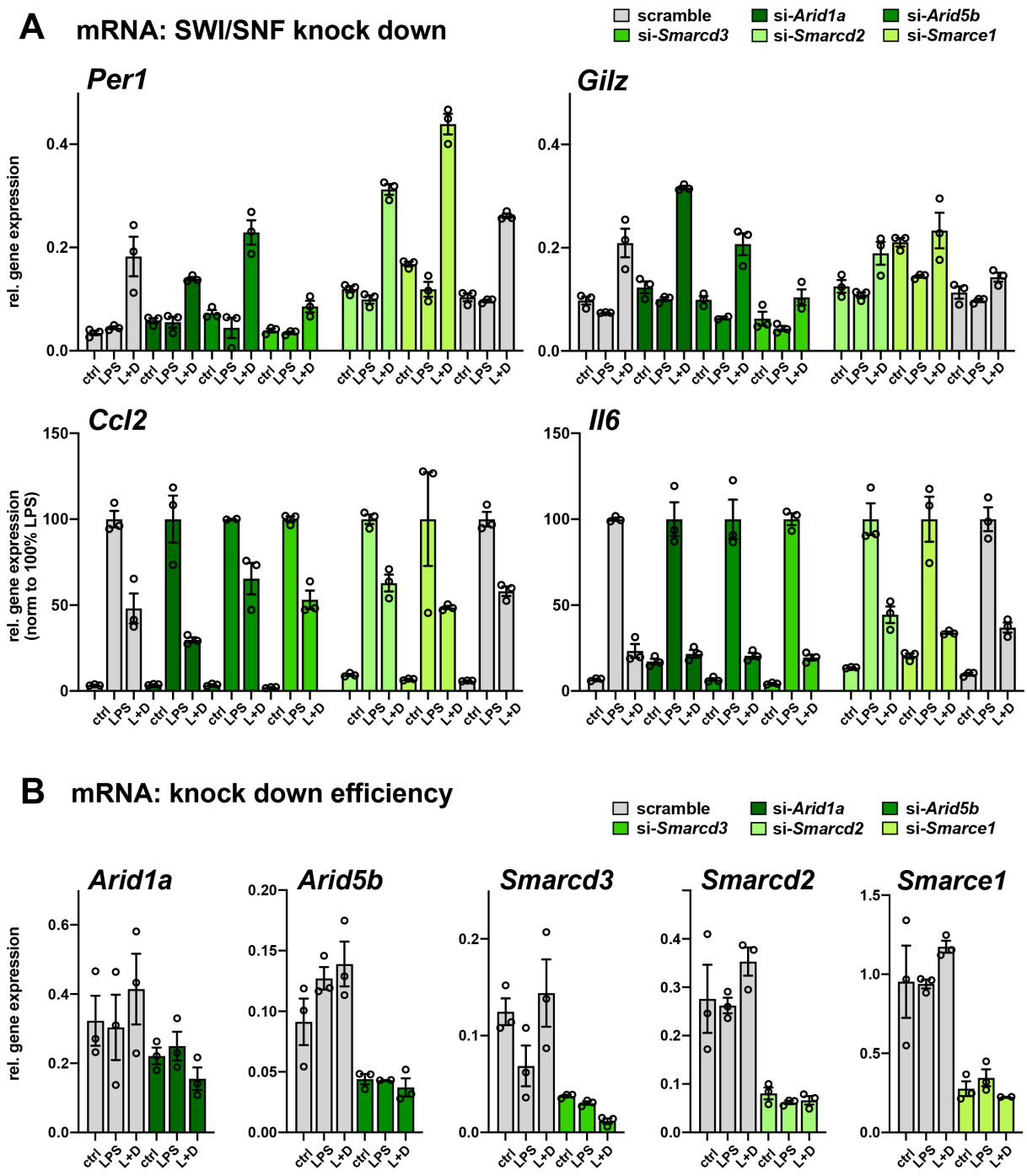

Figure S1. SWI/SNF subunits knock down with no effect on GR target genes in MEFs.
A, qRT-PCR of target genes (normalised to *U36b4*) upon treatment with vehicle (ctrl), 16h Dex, 6h LPS and 6h LPS + 16h Dex (L+D). Wild type GR MEFs with non-targeted siRNA (scramble), siRNA against *Arid1a*, *Arid5b*, *Smarcd3*, *Smarcd2* or *Smarce1*. Values represent mean ± SEM, n = 3, *p<0.05, **p<0.01, ***p<0.001 and ns = not significant. Student's t-test. **B**, qRT-PCR to validate knock down efficiency (normalised to *U36b4*).

Supplementary list 1. Selected GR ChIP-Seq peaks.

Gene	Chromosome	Peak start	Peak end	Gene strand	Position to feature
Per1	chr11	69095005	69095204	+	upstream
Per1	chr11	69096987	69097186	+	inside
Tsc22d3	chrX	140511355	140511554	-	downstream
Tsc22d3	chrX	140513466	140513665	-	downstream
Tsc22d3	chrX	140529263	140529462	-	downstream
Tsc22d3	chrX	140543120	140543319	-	inside
Tsc22d3	chrX	140573122	140573321	-	inside
Cxcl2	chr5	90898695	90898894	+	upstream
Cxcl2	chr5	90900335	90900534	+	upstream
Mmp8	chr9	7560065	7560264	+	inside
Mmp8	chr9	7567442	7567641	+	inside
Dusp1	chr17	26488732	26488931	-	downstream
Dusp1	chr17	26503663	26503862	-	downstream
Dusp1	chr17	26504222	26504421	-	downstream
Dusp1	chr17	26505191	26505390	-	downstream
Dusp1	chr17	26505558	26505757	-	overlapEnd
Dusp1	chr17	26507478	26507677	-	inside
Dusp1	chr17	26512650	26512849	-	upstream
Dusp1	chr17	26514778	26514977	-	upstream
Dusp1	chr17	26529953	26530152	-	upstream
Dusp1	chr17	26530753	26530952	-	upstream
Dusp1	chr17	26533869	26534068	-	upstream
Cp	chr3	19957083	19957282	+	inside
Ccl2	chr11	82015138	82015337	+	upstream
Ccl2	chr11	82022606	82022805	+	upstream
Ccl2	chr11	82028172	82028371	+	upstream
Ccl20	chr1	83091386	83091585	+	upstream
Ccl20	chr1	83096143	83096342	+	upstream
Ccl20	chr1	83096524	83096723	+	upstream
Ccl20	chr1	83099822	83100021	+	upstream
Ccl20	chr1	83116540	83116739	+	upstream
Ccl20	chr1	83117587	83117786	+	inside
Ccl20	chr1	83118291	83118490	+	inside
Il6	chr5	29936032	29936231	+	upstream
Il6	chr5	30007125	30007324	+	upstream
Il6	chr5	30012998	30013197	+	overlapStart
Il6	chr5	30014779	30014978	+	inside
Il6	chr5	30018358	30018557	+	inside
Il6	chr5	30020625	30020824	+	downstream
Vcam1	chr3	116076758	116076957	-	downstream
Vcam1	chr3	116080171	116080370	-	downstream
Vcam1	chr3	116114331	116114530	-	inside
Vcam1	chr3	116116140	116116339	-	inside
Vcam1	chr3	116121053	116121252	-	inside
Vcam1	chr3	116138168	116138367	-	upstream
Vcam1	chr3	116189557	116189756	-	upstream

Supplementary list 2. Differentially expressed genes LPS vs LPS and Dex.

Genes are sorted by log2 fold change (FC)

Gene name	base mean	log2FC WT	Padj WT	log2FC ΔZn	Padj ΔZn
Serpina3n	300,08	3,81	0,00	0,26	1,00
Fkbp5	2444,32	2,69	0,00	0,00	1,00
Fabp4	227,16	2,62	0,00	0,11	1,00
Mt2	4844,90	2,61	0,00	0,11	1,00
Fam46b	491,60	2,37	0,00	-0,16	1,00
Tsc22d3	991,06	2,26	0,00	0,04	1,00
Mt1	3225,84	2,25	0,00	0,04	1,00
Pdk4	551,95	2,16	0,00	-0,10	1,00
Clca3a1	976,47	2,06	0,00	0,11	1,00
Sorbs2	577,40	1,98	0,00	0,10	1,00
Dpep1	285,76	1,90	0,00	-0,10	1,00
Crispld2	2982,28	1,88	0,00	0,03	1,00
Per1	1014,82	1,87	0,00	0,03	1,00
Vegfd	665,55	1,85	0,00	0,16	1,00
Tmem119	1655,51	1,84	0,00	0,11	1,00
Suox	494,69	1,84	0,00	0,24	0,67
Jade2	403,93	1,76	0,00	-0,13	1,00
Snta1	635,06	1,76	0,00	-0,10	1,00
Pi15	362,22	1,70	0,00	0,05	1,00
Sphk1	752,46	1,67	0,00	0,02	1,00
Deptor	298,31	1,67	0,00	-0,13	1,00
Mtus2	257,01	1,65	0,00	0,22	1,00
Rtl3	661,33	1,58	0,00	0,13	1,00
Ablim1	769,20	1,55	0,00	0,06	1,00
Ror1	292,80	1,53	0,00	0,17	1,00
Adgrg2	436,00	1,52	0,00	-0,05	1,00
Sgk1	3101,25	1,51	0,00	0,05	1,00
Tmem38b	351,71	1,49	0,00	-0,13	1,00
Ctla2a	933,39	1,45	0,00	0,17	1,00
Cdo1	601,87	1,43	0,00	0,02	1,00
Col11a1	13295,75	1,43	0,00	-0,01	1,00
Mum1l1	899,66	1,39	0,00	0,18	1,00
Tgm2	643,41	1,38	0,00	0,04	1,00
Plce1	318,13	1,38	0,00	0,02	1,00
Ankrd44	975,24	1,36	0,00	0,10	1,00
4930523C07Rik	214,67	1,36	0,00	0,10	1,00
Gas6	5943,00	1,30	0,00	0,18	0,78
Glul	1093,88	1,30	0,00	-0,07	1,00
Gprc5b	683,49	1,29	0,00	-0,05	1,00
Ptx3	5345,43	1,29	0,00	0,04	1,00
Cryab	2432,68	1,27	0,00	0,11	1,00
Tnn	510,06	1,23	0,00	-0,02	1,00
Ndrg2	544,71	1,22	0,00	0,03	1,00

Gene name	base mean	log2FC WT	Padj WT	log2FC ΔZn	Padj ΔZn
Smad9	206,78	1,21	0,00	-0,03	1,00
Tcp11l1	544,31	1,21	0,00	0,00	1,00
Hspb1	2336,58	1,19	0,00	0,00	1,00
Pmp22	2548,12	1,18	0,00	0,00	1,00
Saa3	529,92	1,18	0,00	0,23	1,00
Vdr	511,80	1,18	0,00	0,04	1,00
Ampd3	555,71	1,17	0,00	-0,09	1,00
Atoh8	437,01	1,17	0,00	0,07	1,00
Selenop	423,65	1,16	0,00	-0,31	1,00
Rab3il1	272,04	1,14	0,00	0,10	1,00
Cp	434,49	1,13	0,00	0,02	1,00
Osr1	318,16	1,13	0,00	0,00	1,00
Bdh1	230,95	1,13	0,00	0,12	1,00
Adamts1	4611,83	1,12	0,00	0,07	1,00
Angpt2	318,51	1,12	0,00	0,11	1,00
Ust	732,80	1,12	0,00	0,08	1,00
Fibin	1619,00	1,11	0,00	0,04	1,00
Daam2	769,96	1,11	0,00	0,03	1,00
Adm	1180,55	1,10	0,00	0,02	1,00
Dhrs3	388,85	1,10	0,00	-0,03	1,00
Cry1	460,40	1,09	0,00	-0,05	1,00
Itgbl1	542,66	1,08	0,00	0,04	1,00
Cpm	275,10	1,06	0,00	0,04	1,00
Tead4	231,74	1,04	0,00	-0,26	1,00
Trnp1	417,92	1,04	0,00	0,31	0,65
Prune2	353,24	1,03	0,00	0,14	1,00
Wee1	569,01	1,03	0,00	-0,02	1,00
Sdc4	5043,27	1,01	0,00	0,15	0,29
Sik1	815,26	1,01	0,00	0,08	1,00
Atp1b1	1108,93	1,00	0,00	-0,03	1,00
Lmod1	1846,02	0,99	0,00	0,05	1,00
Ezr	1385,88	0,98	0,00	-0,11	1,00
P2rx5	260,09	0,97	0,00	0,10	1,00
Klf9	1069,47	0,94	0,00	-0,02	1,00
Cdkn1c	706,08	0,92	0,00	0,04	1,00
Tom1l1	730,43	0,92	0,00	-0,03	1,00
Cry2	514,93	0,91	0,00	-0,05	1,00
Rras2	2548,47	0,91	0,00	-0,01	1,00
Cep85	866,31	0,91	0,00	-0,09	1,00
Samhd1	3670,59	0,91	0,00	0,13	1,00
Postn	61302,39	0,90	0,00	0,07	1,00
Gadd45g	1045,66	0,90	0,00	-0,08	1,00
Id3	3095,65	0,90	0,00	-0,02	1,00
Col6a2	10655,01	0,90	0,00	-0,02	1,00
Nedd9	1950,27	0,90	0,00	0,13	1,00

Gene name	base mean	log2FC WT	Padj WT	log2FC ΔZn	Padj ΔZn
Gclc	1470,42	0,88	0,00	-0,08	1,00
Nrbp2	335,27	0,88	0,00	0,13	1,00
Agfg2	635,64	0,88	0,00	-0,08	1,00
Whrn	290,64	0,87	0,00	-0,21	1,00
Ehd3	683,11	0,86	0,00	0,10	1,00
1700025G04Rik	795,63	0,86	0,00	-0,04	1,00
Vldlr	1083,71	0,86	0,00	0,05	1,00
Irak3	270,82	0,86	0,00	0,08	1,00
Pcdh9	706,53	0,85	0,00	-0,12	1,00
Fam160a1	356,84	0,85	0,00	0,23	1,00
Itga8	769,77	0,85	0,00	-0,07	1,00
Eef2k	1389,65	0,84	0,00	-0,02	1,00
Adam33	335,48	0,84	0,00	0,13	1,00
Mvd	1186,09	0,84	0,00	0,12	1,00
Ada	625,80	0,83	0,00	0,17	1,00
Mrvi1	319,41	0,83	0,00	-0,14	1,00
Mylk	931,51	0,82	0,00	0,07	1,00
Tns2	1669,18	0,82	0,00	0,03	1,00
Adcy1	254,65	0,82	0,00	-0,09	1,00
Slc43a2	313,29	0,82	0,00	-0,07	1,00
Phka2	452,43	0,82	0,00	-0,03	1,00
Pla2g15	1110,89	0,81	0,00	0,04	1,00
Rhoj	2145,33	0,81	0,00	0,12	0,95
Sesn1	394,27	0,81	0,00	0,06	1,00
Aspn	3123,06	0,80	0,00	0,18	1,00
Mgll	724,82	0,80	0,00	0,08	1,00
Ly6c1	313,67	0,80	0,00	0,16	1,00
Pid1	552,69	0,80	0,00	-0,12	1,00
Sdf2l1	472,80	0,80	0,00	0,07	1,00
Col6a1	18857,02	0,79	0,00	0,02	1,00
Klf13	1823,12	0,79	0,00	0,01	1,00
Syk	573,39	0,78	0,00	-0,09	1,00
Acss2	405,34	0,78	0,00	0,29	0,33
Rin3	979,28	0,78	0,00	-0,11	1,00
Irx1	476,79	0,77	0,01	-0,13	1,00
Irs2	318,44	0,77	0,00	-0,37	1,00
Fabp5	2849,27	0,76	0,00	0,02	1,00
Cdkn2d	387,81	0,76	0,00	0,05	1,00
Ap1s2	1446,30	0,75	0,00	0,03	1,00
Nfil3	1124,88	0,75	0,00	0,23	0,27
H6pd	2861,15	0,75	0,00	0,00	1,00
Plpp1	2359,95	0,74	0,00	0,04	1,00
Izumo4	203,32	0,74	0,00	0,21	1,00
Prkd1	757,46	0,74	0,00	-0,03	1,00
Slc39a8	207,51	0,74	0,00	0,16	1,00

Gene name	base mean	log2FC WT	Padj WT	log2FC ΔZn	Padj ΔZn
Pde5a	503,41	0,73	0,00	0,05	1,00
Tubb3	1470,27	0,73	0,00	-0,04	1,00
Serpina3g	2982,27	0,73	0,00	0,28	0,00
Bnip3	934,03	0,73	0,00	-0,01	1,00
Adamtsl4	516,85	0,73	0,00	-0,02	1,00
Bcl2l1	2497,42	0,73	0,00	0,02	1,00
C1qb	256,17	0,73	0,00	0,03	1,00
Rasl11b	317,11	0,72	0,00	-0,15	1,00
Tns1	9838,53	0,71	0,00	-0,13	1,00
Medag	398,03	0,70	0,00	0,14	1,00
Commd9	597,95	0,70	0,00	0,12	1,00
Syde2	440,51	0,70	0,00	0,08	1,00
Hdac7	2679,52	0,70	0,00	-0,02	1,00
Parm1	621,95	0,70	0,00	0,10	1,00
Epas1	668,59	0,70	0,00	0,00	1,00
Cyp4v3	241,01	0,70	0,00	0,05	1,00
Cavin3	1181,38	0,69	0,00	0,08	1,00
Slc4a4	352,54	0,69	0,00	-0,14	1,00
Mvk	1187,07	0,68	0,00	0,15	1,00
Znhit6	955,70	0,68	0,00	0,04	1,00
Cavin2	3462,06	0,68	0,00	-0,14	1,00
Hdac5	1066,92	0,68	0,00	-0,04	1,00
Peli2	306,40	0,67	0,00	-0,09	1,00
Nrk	650,08	0,67	0,00	0,04	1,00
Dact1	254,96	0,66	0,00	0,08	1,00
E2f6	1569,12	0,66	0,00	0,04	1,00
Pdlim2	246,58	0,66	0,00	0,07	1,00
Ctgf	20621,74	0,66	0,00	0,10	0,82
Pcx	443,01	0,66	0,00	0,14	1,00
Casp12	615,78	0,66	0,00	0,16	1,00
Atp10a	1200,02	0,66	0,00	0,06	1,00
Arxes2	362,43	0,66	0,00	0,33	0,68
Acot11	208,22	0,66	0,00	-0,05	1,00
Dhrs7	299,86	0,66	0,00	0,26	0,80
Bok	584,96	0,65	0,00	-0,10	1,00
Pik3ip1	299,35	0,65	0,00	0,05	1,00
Nuak2	651,77	0,65	0,00	-0,11	1,00
Pak3	938,83	0,65	0,00	-0,03	1,00
Rasa3	2262,38	0,65	0,00	-0,02	1,00
Rtl8a	316,27	0,65	0,00	0,06	1,00
Gopc	1796,07	0,64	0,00	0,03	1,00
Cdh2	4267,43	0,64	0,00	-0,11	1,00
Adcy2	346,65	0,64	0,00	0,10	1,00
Nkd2	234,92	0,64	0,00	0,00	1,00
Fos	243,83	0,64	0,00	0,27	0,89

Gene name	base mean	log2FC WT	Padj WT	log2FC ΔZn	Padj ΔZn
Smarcd3	271,72	0,64	0,00	-0,08	1,00
Kcnj15	515,46	0,64	0,00	-0,28	1,00
Ebf1	833,15	0,64	0,00	-0,06	1,00
Msmo1	5854,48	0,64	0,00	0,11	1,00
Smad6	288,23	0,63	0,00	-0,19	1,00
Lss	3434,41	0,63	0,00	0,12	0,68
Limch1	926,40	0,63	0,00	-0,01	1,00
Itga3	924,74	0,63	0,00	0,00	1,00
Snx1	1970,89	0,63	0,00	0,02	1,00
Akap12	14516,55	0,63	0,00	-0,08	1,00
Ip6k2	941,55	0,62	0,00	0,06	1,00
Pik3r1	1734,85	0,62	0,00	-0,04	1,00
Fst	2616,61	0,62	0,00	0,11	0,65
Mid1	353,31	0,62	0,00	-0,02	1,00
Flot1	1069,41	0,62	0,00	0,01	1,00
Klhdc8a	1113,09	0,62	0,00	0,14	1,00
Chst12	1313,05	0,62	0,00	-0,01	1,00
Mcf2l	312,76	0,62	0,00	-0,17	1,00
Mtmr1	483,08	0,62	0,00	0,03	1,00
Capn6	1654,53	0,62	0,00	0,12	1,00
Dusp1	971,24	0,62	0,00	0,22	0,33
Lgalsl	1637,35	0,62	0,00	0,05	1,00
Ret	204,85	0,62	0,00	-0,04	1,00
Cyp26b1	593,63	0,61	0,00	-0,16	1,00
Cltb	985,98	0,61	0,00	-0,03	1,00
Mboat2	554,55	0,61	0,00	-0,02	1,00
Ephb2	2060,84	0,61	0,00	0,10	1,00
Il1rn	1816,06	0,61	0,00	0,09	1,00
Rock2	9365,05	0,61	0,00	-0,14	1,00
Gm17501	770,32	0,61	0,00	0,12	1,00
Vav2	966,59	0,61	0,00	-0,16	0,85
Sema3d	233,04	0,61	0,01	-0,15	1,00
Cnksr3	312,48	0,60	0,00	-0,05	1,00
Rnf128	1155,18	0,60	0,00	0,13	1,00
Fgf13	231,20	0,60	0,00	0,04	1,00
B3galnt2	960,63	0,60	0,00	-0,09	1,00
Tead3	1209,95	0,60	0,00	0,04	1,00
Anxa1	34479,37	0,60	0,00	0,00	1,00
Plekhf1	637,63	0,59	0,00	-0,03	1,00
Eda	205,19	0,59	0,00	0,06	1,00
Dennd4a	1153,38	0,59	0,00	-0,16	1,00
Plac8	574,88	0,59	0,00	0,21	1,00
Fam3a	483,51	0,59	0,00	-0,03	1,00
Nox4	617,69	0,58	0,00	0,07	1,00
Pmvk	948,16	0,58	0,00	0,26	0,33

Gene name	base mean	log2FC WT	Padj WT	log2FC ΔZn	Padj ΔZn
Kif26b	1696,03	-0,58	0,00	-0,04	1,00
Fam46a	1045,45	-0,58	0,00	0,01	1,00
Enpp2	337,33	-0,58	0,00	0,01	1,00
Enpp1	884,98	-0,58	0,00	-0,07	1,00
Rnf24	1076,71	-0,58	0,00	-0,04	1,00
Pdpn	3102,55	-0,58	0,00	0,06	1,00
Plaur	1336,08	-0,59	0,00	-0,10	1,00
Rnf122	295,77	-0,59	0,00	0,08	1,00
Col10a1	389,26	-0,59	0,00	0,16	1,00
Serpinb9b	802,82	-0,59	0,00	0,05	1,00
Cd34	451,02	-0,59	0,00	0,21	0,85
Spred1	2243,59	-0,59	0,00	-0,02	1,00
Cep170	4178,97	-0,59	0,00	-0,13	1,00
Tnc	97010,79	-0,59	0,00	-0,08	1,00
Ttyh2	1245,70	-0,59	0,00	0,12	1,00
Tmtc2	235,48	-0,59	0,00	0,09	1,00
Malt1	269,29	-0,59	0,00	0,03	1,00
Slc25a37	1937,26	-0,60	0,00	0,02	1,00
Stambpl1	757,43	-0,60	0,00	0,07	1,00
Ube2l6	437,85	-0,61	0,00	0,34	0,18
Lrrc4c	217,93	-0,61	0,00	0,05	1,00
Noct	1528,06	-0,61	0,00	0,04	1,00
Unc5c	1103,83	-0,61	0,00	0,00	1,00
Rab7b	205,83	-0,62	0,00	0,07	1,00
Mcc	650,09	-0,62	0,00	-0,09	1,00
Fhdc1	568,65	-0,62	0,00	-0,11	1,00
Ccl20	2114,17	-0,62	0,00	0,03	1,00
Fam84b	560,70	-0,62	0,00	0,04	1,00
Mitd1	552,86	-0,62	0,00	0,18	0,95
Zfhx3	695,84	-0,62	0,00	-0,33	0,98
Ak5	546,54	-0,62	0,00	0,05	1,00
Rasal2	1273,16	-0,62	0,00	-0,16	1,00
Rnf135	247,37	-0,62	0,00	0,07	1,00
Sgms2	835,72	-0,62	0,00	-0,06	1,00
Zeb1	2661,83	-0,63	0,00	-0,10	1,00
Insig2	1153,63	-0,63	0,00	0,05	1,00
Ptgir	201,75	-0,63	0,00	0,09	1,00
Nes	4825,81	-0,63	0,00	0,03	1,00
Itgb8	226,56	-0,63	0,01	-0,30	1,00
Notch1	1173,51	-0,63	0,00	-0,08	1,00
Apln	308,10	-0,63	0,00	-0,14	1,00
Irs1	767,01	-0,63	0,00	-0,09	1,00
Arid5a	310,80	-0,63	0,00	0,16	1,00
Egr2	340,62	-0,63	0,00	0,13	1,00
Neto2	424,09	-0,63	0,00	-0,04	1,00

Gene name	base mean	log2FC WT	Padj WT	log2FC ΔZn	Padj ΔZn
Hk2	2048,61	-0,63	0,00	-0,01	1,00
Adamtsl3	738,46	-0,64	0,00	-0,07	1,00
Serpinb9	501,68	-0,64	0,00	0,21	0,84
Sesn3	358,66	-0,64	0,01	-0,08	1,00
Glis3	940,85	-0,64	0,00	-0,04	1,00
Ccl2	20141,42	-0,64	0,00	0,13	1,00
Tnfaip6	270,52	-0,65	0,00	0,20	0,85
Arhgap28	921,29	-0,65	0,00	0,00	1,00
Nrg1	363,54	-0,65	0,00	-0,05	1,00
Slc5a3	1487,07	-0,65	0,00	-0,03	1,00
Rbpj	4025,38	-0,66	0,00	-0,13	1,00
Parvb	538,92	-0,66	0,00	-0,14	1,00
Rgs5	659,61	-0,67	0,00	0,08	1,00
Cxcl2	848,29	-0,67	0,00	0,05	1,00
Ankrd28	1702,67	-0,67	0,00	-0,09	1,00
Nr4a2	224,97	-0,67	0,00	-0,03	1,00
Ern1	692,48	-0,67	0,00	-0,21	1,00
Stat5a	684,85	-0,68	0,00	0,02	1,00
Enpp4	421,28	-0,68	0,00	0,17	1,00
Slc7a2	2500,78	-0,68	0,00	-0,03	1,00
Hivep2	1577,26	-0,68	0,00	-0,05	1,00
D630045J12Rik	331,79	-0,68	0,00	-0,06	1,00
Adam19	5248,56	-0,68	0,00	-0,11	1,00
Mdn1	1243,87	-0,68	0,00	-0,17	1,00
Sod3	833,52	-0,68	0,00	0,06	1,00
Pou2f1	253,75	-0,69	0,02	-0,18	1,00
Pcdh7	2291,40	-0,69	0,00	0,06	1,00
Daxx	1335,09	-0,69	0,00	0,24	0,26
Ripk2	3311,08	-0,69	0,00	0,10	1,00
Fam208b	2055,02	-0,70	0,00	-0,03	1,00
Ralgapa2	280,27	-0,70	0,00	-0,01	1,00
Socs5	2493,82	-0,70	0,00	-0,11	0,98
Ptges	1211,78	-0,70	0,00	-0,07	1,00
Twist2	898,47	-0,71	0,00	0,12	1,00
Hmox1	3332,41	-0,71	0,00	-0,01	1,00
Lifr	541,61	-0,71	0,00	0,02	1,00
Gja1	6212,34	-0,71	0,00	-0,07	1,00
Slc5a7	269,02	-0,71	0,00	0,27	1,00
Slfn2	860,06	-0,72	0,00	0,35	0,01
Rsbn1	437,04	-0,73	0,00	-0,14	1,00
Tm4sf1	7675,40	-0,73	0,00	0,05	1,00
Zfp704	541,59	-0,73	0,00	-0,03	1,00
Sipa1l2	1482,22	-0,74	0,00	-0,08	1,00
Arl4c	2163,01	-0,74	0,00	0,03	1,00
Tmcc3	1162,20	-0,74	0,00	0,02	1,00

Gene name	base mean	log2FC WT	Padj WT	log2FC ΔZn	Padj ΔZn
Ccl9	645,44	-0,74	0,00	0,08	1,00
Irf1	1251,66	-0,74	0,00	0,08	1,00
Ier3	2740,31	-0,75	0,00	-0,10	1,00
Il18rap	413,44	-0,75	0,00	-0,01	1,00
Il1rl1	21122,68	-0,75	0,00	-0,11	1,00
Cd44	21643,38	-0,75	0,00	-0,02	1,00
Plpp3	1815,78	-0,75	0,00	0,02	1,00
Mfap3l	1278,23	-0,76	0,00	-0,07	1,00
Btbd11	205,91	-0,76	0,00	-0,19	1,00
Ncoa7	502,86	-0,76	0,00	0,13	1,00
Ttc9	575,10	-0,77	0,00	-0,06	1,00
Ptch1	937,55	-0,77	0,00	-0,17	1,00
Chst2	1532,95	-0,77	0,00	-0,05	1,00
Itpripl2	8028,74	-0,77	0,00	-0,08	1,00
Mast4	2403,89	-0,77	0,00	-0,07	1,00
Trim56	1901,14	-0,77	0,00	-0,03	1,00
Lhfpl2	2288,75	-0,78	0,00	0,00	1,00
Kctd12	320,74	-0,79	0,00	0,16	1,00
Rictor	2407,85	-0,79	0,00	-0,21	1,00
Ptprb	326,57	-0,79	0,00	-0,08	1,00
Cxcl14	1257,92	-0,80	0,00	0,17	1,00
Nrp2	7406,18	-0,80	0,00	-0,07	1,00
Ubash3b	358,26	-0,80	0,00	-0,13	1,00
Vcam1	8609,94	-0,80	0,00	0,13	0,95
Kif21b	1295,37	-0,81	0,00	-0,06	1,00
Pde4b	823,49	-0,81	0,00	0,02	1,00
Gpr149	459,02	-0,81	0,00	-0,08	1,00
Zfp618	703,11	-0,81	0,00	-0,12	1,00
Smad3	2532,71	-0,82	0,00	0,00	1,00
Dusp4	610,38	-0,82	0,00	-0,03	1,00
Ccl3	796,43	-0,82	0,00	0,15	1,00
Wisp1	11962,40	-0,82	0,00	-0,10	1,00
Pde8b	442,15	-0,82	0,00	0,19	0,98
Htr2a	912,06	-0,83	0,00	-0,16	1,00
Itgb3	1633,53	-0,83	0,00	-0,07	1,00
Prkg2	1430,60	-0,84	0,00	-0,02	1,00
Rgs16	2495,88	-0,84	0,00	0,00	1,00
Trim66	229,71	-0,85	0,00	-0,06	1,00
Ano1	298,09	-0,85	0,00	-0,22	1,00
Npr3	766,58	-0,86	0,00	-0,37	0,16
Megf10	1090,32	-0,86	0,00	-0,04	1,00
Gbp2	2483,47	-0,88	0,00	0,42	0,16
Rab11fip1	334,41	-0,88	0,00	0,10	1,00
Pla2g4a	2858,73	-0,88	0,00	-0,01	1,00
Tap1	716,51	-0,88	0,00	0,40	0,07

Gene name	base mean	log2FC WT	Padj WT	log2FC ΔZn	Padj ΔZn
Uba7	322,17	-0,89	0,00	0,47	0,12
Ank	2165,63	-0,90	0,00	-0,03	1,00
Mex3b	613,12	-0,90	0,00	-0,17	1,00
Gm6548	517,75	-0,91	0,00	0,36	0,00
Vegfa	3517,50	-0,91	0,00	0,04	1,00
Ddx58	2551,18	-0,91	0,00	0,14	1,00
Ifi211	543,46	-0,92	0,00	0,31	1,00
Grem1	6523,30	-0,92	0,00	-0,03	1,00
Bcl2l11	731,29	-0,92	0,00	-0,16	0,80
Phlda1	379,68	-0,93	0,00	0,18	1,00
Rdh10	485,80	-0,94	0,00	-0,06	1,00
Znfx1	1725,48	-0,94	0,00	0,18	1,00
Ntn1	973,02	-0,95	0,00	-0,01	1,00
Eif2ak2	2035,63	-0,95	0,00	0,11	1,00
Parp12	1097,27	-0,95	0,00	0,36	0,12
Scube3	255,01	-0,95	0,00	0,08	1,00
Herc6	414,02	-0,95	0,00	0,49	0,32
Adar	1600,35	-0,95	0,00	0,11	1,00
Samd5	228,90	-0,95	0,00	-0,06	1,00
Dcp2	1307,83	-0,96	0,00	-0,07	1,00
Icosl	252,29	-0,96	0,00	0,12	1,00
Zc3hav1	2350,42	-0,97	0,00	0,14	1,00
H2-Q4	425,59	-0,98	0,00	0,30	0,52
Plat	2631,72	-0,98	0,00	0,08	1,00
Gas2	920,71	-0,99	0,00	0,01	1,00
Lum	609,42	-0,99	0,00	-0,01	1,00
Trim30d	228,20	-1,00	0,00	0,45	0,68
F2rl1	999,61	-1,00	0,00	-0,17	0,49
Plxna4	427,91	-1,00	0,00	0,10	1,00
Hbegf	2070,12	-1,00	0,00	0,11	1,00
Parp10	330,32	-1,01	0,00	0,42	0,02
Igfbp5	12957,81	-1,01	0,00	-0,04	1,00
Ccl4	417,36	-1,02	0,00	0,02	1,00
Dkk2	594,37	-1,03	0,00	-0,11	1,00
Ggct	235,76	-1,03	0,00	0,07	1,00
Timp3	8983,15	-1,03	0,00	-0,11	1,00
Gjb2	1916,28	-1,04	0,00	0,06	1,00
Slc6a17	1093,91	-1,05	0,00	-0,03	1,00
Ptpre	286,66	-1,06	0,00	0,04	1,00
Gbp5	445,94	-1,06	0,00	0,31	1,00
Ngf	667,54	-1,06	0,00	0,00	1,00
B4galt5	3348,43	-1,07	0,00	0,05	1,00
Adamts4	805,29	-1,07	0,00	-0,06	1,00
Meox1	256,57	-1,07	0,00	-0,02	1,00
Bst2	559,42	-1,08	0,00	0,40	0,59

Gene name	base mean	log2FC WT	Padj WT	log2FC ΔZn	Padj ΔZn
Tlr3	277,09	-1,08	0,00	0,46	0,83
Trim12a	250,71	-1,09	0,00	0,26	0,68
Cx3cl1	2845,45	-1,09	0,00	0,12	0,90
Irf9	1017,37	-1,11	0,00	0,17	1,00
Pdgfb	400,82	-1,11	0,00	0,09	1,00
Cxcl16	583,80	-1,13	0,00	0,07	1,00
Slc4a7	1512,38	-1,13	0,00	-0,17	1,00
Parp9	1109,91	-1,14	0,00	0,35	0,33
Cd40	290,66	-1,15	0,00	0,01	1,00
Penk	579,00	-1,15	0,00	0,00	1,00
S1pr1	1103,33	-1,18	0,00	0,04	1,00
Tnfsf11	234,70	-1,19	0,00	0,01	1,00
Ifi204	346,60	-1,20	0,00	0,47	0,33
Tnfrsf11b	989,68	-1,24	0,00	0,02	1,00
Hgf	448,62	-1,24	0,00	-0,10	1,00
Piezo2	1970,73	-1,24	0,00	0,00	1,00
Ahr	534,33	-1,24	0,00	-0,07	1,00
Nr1d2	769,74	-1,25	0,00	-0,16	1,00
Trim12c	344,81	-1,25	0,00	0,21	1,00
Car8	220,22	-1,30	0,00	-0,01	1,00
Stat2	2055,13	-1,33	0,00	0,18	0,99
Ccl5	553,43	-1,34	0,00	0,26	1,00
Gm20559	292,22	-1,34	0,00	0,43	0,34
Ch25h	792,42	-1,35	0,00	-0,03	1,00
Angptl4	473,36	-1,37	0,00	-0,13	1,00
Inhba	4036,47	-1,38	0,00	-0,28	1,00
Samd9l	1251,46	-1,39	0,00	0,37	0,68
Ifit2	1448,99	-1,40	0,00	0,44	0,65
Mmp3	985,55	-1,42	0,00	-0,04	1,00
Gbp3	773,17	-1,43	0,00	0,46	0,23
Tor3a	1298,40	-1,45	0,00	0,37	0,00
Nr1d1	558,15	-1,48	0,00	-0,07	1,00
Stc1	232,76	-1,50	0,00	-0,09	1,00
Thbd	1664,67	-1,50	0,00	-0,11	1,00
Stat1	641,57	-1,57	0,00	0,47	0,03
Trim25	2304,96	-1,59	0,00	0,07	1,00
Ifih1	804,24	-1,61	0,00	0,41	0,68
Gbp7	644,37	-1,63	0,00	0,28	1,00
Lif	3855,46	-1,63	0,00	0,07	1,00
Helz2	2432,84	-1,63	0,00	0,12	1,00
Nos2	438,58	-1,64	0,00	0,23	1,00
Trim21	518,49	-1,64	0,00	0,37	0,22
Ptgs2	12071,02	-1,66	0,00	-0,01	1,00
Has2	1532,89	-1,66	0,00	-0,03	1,00
Slfn9	1043,24	-1,69	0,00	0,19	1,00

Gene name	base mean	log2FC WT	Padj WT	log2FC ΔZn	Padj ΔZn
Tnf	953,93	-1,69	0,00	0,01	1,00
Ifi47	232,86	-1,71	0,00	0,63	0,01
Ifi203	440,17	-1,73	0,00	0,36	1,00
Dtx3l	940,52	-1,80	0,00	0,29	0,99
Irgm1	3695,11	-1,81	0,00	0,34	0,15
Trim30a	270,33	-1,82	0,00	0,49	0,84
Irf7	531,64	-1,92	0,00	0,49	0,54
Mmp9	517,04	-1,97	0,00	-0,11	1,00
Neurl3	251,40	-1,99	0,00	0,09	1,00
Xaf1	313,26	-2,02	0,00	0,48	0,24
Sema7a	331,62	-2,06	0,00	-0,18	1,00
Rnf213	5035,17	-2,08	0,00	0,18	1,00
Parp14	1622,91	-2,10	0,00	0,31	1,00
Aldh1a3	411,23	-2,15	0,00	-0,17	0,80
Il6	551,11	-2,17	0,00	0,06	1,00
Oasl2	860,24	-2,21	0,00	0,45	0,66
Mmp10	202,80	-2,22	0,00	-0,23	0,85
Il1a	247,20	-2,29	0,00	-0,01	1,00
Mmp13	420,19	-2,30	0,01	0,29	1,00
Cd274	304,31	-2,31	0,00	0,46	0,83
Irgm2	1005,38	-2,36	0,00	0,28	1,00
Rsad2	1508,20	-2,38	0,00	0,42	0,58
Igtp	600,99	-2,38	0,00	0,47	0,31
Slfn8	268,75	-2,40	0,00	0,41	0,95
Cmpk2	814,22	-2,46	0,00	0,52	0,32
Isg15	1037,29	-2,50	0,00	0,49	0,57
Mx1	209,74	-2,58	0,00	0,60	0,32
Usp18	766,93	-2,59	0,00	0,58	0,02
Il1b	561,71	-2,62	0,00	0,07	1,00
Rtp4	465,23	-2,69	0,00	0,35	0,95
Cxcl10	5874,42	-2,74	0,00	0,46	0,01
Iigp1	658,27	-2,99	0,00	0,64	1,00
Oasl1	258,69	-2,99	0,00	0,49	0,02
Cxcl9	427,57	-3,05	0,00	0,68	0,15
Ifi44	345,64	-3,12	0,00	0,57	1,00
Ifit1	3018,64	-3,24	0,00	0,51	0,98
Ifit3	2028,82	-3,27	0,00	0,59	0,15
Mx2	245,08	-3,29	0,00	0,53	0,02
Ifit3b	777,00	-3,69	0,00	0,56	0,98

Supplementary list 3. Peptide counts from ChIP-MS.

Proteins significantly enriched over IgG in GR^{WT}

A2M;PZP	ASNS	CGGBP1	DAPK3	EIF4A1	GGA1
ABCB10	ATF1	CHD4	DDB1	EIF4B	GLRX3
ACAP3	ATP5B	CHMP1A	DDX1	EIF4G1	GLYR1
ACTA2/ACTG2	ATP5C1	CHMP4B	DDX18	EIF4G2	GMFB
ACTL6A	ATP5E	CHTOP	DDX23	EIF4H	GMPR2
ACTN1	ATRX	CKAP4	DDX39B	EIF5	GMPS
ACTN1	ATXN2	CLIC1	DDX3Y	EP300	GNL3
ACTN4	ATXN2L	CLIC4	DDX42	ERH	GNL3L
ACTR3	BICC1	CLINT1	DDX50	ESCO2	GOLGB1
ADNP	BNC2	CLIP1	DDX58	ESD	GPHN
ADSS	BOLA2	CLIP2	DEK	ESYT1	GRB10
AGO2	BRD4/3	CLK3	DGCR8	FABP5	GSN
AHCYL1/2	BUB3	CLTA	DHX15	FAM120A	GSPT1/2
AHDC1	BZW1	CMPK1	DIS3	FAM76B	GTF2I
AHNAK	C1QA	CNN1	DNAJA1	FARSA	H1F0
AKAP1	C1QB	CNN2	DNAJA2	FAU	H2AFJ
AKAP2	C3	CNN3	DNAJC7	FBLIM1	H2AFV/H2AFZ
AKAP8	CALM1/3	COL6A2	DNAJC8	FBN2	HBB-Y
AKAP9	CALU	COPB1	DNM1L	FDPS	HCFC1
AKR1B1/3	CAMK2D	COPB2	DNM2	FEN1	H2AFJ
AKT1	CAND1	CPNE1	DNMT1	FHL1	H2AFV/H2AFZ
AMPD2	CAPG	CPNE3	DOCK7	FHL2	HBB-Y
ANKFY1	CAT	CPSF2	DPF2	FHL3	HCFC1
ANKHD1	CBFB	CPSF7	DROSHA	FILIP1L	HDAC1
ANKRD17	CBX3	CREBBP	DTX3L	FKBP1A	HDAC2
ANLN	CCAR1	CSE1L	DUSP3	FKBP4	HELZ2
ANXA6	CCDC88A	CSRP1	DYNC1H1	FKBP5	HIBADH
ANXA7	CCT3	CSRP2	DYNC1I2	FSCN1	HINT1
AP2B1	CCT4	CSTB	DYNLL1	FTSJ3	HIST1H1A/B/C/E
AP2M1	CDC37	CTBP2	EEA1	FUBP3	HIST1H2B
APOB	CDC5L	CTCF	EED	FXR1	HIST1H4A
ARCN1	CDK1	CTGF	EEF2	FXR2	HIST2H2A
ARF1/2/3/5	CDK5RAP2	CTH	EFTUD2	FYCO1	HIST3H2BA/B
ARF4	CEBPB	CTNNA1	EHMT1	G3BP1	HK2
ARFGAP1	CELF1	CTNND1	EIF1	G3BP2	HMGA1
ARID1A	CELF2	CTTN	EIF2S2	GALK1	HMGA2
ARID5B	CELSR2	CTTNBP2NL	EIF3A	GAPVD1	HMGN1
ARIH1	CENPE	CUL1	EIF3B	GARS	HMGN2
ARL8B	CEP170	CUL4A	EIF3D	GART	HNRNPDL
ARPC1B	CEP78	CWF19L2	EIF3E	GATAD2A	HP
ARPC4	CFDP1	CYLD	EIF3H	GATAD2B	HSP90AA1

Proteins significantly enriched over IgG in GR^{WT}

HSP90AB1	**LUC7L**	**NCOA2**	**PCNA**	**PTPN23**	**GM3550;GM5218**
HSPA4	**LUC7L2**	**NCOA3**	**PDCD6IP**	**PUF60**	**RPL36**
HSPD1	**LUC7L3**	**NCOA5**	**PDE4DIP**	**PUM1**	**RPL4**
HSPG2	**LZTS2**	**NCOR2**	**PDLIM1**	**PYGB**	**RPL6**
IARS	**MAGOHB**	**NDC1**	**PDLIM2**	**RAB10**	**RPN2**
IFI204	**MAP1B**	**NEDD4**	**PDLIM4**	RAB13	**RPS15**
IFI205B	**MAP2**	**NEDD8**	**PDLIM5**	**RAB14**	**RPS21**
IFIT1	**MARF1**	**NEK7**	**PDLIM7**	**RAB6A**	**RPS28**
IFITM3	**MASP1**	**NEK9**	**PDS5B**	**RAB8A/B**	**RUNX1T1;CBFA2T3**
IGF2BP1	**MBNL2**	**NFIX**	**PDXDC1**	**RABEP1**	**SACS**
IGF2BP2	**MCCC2**	**NFKB2**	**PGD**	**RABGEF1**	**SAFB**
IGF2BP3	**MCM2**	**NIFK**	**PGK1**	**RAC1/3**	**SAFB2**
IK	**MCM3**	**NMD3**	**PGP**	**RAD50**	**SART3**
IKBIP	**MCM4**	**NME2**	**PHIP**	**RAE1**	**SBDS**
IKBIP	**MCM5**	**NOL9**	**PHLDB2**	**RANBP1**	**SDHA**
IMPDH2	**MCM6**	**NONO**	**PIN1**	**RAP1B**	**SDK1**
IPO5	**MCM7**	**NOSIP**	**PKD2**	**RARS**	**SEC13**
IQGAP1	**MEMO1**	**NPLOC4**	**PKM**	**RBBP4**	**SENP3**
IRF2BP2	**METAP1**	**NR3C1**	**PML**	**RBBP7**	**SERPINB6**
IST1	**MICALL2**	**NRIP1**	**PMM2**	**RBFOX1/2/3**	**SETDB1**
ITIH2	**MKI67**	**NUDT5**	**POLDIP3**	**RBM15**	**SF3A3**
KIF20B	**MNAT1**	**NUFIP2**	**PON1**	**RBM17**	**SF3B1**
KIF2A	**MOB4**	**NUP153**	**PPAT**	**RBM22**	**SF3B2**
KIF2C	**MOV10**	**NUP155**	**PPFIA1**	**RBM25**	**SF3B3**
KIF4	**MPRIP**	**NUP205**	**PPID**	**RBM26**	**SGOL2**
KPNA4	**MRTO4**	**NUP35**	**PPM1G**	**RBM28**	**SH3GL1**
KPNB1	**MSH2**	**NUP50**	**PPP1CB**	**RBM39**	**SIPA1L1**
KTN1	**MSH3**	**NUP93**	**PPP1R12A**	**RBM8**	**SKIV2L2**
LAP3	**MSH6**	**NUP98**	**PPP1R8**	**RBMS1**	**SLC4A2**
LARP1	**MTA1**	**NXF1**	**PPP2R1A**	**RBMS2**	**SLTM**
LARP4	**MTA2**	**OGT**	**PRDX6**	**RDX**	**SMAD1**
LARS	**MTHFR**	**OSBPL1A**	**PRKAR1A**	**RELA**	**SMARCA4**
LASP1	**MTPN**	**OSTF1**	**PRPF31**	**RNF20**	**SMARCA5**
LDB1	**MUT**	**PABPC4**	**PRPF40A**	**RNF213**	**SMARCAD1**
LGALS9	**MYEF2**	**PAFAH1B1**	**PRRC2C**	**RNF40**	**SMARCB1**
LIMA1	**MYL1/3**	**PAK1IP1**	**PRRX1/2**	**RNH1**	**SMARCC1**
LIMS1/2	**MYOF**	**PALLD**	**PRSS23**	**RPA1**	**SMARCC2**
LMO7	**NAA15**	**PARP1**	**PSIP1**	**RPL13A**	**SMARCD2**
LPP	**NAB2**	**PARP12**	**PSMD9**	**RPL14**	**SMARCD3**
LTA4H	**NACC1**	**PARP9**	**PSPC1**	**RPL27**	**SMARCE1**
LTBP1	**NAPA**	**PCK2**	**PTBP3**	**RPL29**	**SMC1A**

Proteins significantly enriched over IgG in GR^{WT}

SMC3	**SWAP70**	**TRIM33**	**YTHDF2**
SNAP29	**SYNCRIP**	**TRIP11**	**YTHDF3**
SNRNP200	**SYNPO**	**TRIP12**	**YWHAB**
SNRNP40	**TAGLN2**	**TRIP12**	**YWHAE**
SNRPA	**TAX1BP1**	**TRIP6**	**YWHAG**
SNRPA1	**TBL1X**	**TSC1**	**YWHAH**
SNRPC	**TCEA1**	**TSC2**	**YWHAQ**
SNRPD2	**TCEB1**	**TSN**	**YWHAZ**
SNX5	**TCERG1**	**TSNAX**	**ZC3H10**
SOAT1	**TCF20**	**TUBB3**	**ZC3H11A**
SON	**TCF25**	**TUBB6**	**ZC3H18**
SPECC1	**TEAD1/2/3/4**	**TXLNA**	**ZEB2**
SPTAN1	**TES**	**TXN**	**ZFR**
SQSTM1	**TEX10**	**TXNDC17**	**ZMYM4**
SRRM1	**TGM2**	**TXNL1**	**ZMYND8**
SRRM2	**THRAP3**	**U2AF1**	**ZNF281**
SRSF1	**THYN1**	**U2SURP**	**ZNF326**
SRSF10	**TIA1**	**UAP1L1**	ZFP326
SRSF9	**TIAL1**	**UBAP2L**	**ZNF592**
SSBP1	**TJP1**	**UBE2M**	**ZRANB2**
SSFA2	**TLE3**	**UBE2N**	**ZYX**
SSRP1	**TMEM209**	**UBL5**	
SSU72	**TMPO**	**UBTF**	
ST13	**TNIP1**	**UHRF1**	
STAT1	**TNKS1BP1**	**UPF1**	
STAT3	**TNPO1**	**USP25**	
STAU1	**TNS3**	**USP5**	
STIP1	**TOMM34**	**USP7**	
STRAP	**TOP2A**	**USP9X**	
STRIP1	**TPCN2**	**VAPA**	
STRN	**TPR**	**VARS**	
STRN3	**TPT1**	**VCL**	
STRN4	**TPX2**	**VWA5A**	
STT3A	**TRA2A**	**WDHD1**	
STUB1	**TRA2B**	**WDR18**	
SUGT1	**TRAPPC12**	**WDR5**	
SUMO1	**TRIM21**	**XPO1**	
SUMO2	**TRIM25**	**XPO5**	
SUMO3	**TRIM26**	**XRN2**	
SUPT16	**TRIM27**	**YLPM1**	
SUPT5H	**TRIM3**	**YTHDC1**	

List of publications

1. **Escoter-Torres, L**.*, Greulich, F., Quagliarini, F., Wierer, M., Uhlenhaut, N.H. Anti-inflammatory functions of the Glucocorticoid Receptor require DNA binding. (Under consideration)

2. **Escoter-Torres, L**.*, Caratti, G.*, Mechtidou, A.*, Tuckermann, J., Uhlenhaut, N.H., Vettorazzi, S. (2019) Fighting the fire: mechanisms of inflammatory gene regulation by the glucocorticoid receptor. *Frontiers in Immunology*. 10:1859. DOI:10.3389/fimmu.2019.01859
   * equal contribution

3. Clauss, K.*, Popp, A.P.*, Schulze, L., Hettich, J., Reisser, M., **Escoter Torres, L.**, Uhlenhaut, N.H., Gebhardt, J.C.M. (2017) DNA residence time is a regulatory factor of transcription repression. *Nucleic Acids Res*., 45, 11121-11130. DOI:10.1093/nar/gkx728

   *These authors contributed equally to the paper as first authors.

Conference attendance and poster presentations

1. Essential functions of the Glucocorticoid Receptor require direct DNA binding. *Transcriptional Regulation in Evolution, Development, and Disease,* Cell Symposia (Chicago, USA, Oct. 2019)

2. Essential functions of the Glucocorticoid Receptor require direct DNA binding. *Nuclear receptors and biological networks,* EMBO (Kolymbari, Greece, Sept. 2018)

3. Identification of GR coregulators by ChIP-MS and ReChIP. *Nuclear Receptors and Epigenomic Mechanisms in Human Disease and Aging*, FEBS Advanced Lecture Course (Spetses, Greece, Sept. 2017)